ELSEVIER

Inorganica Chimica Acta 226 (1994) 293–340

Inorganica Chimica Acta

Chemical and electrochemical approaches to the investigation of redox reactions of simple electron transfer metalloproteins

A.M. Bond

Department of Chemistry, La Trobe University, Bundoora, Vic. 3083, Australia

Received 31 March 1994

Abstract

The redox chemistry of simple metalloproteins such as cytochrome, plastocyanin and ferredoxin has been studied extensively by both chemically and electrochemically based techniques. However, despite the fact that complementary information can be obtained, in practice the results of the two methods generally have been reported and interpreted in an independent manner. In this paper an overview of the information that can be gained from the two approaches is presented. In both areas, a complex range of problems exists that are often considerably more challenging than those commonly encountered in studies on smaller redox active molecules. Consequently, interpretation of data obtained from either method when based on standard approaches and concepts is often fraught with danger. Nevertheless, knowledge related to important thermodynamic relationships, rates of electron transfer and structural changes associated with electron transfer processes are slowly being unravelled from both fields of endeavour. It is therefore proposed that the inherently difficult challenge of using both forms of methodology could now be attempted more frequently than currently is the case and that the dual approach provides an opportunity to synergistically enhance knowledge related to biologically important electron transfer processes of redox active metalloproteins.

Keywords: Chemistry; Electrochemistry; Redox reactions; Electron transfer; Metalloproteins

1. Principles and relationships of chemical and electrochemical methods used to study the redox properties of metalloproteins

Since electron transfer reactions within and between metal containing proteins play such an important role in biological energy transduction processes such as photosynthesis and respiration, it is not surprising that there has been extensive interest over a long period of time in the study of metalloprotein redox chemistry. Current interest in the subject is highlighted by the recent publication of Volume 226 of Advances in Chemistry entitled *Electron Transfer in Biology and the Solid State*, Volume 27 of Metal Ions in Biological Systems entitled *Electron Transfer Reactions in Metalloproteins*, Volume 36 of Advances in Inorganic Chemistry and the Proceedings of the Fifth International Symposium on Redox Mechanisms and Interfacial Properties of Molecules of Biological Importance (1993) which are either entirely or extensively devoted to the subject.

The process of moving an electron from one site (the donor) to another site (the acceptor) is a seemingly simple process in biological systems. However, the processes are exceedingly complex and many of the reactions involve rapid electron transfer through electron transfer chains over distances in excess of 10 Å and even up to 40 Å according to a recent report [1]. Thus, despite the significant advances that have taken place in the understanding of the thermodynamics (free energy) and kinetics (rates and mechanisms) of biologically important electron transfer reactions by ingenious application of a plethora of experimental approaches and theoretical concepts, it is evident that a great many aspects of the processes still need to be unravelled [2].

A substantial component of existing knowledge on biologically important electron transfer reactions is based on the results of investigations of the redox chemistry of simple electron transfer proteins such as the iron containing cytochrome *c* (Cyt.c) proteins and the blue copper containing plastocyanin (Pc) proteins. These proteins may be isolated from a range of sources in significant amounts and the study of homogeneous reactions with conventional inorganic redox reagents in a buffered aqueous solution phase has given rise to thermodynamically important standard (formal) redox potentials for the half cell reactions

SSDI 0020-1693(94)04082-7

$$[\text{Cyt.c, Fe(III)}]+e^- \rightleftharpoons [\text{Cyt.c, Fe(II)}] \quad (1)$$

and

$$[\text{Pc, Cu(II)}]+e^- \rightleftharpoons [\text{Pc, Cu(I)}] \quad (2)$$

Charges on the protein, which are in fact a very important component of protein redox reactions, are omitted for simplicity in this article when writing the reactions in equation form.

Rate data generally obtained from solution phase studies are also available for many intermolecular electron transfer reactions between proteins and inorganic redox reagents and the rate laws derived from them have given rise to the postulation of electron transfer reaction mechanisms. Similarly, biologically important redox reactions have been extensively studied in the solution phase and shown to involve electron transfer processes between different metalloproteins. For example, a model of the cytochrome *c*–cytochrome *c* peroxidase complex [3] indicates that it is stabilised by specific salt bridges with the hemes in parallel planes with an Fe–Fe distance of about 24 Å and an edge-to-edge distance of about 18 Å. Recently [4], a crystal structure of the complex confirmed that cytochrome *c* interacts with its redox partners in a highly specific manner. The structure also led to the postulation of a new electron transfer pathway between these biologically important redox partners, although it is not yet clear how this solid state structure is connected to solution phase rates.

For even an elementary intermolecular homogeneous electron transfer reaction, involving a metalloprotein and an inorganic redox reagent or two different metalloproteins, several steps will be required to achieve the transfer of an electron from a protein (designated species A) to the inorganic redox reagent or a different protein (designated species B) in the overall reaction

$$A+B \rightleftharpoons A^{x+}+B^{x-} \quad (3)$$

In many studies the kinetics of the overall reaction given in Eq. (3) fits the second-order rate law expected for a simple outer-sphere bimolecular process. That is, a second-order rate constant is obtained having the units of $M^{-1}\,s^{-1}$. However, this deceptively simple rate law will almost certainly not be the result of an outer-sphere reaction. Rather, it will correspond to a limiting case of a complex reaction scheme. For example, it may be postulated that, even in a minimal reaction scheme, the initial step of (i) the diffusion of the reactants A and B is followed sequentially by (ii) molecular interaction of the two reactants (donor and acceptor complexes) to form a precursor complex [AB] in which an optimum distance for electron transfer may be achieved (Eq. (4)), (iii) the elementary step of electron transfer to form $[A^{x+}B^{x-}]$ (Eq. (5)), and finally (iv) dissociation of $[A^{x+}B^{x-}]$ (Eq. (6)) to form the products of the overall reaction A^{x+} and B^{x-} which then diffuse back into the bulk solution.

$$A+B \underset{k_{-1}}{\overset{k_1}{\rightleftharpoons}} [AB] \quad (4)$$

$$[AB] \underset{k_{-et}}{\overset{k_{et}}{\rightleftharpoons}} [A^{x+}B^{x-}] \quad (5)$$

$$[A^{x+}B^{x-}] \underset{k_{-d}}{\overset{k_d}{\rightleftharpoons}} A^{x+}+B^{x-} \quad (6)$$

Any of the steps in Eqs. (4)–(6) characterized by forward and back homogeneous chemical rate constants k_1, k_{-1}, k_d and k_{-d} and forward and back electron transfer rate constants k_{et}, k_{-et}, or indeed diffusion, may be rate limiting. Consequently, confusion may easily arise in unambiguously deconvoluting the elementary electron transfer step (Eq. (5)) characterized by k_{et} and k_{-et} from the other reactions when as is often the case an overall rate constant, k_{obs}, is the physically measured parameter.

It is easily shown that with the reaction scheme represented by Eqs. (4)–(6) some limiting simple rate laws may be obtained. For example, if the rate of electron transfer is much faster than the inverse lifetime of the formation of precursor complex [AB] in Eq. (4), then $k_{obs} \approx k_1$, and the rate law is equivalent to that which would be obtained for a simple outer-sphere bimolecular second-order rate process. In contrast, if the rate of electron transfer is small relative to the lifetime of the intermediate, then electron transfer is the rate determining step and $k_{obs} \approx k_1 k_{et}/k_{-1}$. The existence of different schemes to Eqs. (4)–(6) but which still give the same overall reaction (Eq. (3)) in an electron transfer reaction may also result in erroneous assignment of the mechanism and ideally spectroscopic or other forms of identification or even isolation of intermediates and separate studies of the binding properties of A and B should accompany the rate data.

Detailed discussion of the issues involved in correctly assigning mechanisms of electron transfer mechanisms is available in Refs. [2] and [5]. However, in this review, it is important to note that rate constant data derived from chemical redox reactions normally will be designated as k_{obs} values which may either be a measure of the rate constant for the second-order reaction between A and B to form a precursor complex or some other more complex reaction sequence. It follows from the above discussion that k_{obs} values need not be directly related to k_{et} as often implied in discussion of protein electron transfer reactions. Ideally, the symbol k_{et} should be reserved for a first-order rate constant obtained under conditions where it can be confirmed that the contribution of other steps have been correctly deconvoluted from k_{obs} or where it is clear that reaction (5) has been directly and unambiguously measured in the absence of a contribution from other steps.

With the aim of simplifying the mechanistic interpretation of the electron transfer step, the synthesis of proteins containing a redox active centre at what have been proposed to be fixed and known distances from the metal centre have been undertaken [1,2,6]. In complexes of this kind, intramolecular electron transfer between the added redox active site and the redox active metal centre of the metalloprotein may be studied under many circumstances in the absence of diffusion and some of the other complications of the kind represented in reaction sequence (4)–(6) which are present in intermolecular electron transfer reactions. Varying the site of attachment also enables orientation and free energy (driving force) effects on the rate of the electron transfer step to be studied. Consequently, modified proteins have become widely used molecules for studying biologically important electron transfer reactions.

The original modification procedure shown in Scheme 1 involved the direct reaction of aquopentaammineruthenium(II) complex designated as $[a_5Ru(H_2O)]$, with the imidazole of a surface histidine, to give $[a_5Ru(histidine)]$, where charges have again been omitted for simplicity in writing the chemical formulae. Subsequently, many forms of modified protein have been prepared for studying biologically relevant electron transfer processes [2]. Electron transfer reactions in modified proteins generally have been studied by pulse radiolysis or flash photolysis. In Scheme 2, the electron transfer reaction is initiated by photogenerated

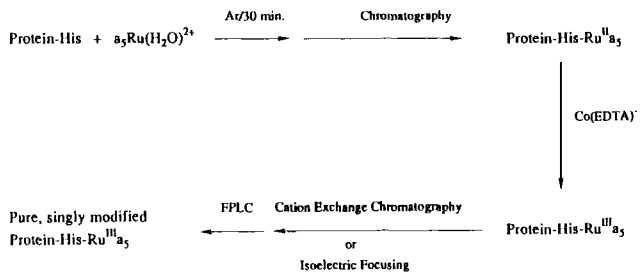

Scheme 1. Preparation and purification of $a_5Ru(His)$ modified proteins. Reproduced by courtesy: *Prog. Inorg. Chem., 38* (1990) 259.

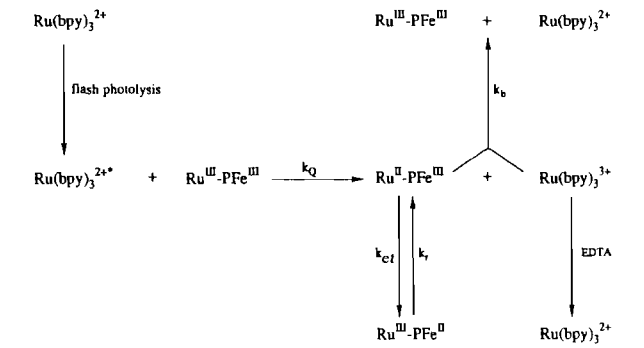

Scheme 2. Method for studying the rate of the Ru(II) → Ru(III) electron transfer process (k_{et}) in ruthenium modified heme proteins. Reproduced by courtesy: *Prog. Inorg. Chem., 38* (1990) 259.

($[Ru(bpy)_3]^{2+}$)* which rapidly reduces the surface ruthenium synthetically introduced into the protein. The $[Ru(bpy)_3]^{3+}$ is then scavenged by EDTA before it can back react with $a_5Ru(II)$(histidine). Electron transfer to the protein metal centre is then monitored spectroscopically. Scheme 3 shows the general case where k_{et} values for both reduction and oxidation processes may be measured for the modified protein designated as A–O–D where the electron donor metal centre, O, has a more negative reduction potential than the electron acceptor metal centre, A, but where either can be in the oxidised or reduced state.

In interpreting data obtained from intramolecular electron transfer studies on modified proteins, it is assumed that the structure of the surface modified protein is the same as that of the native protein and that the distance and the intervening medium associated with the electron transfer process are both known and can be deliberately varied by altering the site of attachment of the surface redox centre relative to the protein redox centre. However, the inorganic redox centre is often in a hydration sphere of unknown mobility. To complicate matters the mobility may vary with oxidation state. If this redox centre is at all mobile on the surface of the protein in either oxidation state, then the distance between the protein and added redox sites may not be as well defined as in the ideal representation where redox sites are assumed to be completely rigid. Furthermore, in reaction Scheme 2, homogeneous reactions as in Eqs. (4)–(6) must occur concomitantly with the intramolecular reaction and it must be verified that such homogeneous reactions are not contributing to the value of k_{et} assigned to the intramolecular electron transfer reaction. This is a potentially significant problem when slow values of k_{et} are obtained for the intramolecular reaction since this kinetic regime is where it is most likely that the time domains of the intra- and intermolecular reactions will overlap. Consequently, though perhaps not as widely recognised, there also may be ambiguities in the interpretation of redox data obtained from modified proteins

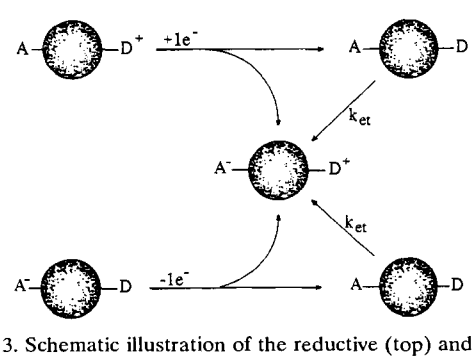

Scheme 3. Schematic illustration of the reductive (top) and oxidative (bottom) methods of studying intramolecular electron transfer (k_{et}) within a chemically modified protein A–O–D. Reproduced by courtesy: *Met. Ions Biol. Syst., 27* (1991) 214.

as is the case with homogeneous redox data and extreme caution always needs to be displayed in interpreting the rate laws in the mechanistic sense. However, it is also clear that many scientists are currently undertaking the necessarily laborious experiments and solving the demanding theories that are required to address these issues. Optimistically, a natural progression from simple qualitative explanations to complex quantitative ones will emerge from these endeavours.

Electrochemical studies of the redox chemistry of metalloproteins, while usually reported in isolation to the chemical redox studies, are also very widespread and also have been extensively reviewed [7]. In the electrochemical technique, the electrode provides the source (reduction) or sink (oxidation) for electrons and variation of the applied potential provides the driving force which enables the redox reaction to occur. In a typical electrochemical reaction involving solution soluble proteins it would be assumed that metalloproteins such as [Cyt.c, Fe(III)] or [Pc, Cu(II)] diffuse towards the electrode surface until they are sufficiently close to the electrode (double layer region) to accept electrons from the electrode at which stage the proteins are reduced to [Cyt.c, Fe(II)] or [Pc, Cu(I)] etc. The product of the electrode process would then be assumed to diffuse away from the electrode surface and back into the bulk solution. In a mechanism of this kind, the charge transfer process may be represented as in Eq. 7(a) or 7(b).

$$[\text{Cyt.c, Fe(III)}] + e^- \overset{E_f^0,\, k_s,\, \alpha}{\rightleftharpoons} [\text{Cyt.c, Fe(II)}] \qquad (7a)$$

$$[\text{Pc, Cu(II)}] + e^- \overset{E_f^0,\, k_s,\, \alpha}{\rightleftharpoons} [\text{Pc, Cu(I)}] \qquad (7b)$$

where E_f^0 is the formal reversible potential which is often close to the standard redox potential (E° value), k_s is the heterogeneous charge transfer rate constant at E_f^0 and α is the charge transfer coefficient [8]. The complete electrode process for solution soluble proteins involves coupling the diffusion component of the experiment with the electrochemically induced electron transfer step.

In principle, the heterogeneous charge transfer rate constant is related to the driving force of the potential in a way predicted by the Butler–Volmer equation (8) whereas k_{et} for homogeneous chemically based redox reactions is related to the driving force of free energy of the reaction by the Marcus relationship [5]. Obviously, under some circumstances a correlation may be expected between k_s and k_{et} and these will be considered at a later stage in this review. However, it needs to be recognised that k_s is a heterogeneous rate constant for electron transfer across an electrode/solution interface. Since k_s is a measure of a reaction that necessarily occurs between two phases, k_s therefore has the units of m s^{-1} (or cm s^{-1} in much of the electrochemical literature) rather than s^{-1} as is the case for k_{et} which is a homogeneous rate constant for a reaction in a single phase. For a reaction of the kind given in Eq. (7), a close parallel with the intramolecular redox reaction in chemically modified proteins or reaction (5) in a homogeneous redox reaction could be expected provided the diffusion component can be correctly deconvoluted from the electron transfer step in the electrochemical method. Additionally, a correlation of k_s with second-order k_{obs} values would be expected if reactions mimicked a bimolecular outer-sphere process, but as noted above, this may be unlikely, since protein redox reactions are more like inner-sphere than outer-sphere processes.

Eq. (7) and the above discussion refer to the common electrochemical method where diffusion of a solution soluble protein and electron transfer are coupled. Alternatively, in electrochemical studies it is sometimes possible that the metalloprotein may be adsorbed or chemically attached to the electrode surface via say a lysine or a histidine group [9] and the electrochemical electron transfer reaction studied as in Eq. (8).

$$[\text{Cyt.c, Fe(III)}]_{\text{attached}} + e^- \overset{(E_f^0)_{\text{attached}},\ (k_s)_{\text{attached}},\ (\alpha)_{\text{attached}}}{\rightleftharpoons} [\text{Cyt.c, Fe(II)}]_{\text{attached}} \qquad (8)$$

In this case, assuming the product of the electron transfer process remains attached to the electrode surface, then an even closer parallel with modified protein intramolecular electron transfer reactions may be expected to exist because ideally in neither case is diffusion from the bulk solution relevant. If the structures of the surface attached and bulk solution forms are similar, then the electrochemical parameters derived for the two kinds of electrode mechanism should be related to each other as well as to their chemical redox counterparts. However, unfortunately the structure of $[\text{Cyt.c, Fe(III)}]_{\text{attached}}$ or any other surface attached protein need not be the same as the solution soluble native form and if structural changes occur on attachment to the electrode surface the $(E_f^0)_{\text{attached}}$ value derived from the reaction in Eq. (8) may be distinctly different from the E_f^0 value as derived from the reaction in Eq. (7). Similarly, $(k_s)_{\text{attached}}$ and $(\alpha)_{\text{attached}}$-values associated with Eq. (8) are not expected to be related to analogous parameters derived from Eq. (7) in any simple manner when the structure of the surface attached protein is distinctly different from the solution soluble form.

Obviously, an intermediate kind of electrochemical mechanism as given in Eq. (9) may also apply where electron transfer takes place in the surface confined or attached state, but where mass transport between the bulk solution and the electrode surface occurs by diffusion

$$[\text{Cyt.c, Fe(III)}]_{\text{bulk}} \rightleftharpoons [\text{Cyt.c, Fe(III)}]_{\text{attached}} \quad (9a)$$

$$[\text{Cyt.c, Fe(III)}]_{\text{attached}} + e^- \rightleftharpoons [\text{Cyt.c, Fe(II)}]_{\text{attached}} \quad (9b)$$

$$[\text{Cyt.c, Fe(II)}]_{\text{attached}} \rightleftharpoons [\text{Cyt.c, Fe(II)}]_{\text{bulk}} \quad (9c)$$

This latter kind of mechanism was proposed by Albery et al. [10], and may be the cause of ambiguities in deconvoluting the 'true' electrochemical electron transfer rate k_s from other steps as is the case when measuring 'true' k_{et} in chemical redox studies. That is, published k_s and k_{et} values may often be 'apparent' rather than 'true' values. More details on the nuances of electron transfer process at an electrode may be gained by consulting Ref. [8].

The above introduction has been presented to illustrate the substantial versatility and commonality, as well as potential ambiguities of the chemical and electrochemical methods of studying the redox properties of metalloproteins. However, to date the results of the chemical and electrochemical studies generally have been considered in isolation. The purpose of this article is to present an overview of data obtained from the two methodologies in an endeavour to demonstrate how results obtained from the two approaches are in fact mutually beneficial to the understanding of electron transfer reactions in a synergistic sense and to suggest that a great deal may be gained in future studies by concurrently undertaking redox studies by both chemical and electrochemical means rather than solely by one method or the other as is the currently accepted practice. At the same time, the considerable ambiguities that have arisen in both data sets when convoluting factors other than electron transfer from the process are highlighted in order to indicate how far we are from a complete understanding of this field even after considering the vast data available for electron transfer reactions of simple metalloproteins.

Of course, it will be well recognised from the above discussion that electron transfer reactions of metalloproteins are among the most reviewed class of chemical reactions. In several areas, the data required for the narrow purposes of this particular review therefore have already been compiled. For convenience, where reviews are available they are used as the data base, but of course the primary literature should be consulted for experimental details. The feature that is new in this overview is that a comparison of chemical and electrochemically derived data has been considered in detail for the first time.

2. Structural changes that accompany metalloprotein electron transfer reactions

It must always be remembered that a redox process commonly involves more than just the transfer of an electron, e.g. Eqs. (5), (7), (8), (9b). Thus, if a chemical transformation reaction accompanies the electron transfer, then this step needs to be deconvoluted from the electron transfer step. While it may be argued that little structural change takes place in proteins during the actual electron transfer step (Frank–Condon principle), the overall structural changes accompanying electron transfer are undoubtedly biologically significant and do govern the biologically effective overall rate of the redox process. In many instances, these structural changes may be inadvertently or unknowingly included in the rate studies to give what are in fact only apparent k_{obs}, k_{et} and k_s values.

Overall structural changes accompanying electron transfer reactions have generally been elucidated [11] by X-ray crystallographic (solid phase) and NMR (solution phase) techniques on well characterised samples of oxidised and reduced forms of the metalloprotein. As a simple way of illustrating how redox reactions with different proteins may involve distinctly different structural changes it has been demonstrated that redox reactions taking place in crystals of cytochrome *c* crack the crystals, whereas of cytochrome b_5 remain intact [11]. It may be argued on the basis of this qualitative observation that a considerably greater overall structural change takes place in the case of a redox reaction involving cytochrome *c* than is the case of cytochrome b_5. However, as will be seen subsequently, this feature does not necessarily translate into considerably higher reorganisational energies or slower self-exchange electron transfer rates. Thus, macroscopic aspects related to the overall structural changes and microscopic details associated with the electron transfer step need not necessarily correlate.

As pointed out by Williams [11], NMR data coupled with knowledge from X-ray studies may be used effectively to elucidate the influence of overall chemical changes on features of structure and mobility of the protein. Proton transfer, which is usually a very rapid process, commonly accompanies metalloprotein electron transfer reactions. Consequently, a knowledge of protein movement that occurs concomitantly with or sequentially to the electron transfer step involved in a change in redox state is essential in understanding the overall mechanism of the electron transfer reaction and may also need to be deconvoluted from k_{obs}, k_{et} or k_s values to calculate true values of the electron transfer rate.

From a theoretical point of view, the central requirements for the occurrence of rapid intramolecular electron transfer have been explored for almost 40 years under the heading of the Marcus [12] or related

theory [5]. Application of the Marcus type theory leads [5,12] to the conclusions that: (i) the electron transfer or total electron hop distance must be less than about 20 Å (however, note Ref. [1] where 40 Å distances are believed to be involved), (ii) that the medium through which electron transfer takes place is important, (iii) the driving force or free energy of the reaction is important, and (iv) that the rate of electron transfer will be impeded if the metal ion centre is involved in considerable structural change when the reduction or oxidation process takes place.

With respect to point (iv) which is being emphasised in this section of the review, careful crystallographic and NMR studies on the blue copper proteins, azurin and plastocyanin show that over the biologically important pH range effectively no change in either the protein lattice or metal centre occurs. In these blue copper proteins, Vallee and Williams [13] have argued that at biologically important pH values the copper ion is in a constrained entatic state which may have been 'designed' to minimise conformational change. However, interestingly at low pH values the situation appears to be more complex and significant structural changes do in fact accompany electron transfer. In understanding the structural role of proton transfer and electron transfer at different pH values, the studies of Freeman et al. [14] are important in that they reveal that in the oxidised form of poplar Pc, [Pc, Cu(II)], the coordination of the copper atom is independent of pH whereas in the reduced form, [Pc, Cu(I)], the protein exists as a mixture of two structural forms of copper, Pc and HPc, which can be related by the equilibrium represented by Eq. (10).

$$[\text{Pc, Cu(I)}] + \text{H}^+ \rightleftharpoons [\text{HPc, Cu(I)}] \qquad (10)$$

While this structural change for Pc only becomes important at acidic pH values which lie outside the biologically important range and is in some senses different to the protein lattice changes considered by Williams [11], it represents a case where the proton and electron transfer step clearly can be separated, and is therefore relevant to understanding the role of structural change in protein redox chemistry. In the high pH copper(I) or [Pc, Cu(I)] form, the distorted tetrahedral NNSS′ coordination of the copper atom, also found in [Pc, Cu(II)], is preserved with only minor dimensional changes, so that according to the conclusions summarised above, it would be expected that rapid electron transfer may take place between the [Pc, Cu(II)] and [Pc, Cu(I)] forms of poplar plastocyanin at biologically important pH values around 7. However, in [HPc, Cu(I)] which is formed in acid media the imidazole ring of His87 is protonated and dissociated from the copper atom and rotated by 180° about C_β–C_γ giving rise to trigonal NSS′ coordination. Again, consistent with concepts noted above, [HPc, Cu(I)], or the acid form of reduced plastocyanin, has been proposed to be redox inactive due to a high reorganisation barrier that would be required to oxidise this species to [Pc, Cu(II)]. The hypothesis is said to be supported by data obtained from kinetic measurements of the redox reactions of plastocyanin with small inorganic complexes [15a,b,c]. In contrast, voltammetrically obtained electrochemical data (see later) exhibit reversibility (chemical and electrochemical senses) at both low and high pH values and the redox process as monitored electrochemically is diffusion controlled at all accessible pH values [16]. The electrochemical data have been explained by treating the process in solution under voltammetric conditions as a two-step process

$$[\text{Pc, Cu(II)}] + e^- \overset{E_f^0}{\rightleftharpoons} [\text{Pc, Cu(I)}] \qquad (11a)$$

$$[\text{Pc, Cu(I)}] + \text{H}^+ \overset{K_a}{\rightleftharpoons} [\text{HPc, Cu(I)}] \qquad (11b)$$

with both reactions (11a) and (11b) being very fast on the voltammetric time scale, so that the overall process is diffusion controlled irrespective of the pH value. However, alternative interpretations which include the existence of transient forms of [HPc, Cu(II)] and square reaction schemes (Eq. (12))

$$\begin{array}{ccc} [\text{Pc, Cu(II)}] + e^- & \overset{(E_f^0)_1}{\rightleftharpoons} & [\text{Pc, Cu(I)}] \\ -\text{H}^+ \downarrow\uparrow +\text{H}^+ & & -\text{H}^+ \downarrow\uparrow +\text{H}^+ \\ [\text{HPc, Cu(II)}] + e^- & \overset{(E_f^0)_2}{\rightleftharpoons} & [\text{HPc, Cu(I)}] \end{array} \qquad (12)$$

may equally well explain the pH dependence of the Pc data, although separate electron transfer steps with different E_f^0 values have yet to be observed.

In the case of cytochrome *c*, two distinct voltammetric processes at well separated potentials are in fact observed in alkaline media and the data almost certainly correspond to a square reaction scheme of the type given in Eq. (13) (see later discussion for further details).

$$\begin{array}{ccc} [\text{Cyt.c, Fe(III)}]_{\text{native}} + e^- & \overset{(E_f^0)_1}{\rightleftharpoons} & [\text{Cyt.c, Fe(III)}]_{\text{native}} \\ \text{acid} \downarrow\uparrow \text{base} & & \text{acid} \downarrow\uparrow \text{base} \\ [\text{Cyt.c, Fe(III)}]_{\text{base}} + e^- & \overset{(E_f^0)_2}{\rightleftharpoons} & [\text{Cyt.c, Fe(III)}]_{\text{base}} + e^- \end{array} \qquad (13)$$

The complete story with respect to separation of the electron transfer and structural changes accompanying a redox change may not yet have been completely unravelled, particularly since more subtle forms of conformational change may occur than considered in Eqs. (12) and (13). It must be noted that any conformational change or series of changes in principle can be treated in an analogous way to these square schemes and indeed in voltammetric studies the square

scheme has been commonly invoked as a means of accounting for structural change accompanying the electron transfer process [17]. Importantly, in electrochemical studies, treating the process as a square scheme rather than a single-step process has frequently led to modification of initial postulates concerning both thermodynamic and kinetic aspects of a redox process [17]. While the square reaction scheme has yet to be introduced widely in chemical redox studies of proteins, it is suggested in this article that some data also could be profitably re-examined via the 'square' reaction scheme concept.

As is the case with the blue copper proteins, virtually no change takes place in the cytochrome b_5 protein lattice when a redox state change takes place in solution at the biologically relevant pH. Williams [11] emphasises for this redox active protein that not even hydrogen bonding changes accompany the redox state change. Under these circumstances, cytochrome b_5 should almost be the ideal protein for fast electron transfer since it contains a low-spin iron atom where the change in size accompanying a redox reaction is minimal and the protein is held together in a tight field by a β-sheet in a similar way to blue copper proteins where a robust β-panel structure is present in both oxidation states [11]. Consequently, little impediment to electron transfer should occur in redox reactions of cytochrome b_5 since the requirements for structural change to accompany electron transfer are almost as minimal as for a simple inorganic complex. On this basis cytochrome b_5 may be expected to be a relatively simple electron transfer protein whose electron transfer reactions might be expected to be fast and readily interpreted in a systematic and straightforward manner. However, while there is some truth in this simple concept, it will emerge that factors other than structural change are also important in determining the measured electron transfer rates of protein redox reactions and even proteins such as cytochrome b_5 may give rise to data that are difficult to interpret.

The previously noted observation that crystals of cytochrome *c* crack during redox reactions already provides a hint that overall structural changes accompanying electron transfer are large with this protein even at biologically important pH values. Cytochrome *c*, while perhaps the most widely studied metalloprotein, is therefore likely to be one of the most complex metalloproteins with respect to interpreting the influence of protein lattice structural changes accompanying electron transfer and unambiguously deconvoluting these processes from the electron transfer step. However, Brayer and co-workers in recent studies have reported the high resolution X-ray structural analysis of yeast iso-1-cytochrome *c* in the two oxidation states [18,19]. In the introduction to Ref. [19], it is noted that previous studies have been confusing in the sense that some authors report data that give strong indications that cytochrome *c* undergoes a dramatic redox induced conformational change, whereas other data, sometimes based on the use of the same techniques, have led to the conclusion that differences between the reduced and oxidised forms are very small. Thus, it is only recently that considerable clarification has been achieved on this important aspect of metalloprotein redox chemistry [11,19].

The redox induced conformational changes detected in crystals [11] involve the region around one water molecule, WAT 166, which is H bonded to or close to Thr-76, Met-80, Tyr-67, Asn-52 and propionate-7 of the haem (Fig. 1). The water molecule, the haem and several of these residues have all been shown to undergo redox induced movements by NMR methods. Although the fine details of the H bond changes are not well-defined, NMR data show that there are small secondary structure adjustments throughout the regions from residues 38 to 85, including alterations in the short helices. Importantly, on changing the oxidation state of cytochrome *c* there are several large shifts, $\geqslant 1.0$ ppm in the NMR data not due to the paramagnetic effect, which occur in the N*H* of Gly-41, Ala-43, Asp-60, Lys-79 and Met-80 and the side-chains of Thr-78(OH) and Arg-38 C$H_{(\epsilon)}$. In comparison, little change is detected in the α-CH protons of these residues. The large shifts in the N*H* resonances imply for example, that the H bond from Gly-41 to propionate-6 of the haem (Fig. 1(a)) makes and breaks during the redox reaction, which is effectively a proton/electron coupled diffusion change involving proton movements associated with the carboxylate groups of the propionates inside the protein matrix. NMR studies also reveal that a change in redox state alters access of protons from solvent water to this region, since the H/D exchange of protons from one internal group in this region, Tryp-59 ring N*H*, is 100 times faster in the oxidised state relative to the reduced state. The other smaller structural adjustments in the body of the protein are in the nearby helices 50–75 and in their side-chains.

The detailed high resolution structures of yeast iso-1-cytochrome *c* in both oxidation states [18,19] provide a definitive understanding of the solid state oxidation state dependent conformational changes in cytochrome *c*. Results are in broad terms in agreement with those formulated by Williams [11]. Voltammetric studies [20] at high pressure (also see later) also show that a significant volume change occurs during the course of a redox process and that in agreement with structural, chemical and physical studies [Cyt.c, Fe(II)] has a more compact structure than [Cyt.c, Fe(III)]. Thus it may be concluded from studies on the structural changes accompanying the electron transfer process that while the metal centre may not change significantly during

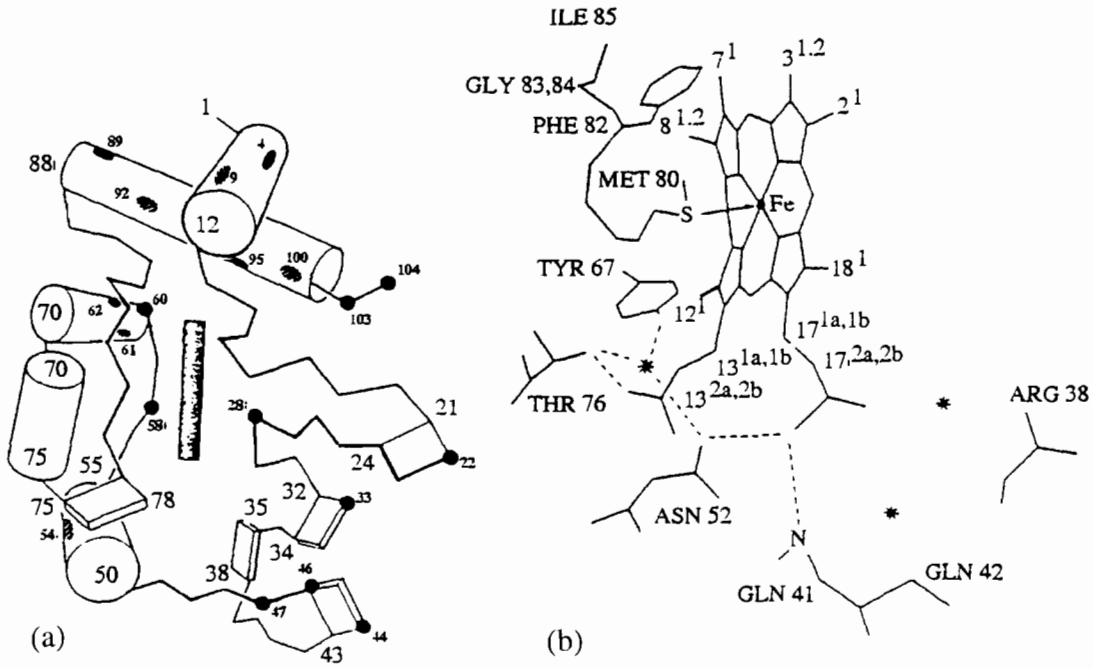

Fig. 1. Structural features of cytochrome *c*. (a) An outline of the structure of cytochrome *c* with the shaded areas representing amino proton (deuteron) sites that have been studied by NMR. (b) The hydrogen bond network of cytochrome *c* over the sequence region 38–41 via 52, (59) 78, 67, 80, heme propionates (13 and 17) and water molecules (*). During a redox reaction, the hydrogen bond network passes through the interior of the protein and therefore is broken and then made in a new way. Reproduced by courtesy: *Biochim. Biophys. Acta, 1058* (1991) 71.

a redox reaction involving cytochrome *c*, the protein lattice structure of cytochrome *c* does in fact change considerably relative to blue copper proteins and cytochrome b_5 where both metal centre and protein lattice structural changes are minimal.

The NMR data available on cytochrome *c* and other metalloproteins, as well as providing structural information, indicate that redox proteins should be considered as dynamic rather than static molecules. Consequently, the dynamics of structural changes may be an important feature of their redox reactions. A further article by Williams [21] includes an excellent overview of the dynamics and other features of structural changes which may take place during a metalloprotein redox process and should be consulted for further details on this aspect of metalloprotein redox chemistry.

While substantial structural changes occur in the protein lattice of proteins such as cytochrome *c* and may complicate the interpretation of electron transfer rate data, the metal centres of the simple metalloproteins such as cytochrome *c*, the blue copper proteins, ferredoxins and cytochrome b_5 are of course ideal electron transfer sites for the following reasons, as elegantly summarised by Williams [21].

(a) The ligands around metal ions in simple electron transfer proteins appear to be selected to facilitate rapid electron transfer rates since they either reduce the central charge on the metal or induce the low-spin rather than the high-spin state of a metal ion. Examples are sulfur, imidazole and porphyrin ligands for iron and copper atoms in all the important simple electron transfer proteins.

(b) The geometry around the metal ion in simple electron transfer proteins is generated by the protein fold which is so strong that there is minimal ligand rearrangement on change of metal oxidation state. Examples are the close-to-tetrahedral, entatic, state of the blue copper proteins in both the Cu(II) and Cu(I) forms and the retention of the coordination geometry when the low-spin iron Fe(III) in cytochrome *c* is reduced to Fe(II).

(c) The metal ion sites are buried up to 10 Å into the protein so that the possibility of adventitious reactions of the metal ions with small ligand containing molecules is minimal. Since the protein fold does not relax readily, the coordination sphere is effectively complete and inviolate. This means that the metal ion sites are also removed from the aqueous solvent.

If only factors (a), (b) and (c) listed above needed to be considered in an electron transfer process and the metal coordination spheres could come into close contact with each other (or to an electrode) so that chemical redox reactions could be regarded as equivalent to simple outer-sphere reactions (or the electrode/protein interface is analogously simple) then the rate constants for both the second-order (bimolecular) homogeneous chemical and heterogeneous electrochemical redox reactions would be expected to be diffusion controlled. This would imply that k_{obs} should be $\geqslant 10^8$

M^{-1} s^{-1} (or $k_s \geqslant 1$ cm s^{-1}) with k_{et} being of the order of 10^{-10} s^{-1} or greater. However, because structural changes of the kind noted above may accompany electron transfer and the metal centres are buried so that electron transfer has to occur over considerable distances, measured electron transfer rates, although adequate for biological systems, may be relatively slow. Consequently, k_{obs} and k_s values are frequently considerably less than predicted for a diffusion controlled process.

In addition to structural features discussed above, the well recognised feature of proteins that the metal centre is buried and not at the edge has obvious implications [21] in determining observed rates of protein redox reactions. Important aspects of this feature of the protein structure include the following.

(i) Placing the metal ion just below the surface of a simple metalloprotein allows the metal redox centre to be covered by a chemical recognition zone. Typically, the electron transfer distance between the coordination spheres of two reaction redox protein centres which are separated by the chemical recognition zone is in the range of 10 Å. Electron transfer occurs over distances of this order via the chemical recognition zone.

(ii) The metal ion redox centre of one protein is specifically oriented towards one quadrant edge of another roughly spherical electron transfer protein to achieve an electron transfer distance of 10 Å with this edge. The electron transfer distances to all other quadrant edges exceed 15 Å.

(iii) The distance constraints in (ii) and the chemical recognition zone constraints in (i) ensure that a highly selective route is available for electrons in and out of electron transfer proteins.

(iv) Thermodynamic control (the redox potential) in proteins is generated by a complex set of factors, including the nature of the coordination sphere and the metal ion geometry, the nature of the surrounding protein lattice and the degree of exposure of the metal redox centre to the solvent. The redox potentials resulting from a combination of these factors have evolved to control the overall rates in biologically important electron transfer processes.

The influence of items (i)–(iii) in electrochemically derived data is not as well established as for chemically based electron transfer reactions since even with simple inorganic systems it has been concluded that rapid electron transfer (large k_s values) may occur at the electrode/solution interface over distances in excess of 10 Å. Discussion on the influence of the distance related terms in electrochemical kinetics will be addressed after summarising some of the data available on metalloprotein redox chemistry.

In summary, in Section 2 it has been noted that available data show that structural changes accompanying redox processes of simple electron transfer metalloproteins are usually small at the metal centre at biologically important pH values. This feature should lead to intrinsically fast rates of electron transfer. However, structural changes can be significant at the metal centre at other pH values, e.g. basic media for cytochrome *c* and acid media for plastocyanin. Furthermore, complex and dynamic rearrangements may take place in the protein lattice at distances well removed from the metal centre which may make the overall rates much slower than predicted if these features are neglected. These kind of structural (conformational) changes may have important implications in the interpretation of both chemical and electrochemical investigations of protein redox reactions where an electron has to be transferred between the outside of the protein lattice and the metal centre over substantial distances through a complex medium. In chemical redox reactions, the structures and dynamics of the protein in both the oxidised and reduced forms of the protein therefore will be important. In electrochemical studies, the electrode and the electrode/protein interfacial properties will provide an additional important factor in determining the influence of the protein structure on the measured rate of electron transfer. Unfortunately, with both homogeneous and heterogeneous methods of studying electron transfer processes, the need to deconvolute the electron transfer process from the structural changes is of paramount importance, but is either impossible or difficult to achieve in most circumstances.

3. Homogeneous chemical redox reactions involving simple electron transfer metalloproteins

Initially, most information on the mechanism of protein electron transfer reactions was based on consideration of data obtained from intramolecular electron transfer redox reactions between a simple electron transfer metalloprotein and an inorganic or organometallic complex. This class of reaction may be classified as a homogeneous chemical redox reaction between a protein and a non-physiological partner. While the relevance to biologically important electron transfer reactions is sometimes rather obscure, such reactions are valuable in understanding the mechanism of the electron transfer process because systematic variation of parameters related to charge, driving force and structure are much more readily achieved than with many other types of reaction. Commonly, a second-order rate constant (k_{obs} value) has been measured as a function of some property of the inorganic complex and conclusions reached are based on the trends in k_{obs} observed with variation in a parameter associated with the inorganic redox reagent. Less frequently, k_{et} values have been derived from this kind of reaction. An important, and inherently simpler, reaction involves the study of electron self-exchange reactions in which

electron transfer occurs between the oxidised and reduced forms of the same protein (as in Eq. (14)).

$$[\text{Cyt.c}^*]_{ox} + [\text{Cyt.c}]_{red} \rightleftharpoons [\text{Cyt.c}]^*_{red} + [\text{Cyt.c}]_{ox} \quad (14)$$

In Eq. (14), $[\text{Cyt.c}^*]_{ox}$ and $[\text{Cyt.c}^*]_{red}$ could, for example, represent isotopically labelled forms of $[\text{Cyt.c}]_{ox}$ and $[\text{Cyt.c}]_{red}$. Alternatively, measurement of line broadening in ESR and NMR spectroscopies, when mixtures of the two oxidation states are present, may enable electron self-exchange rates to be calculated. Since an electron self-exchange reaction does not require the addition of biologically foreign reagents, these class of reactions are likely to more closely mimic the biologically important electron transfer reactions than reactions with inorganic redox reagents. As will be seen later, electron self-exchange reactions occur with virtually no free energy driving force ($\Delta G^\circ = 0$) and also exhibit features that are more akin to electrochemical processes, so data obtained from electron self-exchange reactions must be regarded as intrinsically important with respect to concepts presented in this review.

Studies of electron transfer reaction involving two proteins that are non-physiological partners, for example, cytochrome *c* and cytochrome b_5, represent a further progression towards the study of biologically important electron transfer reactions as do studies in buffered aqueous media between physiological partners. However, until the advent of site directed mutagenesis, studies of this kind, in contrast to studies of metalloproteins with inorganic complexes, did not readily allow systematic variation of the redox properties of the proteins to be achieved. Somewhat ironically therefore, studies on the most biologically relevant intermolecular electron transfer reactions initially were perceived to be of limited value in probing the fundamental parameters that contribute to the rates and the mechanisms of metalloprotein redox reactions.

In the last ten years, investigations of intramolecular electron transfer reactions between two proteins contained within a protein–protein complex or between a protein redox centre and an inorganic or organometallic complex attached to the protein surface have become more favoured as a means of studying protein electron transfer reactions than have homogeneous intermolecular reactions because of the presumed if not always realised simplifying features noted in Section 1. The possibility of separating the electron transfer step from solution diffusional considerations enables attention to be focussed on the influence of distance and the intervening atomic linkages or medium within the protein on the rates of electron transfer. Additionally, the relative orientation of the two redox active metal centres to each other may be studied. However, changes in the protein lattice of the kind described in Section 2 for cytochrome *c* will still occur in the intramolecular electron transfer reactions so that all the complexities and ambiguities need not necessarily be completely eliminated in these kinetic studies. Since problems still remain in interpreting all forms of protein electron transfer reaction, a critical survey of the contribution of both the inter- and intramolecular studies of homogeneous electron transfer reactions of metalloproteins is presented in this section.

3.1. Electron transfer reactions between metalloproteins and inorganic complexes

Commonly, the mechanism assumed to apply in studies of homogeneous chemical redox reactions between metalloproteins and small inorganic molecules in buffered aqueous media is represented by a sequence of the kind given in Eqs. (4)–(6) in which a precursor complex is formed prior to the electron transfer step. Unfortunately, the only kinetic data usually reported in these studies is the second-order (k_{obs}) rate constant (see Section 1). However, if the precursor complex reaction (Eq. (4)) preceding the electron transfer step can be assumed to be an equilibrium reaction with an equilibrium constant K_1 and the electron transfer step is rate determining, then analysis of the data may be based on Eq. (15)

$$k_{obs} = K_1 k_{et} \quad (15)$$

where $K_1 = k_1/k_{-1}$ using the nomenclature given in Eq. (4). In principle the value of k_{et} therefore could be calculated if K_1 is known. However, again unfortunately, even when K_1 is known, its precision and/or accuracy is often very poor so that values of k_{et} obtained from Eq. (15) via intermolecular electron transfer reactions are often unreliable. Consequently, mechanistic conclusions based on reactions between metalloproteins and inorganic complexes are generally based on the systematic variation of the second-order k_{obs} value observed when a relevant parameter of the inorganic complex is varied, rather than on a knowledge of k_{et} values.

A distinguishing feature of metalloproteins which has been shown to be important in intermolecular electron transfer reactions with inorganic compounds, is the very high but asymmetrically distributed overall charge (either positive or negative) that some proteins possess relative to simple inorganic complexes which usually possess overall charges in the range of +3 to −3. For example, cytochrome *c* basically has an overall charge in the range of +7 to +8 at neutral pH, whereas plastocyanin has an overall charge of around −9 and ferredoxin around −19. The exact value of the overall charge is of course dependent on the origin of the species from which protein is isolated and the solution pH value. The charge distribution is frequently very uneven, as indicated, for example, by the dipole movement of around 300 D for cytochrome *c* so that reactivity–charge relationships need not be and indeed

often are not straightforward. Some of the available charge and dipole movement data are summarized in Table 1. Metalloprotein acid–base equilibria (pK_a values) are also frequently important and may influence the overall charge present on the protein. The pH value therefore may be an important parameter in determining the thermodynamics and rates of redox reactions involving metalloproteins, as may the ionic strength when studying reactions of highly charged metalloproteins. Ideally, the dependence on pH and ionic strength should be included in discussion of rate data, but only rarely are these factors considered and accounted for in detail.

In view of the high and asymmetric charge distribution in many proteins, it is not surprising that chemical redox reactions of proteins with inorganic oxidants or reductants of widely varying charge have formed a significant fraction of the systematic studies of this class of reaction and, despite the limited number of k_{et} values available from these studies and a paucity of knowledge of the pH and ionic strength dependence, a good deal of valuable information has been obtained concerning the importance of the charge.

3.1.1. Cytochrome c

Electron transfer reactions of cytochrome *c* with inorganic complexes are governed predominantly by the high overall positive charge resulting from the presence of lysine residues, the asymmetric charge distribution (Table 1) and, although not considered to any significant extent in the literature, presumably by any substantial structural rearrangement of the protein lattice that accompanies the redox reactions.

Table 1
Overall charges and dipole moments of some simple redox active metalloproteins at around pH 7 [a]

Metalloprotein	Charge	Dipole moment (D) [b]
Cytochrome *c*	+7.5 (oxidised)	287
	+6.5 (reduced)	267
Cytochrome c_{551}	−2 (oxidised)	150
	−3 (reduced)	120
Cytochrome b_5	−7.5 (oxidised	−265
	−8.5 (reduced)	−305
Plastocyanin	−8 (oxidised)	
	−9 (reduced)	
[2Fe–2S] ferredoxin	−18 (oxidised)	
	−19 (reduced)	

[a] Values of the parameters reported in this Table are very protein source, media, pH, temperature, technique, calculation method and data source dependent. Values given in this Table are derived from values reported in articles by D.W. Dixon and X. Hong (*Adv. Chem. Ser., 226* (1990) 161) and A.G. Sykes (*Adv. Inorg. Chem., 36* (1991) 377; *Met. Ions Biol. Syst., 27* (1991) 291) and are only provided in this review for use in qualitatively developing arguments. If values of these parameters are required for quantitative calculations or other purposes, the above-mentioned articles and the original publications need to be very carefully consulted.

[b] Average values given (where available) from data obtained by calculations based on X-ray structures and kinetic measurements.

Studies have involved both reduction of [Cyt.c, Fe(III)] as in Eq. (16)

$$[\text{Cyt.c, Fe(III)}] + \text{reductant} \longrightarrow \text{products} \quad (16)$$

and oxidation of [Cyt.c, Fe(II)] as in Eq. (17)

$$[\text{Cyt.c, Fe(II)}] + \text{oxidant} \longrightarrow \text{products} \quad (17)$$

In the main, only second-order rate constants, k_{obs}, obtained from fitting data to the rate law (18) are

$$\text{Rate} = k_{obs}[\text{Cyt.c}][\text{inorganic complex}] \quad (18)$$

available for both the oxidation and reduction directions of the electron transfer reaction [2,22]. Table 2 contains some of the available data on second-order k_{obs} values for reactions of cytochrome *c* with inorganic complexes.

The data in Table 2 suggest that the redox chemistry of cytochrome *c* is complicated. For example, over the pH range 5–8, k_{obs} is a function of pH for oxidation of [Cyt.c., Fe(II)] with some inorganic complexes, but usually independent of pH for reduction of [Cyt.c, Fe(III)]. Obviously, the k_{obs} values in Table 2 are therefore not simply related to k_{et}. However, the importance of charge may be said to be revealed by the much higher overall oxidation rates noted in Table 2 for the oxidation of [Cyt.c, Fe(II)] by inorganic anions rather than cations.

Extensive studies of redox reactions with a wide range of inorganic compounds suggest that at least three sites [2,22] are available on cytochrome *c* for formation of the precursor complex and that different sites are used for binding of cationic and anionic inorganic redox reagents. Site I is positively charged and postulated to include residues Met65 and Lys89, 5, 86, 8. Site II includes Val11, Ala15, Thr19, Lys7, 25, 27 and site III may include residues Ile81, Phe82, Ala83, and Lys 13, 72, 86. The postulate of site specific reaction sites provides an explanation of how positively charged inorganic complexes can react with positively charged proteins such as cytochrome *c* at quite fast rates. That is, despite the very positive overall charge, the asymmetric distribution of charge may allow sites to be available for formation of a precursor complex where electrostatic repulsion terms are minimal. Thus, cationic oxidants such as $[Co(phen)_3]^{3+}$ are believed to interact mainly at site II because of the presence of negatively charged Glu21 and the relative paucity of positively charged side-chains in this region. In contrast, sites I and III which contain positively charged groups are very suitable for formation of precursor complexes with anionic redox complexes including physiological protein partners (see later). The 'intelligence' associated with the redox chemistry of cytochrome *c* therefore may be said to have its origin in the asymmetric nature of the

Table 2
Examples of second-order k_{obs} values obtained for oxidation and reduction reactions of cytochrome *c* with a range of inorganic complexes [a,b]

Reaction	Complex	pH	E_f^0 (mV vs. NHE)	k_{obs} (M^{-1} s^{-1})
Oxidation	$[Co(phen)_3]^{3+}$	8.0	370	1.8×10^3
	$[Co(phen)_3]^{3+}$	5.0		1.1×10^3
	$[Co(terpy)_2]^{3+}$	8.0	270	9.2×10^2
	$[Co(terpy)_2]^{3+}$	5.0		6.3×10^2
	$[Fe(CN)_6]^{3-}$	5–8	410	9.0×10^5
	$[Co(dipic)_2]^-$	5–8	747	1.0×10^4
Reduction	$[Co(terpy)_2]^{2+}$	5–8		1.0×10^3
	$[Ru(NH_3)_5(py)]^{2+}$	5–8	253	4.1×10^3
	$[Co(sep)]^{2+}$	5–8	−260	3.4×10^5

[a] Data mainly reproduced from results reported in Refs. [2] and [22] which should be consulted for exact details of experimental conditions and techniques used.
[b] Relevant points of footnote a in Table 1 should be noted when considering these data.
[c] phen = phenanthroline, terpy = terpyridine, dipic = dipicoline, py = pyridine, sep = sepulchrate.

charge distribution which enables positively charged cytochrome *c* to react at a significant rate even with highly positively charged redox reagents via the existence of a pathway that provides shielding of the unfavourable overall positive charges on both of the redox reagents.

The considerable complexity of the redox reactions between cytochrome *c* and inorganic redox reagents and the difficulty in using k_{obs} values in a simple manner to understand the chemical significance of the rate of electron transfer is further confirmed by the studies of Rush et al. [23] who showed that at low ionic strength, oxidation of [Cyt.c, Fe(II)] by $[Co(bpy)_3]^{3+}$ and $[Co(phen)_3]^{3+}$ is independent of the concentration of the complex and effectively much faster than the second-order process observed at higher ionic strengths. In order to explain the variation in data obtained as a function of ionic strength it was proposed by the authors of Ref. [23] that at low ionic strengths an open conformational form of cytochrome *c* exists with an accessible heme crevice which reacts much faster than a closed form which may be dominant at high ionic strengths after a cation binds to the open form. If the conformational form of the precursor complex is a function of ionic strength then the enhancement in rate of oxidation of [Cyt.c, Fe(II)] at low ionic strength would be explicable if the reorganisational energy in the Fe(II) to Fe(III) process is effectively lowered by the change in conformation from a closed to an open form. This hypothesis also is consistent with remarks made earlier, viz. that it need not only be the structure directly around the metal centre that influences the rate and mechanism and that conformational changes in the protein lattice may be an important structural feature which determines the kinetic behaviour.

Table 2 also includes E_f^0 data for the inorganic oxidants which is a measure of the thermodynamic driving force for the reactions involved. However, given the complex nature of the dependence of k_{obs} on pH, ionic strength and charge it would be optimistic to apply a Marcus type treatment of k_{obs} on driving force for what are certainly not simple outer-sphere reactions. The reality is that second-order k_{obs} values are probably a composite value of a set of complex rate constants reflecting structural change, pK_a values, charge and binding site in addition to the rate of electron transfer. In any given series of reactions with a range of inorganic complexes, the binding sites and hence the electron transfer distances, as well as the charges, are all likely to vary. However, as data in Table 2 reveal, at least for the reaction of cytochrome *c* with $[Co(phen)_3]^{3+}$ and $[Co(terpy)_2]^{3+}$ where the charges and presumably the binding site are constant, the rate constant k_{obs} does in fact increase with an increase in ΔG° (i.e. the more positive E_f^0 for $[Co(phen)_3]^{3+/2+}$ system correlates with the observation of a larger value of k_{obs}) and so the expected influence of both charge and ΔG° are both probably important in the second-order rate constants, but are masked by contributions of many other terms to measured values of k_{obs}.

3.1.2. *Plastocyanin*

Many electron transfer reactions of the blue copper protein plastocyanin with inorganic complexes have been reported [2,15] that are analogous to those discussed above for cytochrome *c*. However, the opposite sign of the charge on plastocyanin relative to cytochrome *c* makes for an interesting comparison of the two data sets. In the higher plant plastocyanins, the His37, His87, Cys84 and Met92 residues provide the coordinating groups for copper. A structural representation of plastocyanin is given in Fig. 2 and as for cytochrome *c* considerable asymmetry exists in the charge distribution so that again it has been postulated that cationic and anionic inorganic redox reagents may utilise different binding sites. For example, the binding site of negatively charged $[Fe(CN)_6]^{3-}$ is believed to be His87 in the

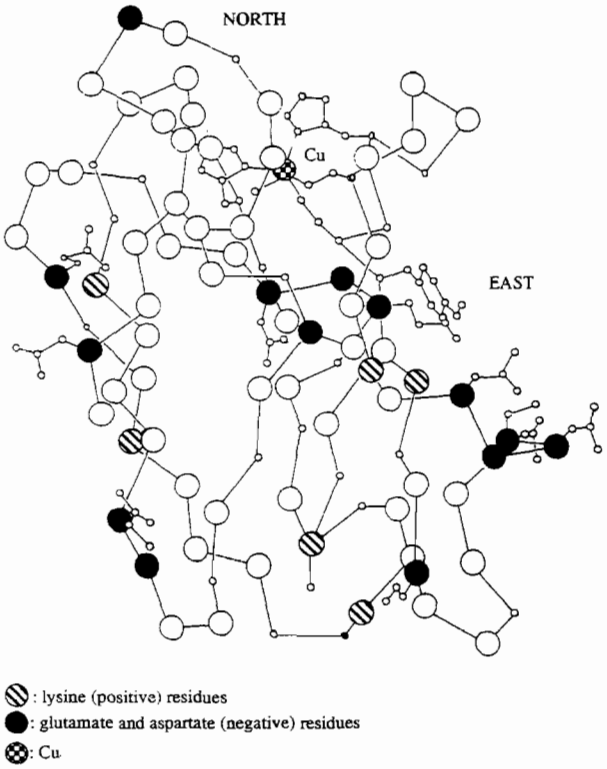

Fig. 2. Structural features of poplar [Pc, Cu(II)] as derived from X-ray crystallographic data. Reproduced by courtesy: *J. Mol. Biol., 169* (1983) 521.

'north' site region whereas positively charged complexes such as $[Cr(phen)_3]^{3+}$ and $[Co(phen)_3]^{3+}$ are believed to bind to the 'east' site. Remarkably, the anionic redox reagents, despite their apparently unfavourable charge for a redox reaction with negatively charged plastocyanin, appear to bind at the His87 residue which, as noted above, also contains one of the Cu ligands and therefore allows an approach to within 6 Å of the Cu atom. On the other hand, cationic species such as $[Cr(phen)_3]^{3+}$, $[Co(phen)_3]^{3+}$, ferrocenium complexes and indeed cytochrome *f*, which are believed to bind at the negative 'east' site patch of active residues 42–45 which is close to Tyr83 (see Fig. 2), are therefore bound at a further distance from the Cu centre than when redox processes of plastocyanin occur with an anion. The close approach possible for formation of the precursor complex in reactions of like-charged species presumably explains how fast reaction rates can still be obtained for redox processes involving negatively charged plastocyanin with negatively charged inorganic redox reagents. Data in Table 3 summarise some of the second-order rate constant data and an interesting feature is that despite the highly negative overall charge associated with higher plant plastocyanins, the second-order rate constants for reaction with both negatively charged $[Fe(CN)_6]^{3-}$ and positively charged $[Co(phen)_3]^{3+}$ are of similar value and moderately fast, and indeed, not too dissimilar to rates observed for reaction of the same inorganic redox reagents with positively charged cytochrome *c*.

As is the case with cytochrome *c*, second-order k_{obs} values for reaction of plastocyanin with simple inorganic redox reagents exhibit a considerable dependence on pH. In particular, rates are reported to be slower at low pH where [Pc, Cu(I)] becomes three-coordinate (see Eq. (11b) and earlier discussion). In summary, despite the lack of significant structural changes in changing from [Pc, Cu(II)] to [Pc, Cu(I)] simple relationships of k_{obs} with various parameters associated with inorganic redox reagents are still difficult to unravel as reported values appear to be a complex function of several variables.

3.1.3. [2Fe–2S] ferredoxins

The redox chemistry of negatively charged [2Fe–2S] ferredoxins has been extensively studied from many perspectives [24]. However, because of the two metal centres versus one in plastocyanin and cytochrome *c* there are some interesting differences with the previously discussed proteins. In the oxidised form (Fig. 3), the two non-heme Fe(III) centres of [2Fe–2S] ferredoxins are bridged by two sulfides, and the tetrahedral coordination at each iron centre is completed by cysteine residues (RS^-) to give a complex which may be formulated as $[Fe_2S_2(SR)_4]^{2-}$. On reduction, one of the Fe(III) centres is reduced to Fe(II) to give $[Fe_2S_2(SR)_4]^{3-}$ so that despite the presence of two metal centres, [2Fe–2S] ferredoxin proteins function as one-electron transfer reagents as do cytochrome *c* and plastocyanin. The two redox states are also commonly referred to as $[Fe_2S_2]^{2+}$ and $[Fe_2S_2]^{+}$ and in this form of notation the redox process can be written as

$$[Fe_2S_2]^{2+} + e^- \rightleftharpoons [Fe_2S_2]^{+} \quad (19)$$

X-ray structures have been determined for *Spirulina platensis* and *Apolothece sacrum* $[Fe_2S_2]^{2+}$ ferredoxins [24]. Despite a 30% difference in the residue sequences, the two structures have a common main chain fold. Importantly, from the point of view of electron transfer reactions, it should be noted that the two Fe atoms are located within 5 Å of the accessible surface. Structural information on the reduced $[Fe_2S_2]^{+}$ form is limited but as for plastocyanin and cytochrome *c* available evidence suggests that the structure around the iron centre is very similar to that in the oxidised from. Spectroscopic data indicate that it is the Fe nearest the surface (Fe_A) and attached to residues Cys41 and Cys46 (see Fig. 3) which is reduced, with the implication being that the $E°$ value for the other iron (Fe_B) is considerably more negative than $E°$ for Fe_A.

Given the extremely high overall negative charge on many ferredoxins (Table 1), it is not surprising that reactions of reduced $[Fe_2S_2]^{+}$ with inorganic oxidants

Table 3
Examples of second-order k_{obs} values obtained for reduction of different copper(II) plastocyanins with inorganic complexes and *Brassica* cytochrome *f* [a]

Plastocyanin	k_{obs} (M^{-1} s^{-1})			
	$[Fe(CN)_6]^{3-}$	$[Co(phen)_3]^{3+}$ (pH 7)	*Brassica* cytochrome *f* (pH 7.5)	*Brassica* cytochrome *f* (pH 5)
Parsley	9.4×10^4	3.0×10^3	2.0×10^2	1.1×10^2
Spinach	8.5×10^4	2.5×10^3	1.6×10^2	1.2×10^2
French bean	5.8×10^4	4.7×10^3		
Poplar	6.9×10^4	2.9×10^3		
Scenedesmus obliquus	9.0×10^4	1.9×10^3		7.8×10^1
Anabena variabilis	6.5×10^5	6.8×10^2	4.0	2.8

[a] Data are reproduced from *Prog. Inorg. Chem., 38* (1990) 259; *J. Am. Chem. Soc., 109* (1987) 6443; *Inorg. Chem., 27* (1988) 2306; *Adv. Inorg. Chem., 36* (1991) 377 and presented in the same context as described in footnote b of Table 2.

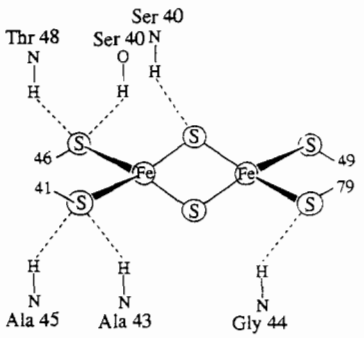

Fig. 3. Structural representation of the iron centres of *S. platensis* $[2Fe–2S]^{2+}$ ferredoxin as derived from X-ray crystallographic data. Reproduced by courtesy: *Met. Ions Biol. Syst., 27* (1991) 291; *J. Biochem., 90* (1981) 1763.

of variable charge have been of considerable interest. Table 4 summarises second-order k_{obs} data obtained with a range of cobalt(III) complexes having charges in the range −3 to +5 for oxidation of reduced parsley ferredoxin. The usual sequence of reactions given in Eqs. (4)–(6) are assumed to occur and the expected dependence of the second-order rate constant K_1k_{et} and K_1 [24] is generally established with cations and anions of variable charge, although the significant exceptions yet again illustrate the complexity of the mechanisms which lead to the reported k_{obs} values. As for plastocyanin, it may be noted from examination of the data contained in Table 4 that the rate of reaction of the negatively charged protein with an anionic oxidant is relatively fast. Data in Tables 2, 3 and 4, considered in a global context, suggest that all metalloprotein electron transfer reagents have the 'intelligence' to provide an electron transfer pathway which can accommodate what appear from an electrostatic point of view to be unfavourable interactions between highly

Table 4
Second-order k_{obs} values obtained for oxidation of $[Fe_2S_2]^+$ ferredoxin and reduction of $[Fe_2S_2]^{2+}$ ferredoxin with inorganic complexes [a]

Reaction	Complex	Protein source	k_{obs} (M^{-1} s^{-1})
Oxidation	$[(NH_3)_5CoNH_2Co(NH_3)_5]^{5+}$	parsley	5.6×10^6
	$[Co(NH_3)_6]^{3+}$	parsley	1.9×10^4
	$[Co(NH_3)_6]^{3+}$	*S. platensis*	8.4×10^3
	$[Co(NH_3)_6]^{3+}$	spinach	1.6×10^4
	$[Co(sep)]^{3+}$	parsley	6.5×10^4
	$[Co(en)_3]^{3+}$	parsley	6.0×10^2
	$[Co(NH_3)_5Cl]^{2+}$	parsley	4.1×10^5
	$[Co(NH_3)_5(C_2O)_4]^+$	parsley	5.7×10^3
	$Co(acac)_3$	parsley	4.3×10^3
	$Co(acac)_3$	*S. platensis*	3.6×10^3
	$[Co(edta)]^-$	parsley	7.2×10^3
	$[Co(edta)]^-$	*S. platensis*	4.4×10^3
	$[Co(C_2O_4)_3]^{3-}$	parsley	3.9×10^3
	$[Pt(NH_3)_6]^{4+}$	parsley	2.1×10^4
Reduction	$[Co(9\text{-}aneN_3)_2]^{2+}$	parsley	1.0×10^3
	$[Cr(15\text{-}aneN_4)(H_2O)_2]^{2+}$	parsley	1.0×10^3

[a] Data are taken mainly from Ref. [24] and were generally obtained at around pH 8.0 in 0.1 M NaCl and at 25 °C, although the primary literature cited in Ref. [24] must be consulted for complete details. Footnote b in Table 2 should also be read in conjunction with this Table.

charged species having the same sign of overall charge. Limited data from reduction of $[Fe_2S_2]^{2+}$ with inorganic reductants are also included in Table 4 and again the values are moderately fast. Data in Table 4 also show that the second-order rate constants are not particularly species-source-sensitive which is expected if the functionally relevant amino acids are conserved.

While the reliability of K_1 and k_{et} values determined from the relationship $k_{obs}=K_1k_{et}$ or more complex expressions must always be queried, K_1 for the binding equilibrium constant (Eq. (4)) and for k_{et} the first-order electron transfer rate constant (Eq. (5)) have been reported for the reaction of the $[Fe_2S_2]^{2+}$ ferredoxin with a range of inorganic oxidants. While it may be argued that trends in K_1 values contained in Table 5 reflect the charge effects, the k_{et} values which are also included in Table 5 do not appear to have any direct relationship with the driving force ($E°$ value of the chemical redox reagent). Consequently, it would be difficult to fit the rate data to a Marcus type relationship. Furthermore, k_{et} values given in Table 5 are also rather small both in the absolute sense and in comparison with values obtained for other proteins by arguably more reliable methods (see later).

Of considerable importance in understanding the mechanism of chemical redox reactions of ferredoxin are studies reporting the influence of charged redox inactive complexes on electron transfer processes. As will be shown later, analogous studies are also very important in understanding the nature of voltammetric processes. For example, data obtained with chemical redox reactions of ferredoxin suggest that some positively charged redox inactive inorganic complexes are able to associate with the very negatively charged ferredoxin at the same site as positively charged redox active reagents, and that this competitive binding reaction gives rise to a blocking mechanism for the reaction with positively charged oxidants. Fig. 4(a) demonstrates the decrease in k_{obs} when reduced parsley ferredoxin is oxidised by $[Co(NH_3)_5(C_2O_4)]^+$ in the presence of redox inactive $[Cr(NH_3)_6]^{3+}$. The data are consistent with $[Cr(NH_3)_6]^{3+}$ inhibiting the electron transfer process by competitive binding at the same site as that occupied by $[Co(NH_3)_5(C_2O_4)]^+$.

Table 5
Values of K_1 and k_{et} reported for the oxidation of $[Fe_2S_2]^+$ ferredoxin with inorganic oxidants [a]

Oxidant	K_1 (M^{-1})	k_{et} (s^{-1})	Protein source
$[(NH_3)_5CoNH_2Co(NH_3)_5]^{2+}$	26400	214	parsley
$[Co(NH_3)_6]^{3+}$	998	19.2	parsley
$[Co(NH_3)_6]^{3+}$	993	15.9	spinach
$[Co(NH_3)_6]^{3+}$	2070	4.9	*S. plantensis*
$[Co(sep)]^{3+}$	1000	65	parsley
$[Co(en)_3]^{3+}$	597	2.7	parsley
$[Co(NH_3)_5Cl]^{2+}$	194	2300	parsley
$[Pt(NH_3)_6]^{4+}$	21000	3.29	parsley

[a] See footnote a in Table 4.

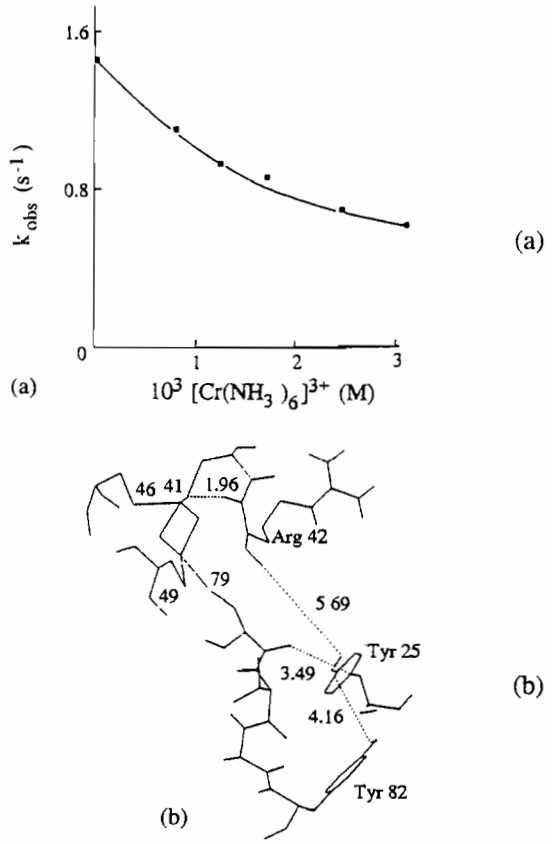

Fig. 4. (a) Inhibition of rate caused by the presence of redox inactive $[Cr(NH_3)_6]^{3+}$ on the oxidation of the reduced form of parsley $[Fe_2S_2]^+$ by a large concentration excess of $[Co(NH_3)_5(C_2O_4)]^+$. (b) Possible electron transfer paths for oxidation of $[Fe_2S_2]^+$ with a cationic inorganic oxidant when the oxidant is bound to the protein of the region around residues Tyr82 and Tyr25 and electron transfer occurs from this region to the iron active site (also see Fig. 3). Reproduced by courtesy: *Met. Ions Biol. Syst., 27* (1991) 291.

Under conditions where competitive protein binding reactions take place with redox active inorganic complex, B, and redox inactive inorganic complex, I, the simplest reaction scheme proposed [24] is

$$A + B \underset{k_{-1}}{\overset{k_1}{\rightleftharpoons}} [AB] \quad (20a)$$

$$A + I \underset{k_{-2}}{\overset{k_2}{\rightleftharpoons}} [AI] \quad (20b)$$

$$[AB] \xrightarrow{k_{et}} \text{products} \quad (20c)$$

For the reaction scheme given in Eq. (20)

$$k_{obs} = \frac{K_1 k_{et}[A]}{1 + K_1[B] + K_2[I]} \quad (21)$$

where $K_1 = k_1/k_{-1}$ and $K_2 = k_2/k_{-2}$

If the concentration of B is sufficiently low so that $K_1[B] \ll 1$, the simpler expression

$$k_{obs} = \frac{K_1 k_{et}[A]}{1 + K_2[I]} \quad (22)$$

is obtained.

In some cases the additional reaction step

$$[AI] + B \xrightarrow{k_I} \text{products} \quad (23)$$

must be included, which means the rate law is modified so that

$$\frac{k_{obs}(1 + K_2[I])}{[B]} = K_1 + k_I K_2[I] \quad (24)$$

^{1}H NMR data on the diamagnetic oxidised $[Fe_2S_2]^{2+}$ ferredoxin form of *Anabena variabilis* [24] show selective paramagnetic line broadening of the Tyr82 residue ^{1}H pair of doublets in the presence of low concentrations of redox inactive $[Cr(NH_3)_6]^{3+}$ which has been shown to inhibit the rate of oxidation of $[Fe_2S_2]^{2+}$ with redox active positively charged chemical oxidants. Other ^{1}H resonances are unperturbed under the same conditions. At higher concentrations of redox inactive $[Cr(NH_3)_6]^{3+}$, other resonances in the aromatic region of the ^{1}H section begin to broaden non-selectively. By contrast, addition of redox inactive but negatively charged $[Cr(CN)_6]^{3-}$ has no effect on the ^{1}H section in the aromatic region indicating that binding of the anion does not take place in the same region of the ferredoxin protein as is the case with cations [24].

Corresponding ^{13}C NMR experiments to the ^{1}H experiment described above [24] have also been used to monitor the reactions that occur on addition of $[Cr(NH_3)_6]^{3+}$ to *A. variabilis* ferredoxin. Changes in the 154–158 ppm region, which contain resonances of Arg and five tyrosines are observed. As the concentration of $[Cr(NH_3)_6]^{3+}$ is increased only two of the resonances assigned to Tyr82 and Tyr25 are affected. These are in fact the only two tyrosine residues close enough together to be affected by selective binding of a single $[Cr(NH_3)_6]^{3+}$ (see Fig. 4(b)). Presumably the ^{1}H resonances of Tyr25, which according to the ^{13}C data should also be affected, are not observed because this residue is too near to the Fe–S centre. Other ^{13}C resonances which are broadened should also be close to Tyr82 and Tyr25 if the NMR method is providing a probe of the binding site for cations on $[Fe_2S_2]^{2+}$ ferredoxin. One of the ^{13}C resonances which is charged by addition of $[Cr(NH_3)_6]^{3+}$ is associated with non-conserved Glu24. However, the conserved negatively charged groups which could be responsible for the binding of $[Cr(NH_3)_6]^{3+}$ include Asp22, Asp23 and Asp63. Further, acidic residues 28, 31 and 32 are close by, which would give rise to a substantially negatively charged patch in this region of the protein and therefore provide a region which constitutes a suitable binding site [24].

The data obtained for the kinetic inhibition of the reaction between $[Fe_2S_2]^{+}$ and cationic oxidants by positively charged complexes such as $[Cr(NH_3)_6]^{3+}$, coupled with the NMR data, offer strong support for the concept of selective binding of inorganic redox reagents prior to the electron transfer step. The cationic inhibitors $[Cr(NH_3)_6]^{3+}$ and $[Cr(en)_3]^{3+}$ when present at sufficient concentration appear in fact to be capable of completely blocking the redox reaction of cationic oxidants with $[Fe_2S_2]^{+}$. A logical interpretation of this result [24] is that these redox inactive complexes effectively compete for the same binding site as the redox active cation, but of course provide a bound AI form of complex which is assumed to be redox inactive. This suggests that in the case of inhibition by $[Cr(NH_3)_6]^{3+}$ and $[Cr(en)_3]^{3+}$, both the cationic oxidant and cationic inhibitors have specificity for the same sites. However, the same cationic complexes only partially inhibit the reaction of $[Fe_2S_2]^{+}$ with neutral inorganic oxidants such as $Co(acac)_3$, $Co(NH_3)_3(NO_2)_3$ and $Co(acac)_2(NH_3)(NO_2)$. Furthermore, when $[Co(edta)]^{-}$ is used as the oxidant, acceleration of the reaction is observed in the presence of $[Cr(NH_3)_6]^{3+}$ and $[Cr(en)_3]^{3+}$ which suggests that Eq. (23) involving oxidation of the AI complex may be important in this particular case. The logical conclusion reached from consideration of this data is that inorganic oxidants of different charges are bound to different sites [24]. Thus inhibition by a cation is predicted for positively charged, but not for negatively charged oxidants. Data of this kind are difficult to quantify because of the range of reaction pathways available. Furthermore, with mixtures of anionic oxidants and positively charged redox inactive inhibitors, the association of the cations and anions themselves needs to be taken into account. Nevertheless, these kind of data demonstrate the importance of charge and binding sites in the overall rate and reaction pathways of proteins like ferredoxin that are highly but asymmetrically charged.

From the NMR data and knowing that paramagnetic line-broadening effects are dependent on distance to the inverse sixth power, it can be concluded that a specific interaction with cationic oxidants occurs in the vicinity of the Tyr82 and Tyr25 residues in the oxidation of ferredoxin. With this information, a question that has been asked is what is the electron transfer pathway from this region of the protein to the metal centre. Alternatively, it is also possible that distance, driving force and reorganisational energy are the main determinants of biological electron transfer rates [6]. However, if one accepts that the pathway is important, then there is generally a number of feasible pathways for electron transfer in proteins. Routes through peptide bonds often involve so many bonds that it is difficult to see how they can be effective pathways. Feasible electron transfer routes in ferredoxin have been obtained

by computer graphics using the crystal structure data [25] and are indicated in Fig. 4(b). It is assumed that Tyr82 and Tyr25 are sufficiently close to readily transmit electrons from one to the other. While there is no direct through-atom link between Tyr25 and the metal centre site coordinated by Cys42, Cys46, Cys49 and Cys79, H bonds and small through-space jumps may be used to provide shortcuts. The most favourable route [25] is likely to consist of a 3.49 Å through-space electron transfer between the aromatic ring of Tyr25 and the carbonyl of Cys79, followed by four through-bond electron transfers over a distance of 9.35 Å from Tyr25 to S(Cys). Rapid electron transfer to or from the S of Cys79 via Fe_B (inner) to Fe_A (outer) is assumed. An alternative route [25] has a through-space electron transfer distance of 5.69 Å from the phenolic group of Tyr25 followed by transfer of the electron through four bonds and an additional through-space distance of 1.96 Å (or an extra 3.21 Å via a through-bond route) from the NH of Arg42 to the S of Cys41 to give a total electron transfer distance of 12.9 Å. This route is less strongly favoured because the 5.69 Å 'through-space' electron transfer distance is not only large but is 'through solvent'. A further through-bond route from Tyr82, via residues 81 and 80 to Cys79 involving 13 bonds and a distance of 19.0 Å to S(Cys), seems even less realistic. From this analysis, and electron transfer pathway via Tyr82, Tyr25, to Cys79 is considered the most likely route [25]. However, as noted in an overview of the debate on long-range electron transfer in biologically important molecules [6], it may be the distance that is the most important factor in determining the rate. That is, exactly which rate, distance and pathway models should be used to interpret data in the theoretical sense is not yet completely clear.

3.2. Electron self-exchange reactions

The second-order electron self-exchange rate constants between the oxidised and reduced forms of the protein molecule (Eq. (14)) are of special significance because the thermodynamic driving force ($\Delta G°$) is zero and thus there is no net driving force. This feature provides a significant simplifying feature in interpreting electron transfer data and makes the reactions more closely related to electrochemically determined heterogeneous charge transfer rate constants that are calculated at the reversible potential. Differences in electron self-exchange rate constants should therefore arise solely from differences in electrostatic, geometric and reorganisational characteristics of the proteins. Protein electron self-exchange rates are usually measured by NMR and ESR line-broadening techniques and some of the available data are contained in Table 6.

Values of the electron self-exchange rate constant for proteins cover a range of at least six orders of magnitude from 10^2 to 10^8 M^{-1} s^{-1}. In the case of ferredoxin, mixtures of the two redox states of the protein give separate NMR responses, implying that the rate constant for electron self-exchange is too slow to be measured on the NMR time scale. The slow self-exchange rate for ferredoxin is not unexpected in view of the high charge estimated at −18 and −19 on the oxidised and reduced forms. From an electrostatic point of view these high charges would make it difficult for the two forms of the protein to form a precursor complex. Similarly, the slow electron transfer self exchange rate constant for plastocyanin may be explained by the large negative charge. However, interestingly, addition of the redox inactive cations such as $Co(NH_3)_6^{3+}$, Mg^{2+} or K^+ increases the self-exchange rate constant significantly, presumably because the cations have the ability to screen the effect of the negative charge.

The importance of charge may also be seen within the cytochrome *c* family. For example, the highly positively charged cytochrome *c* (+7.5 in the oxidised form) has a self-exchange rate constant around 10^4 $M^{-1}s^{-1}$. In contrast both *P. aeruginosa* and *Pseudomonas stutzeri* cytochrome c_{555} which have much lower and oppositely signed estimated charges of −2 in the oxidised form have much faster rate constants around 10^7 M^{-1} s^{-1}. Consequently, as is the case with reactions of proteins with inorganic redox reagents, some features of the electron self-exchange results demonstrate the importance of the charge of the protein. However, arguably, the rate–charge relationship is more readily detected because of the simplifying feature of zero driving force and the nulling effects of structure and other changes caused by the structural symmetry features present in both sides of Eq. (14).

A slow rate of electron self-exchange is also expected for two ions of different geometry since considerable reorganisational energy accompanies the electron transfer process. As noted in Section 1, the geometry around the metal is highly conserved in the different oxidation states of simple metalloproteins. On this basis, it may be explained why self-exchange rate constants for blue copper proteins are much faster than the estimated value of 10^{-5} M^{-1} s^{-1} for the electron self-exchange reaction between aquated Cu^{2+} and Cu^+. In the protein complex, virtually no structural change accompanies electron transfer whereas for the aquated copper ions a considerable change from distorted octahedral to tetrahedral geometry takes place which requires a reorganisation energy.

Dixon and Hang [26] have reviewed the electron self-exchange data available on the cytochrome *c*, c_{551} and b_5 proteins and elegantly demonstrate how this kind of data may be used to probe some of the factors that control electron transfer rates. For a bimolecular

Table 6
Electron self-exchange rate constants, k_{se}, of some metalloproteins [a]

Protein	k_{se} (M^{-1} s^{-1})
Horse heart cytochrome *c*	5×10^4
Cytochrome b_5	2.6×10^3
Pseudomonas aeruginosa cytochrome c_{551}	1.2×10^7
Pseudomonas mendocina cytochrome c_{551}	10^6–10^7
Pseudomonas stutzeri cytochrome c_{551}	4×10^6
Cytochrome b_{562}	4×10^6
Desulfovibrio vulgaris cytochrome c_{553}	slow
Desulfovibrio desufuricans cytochrome c_{553}	slow
Paracoccus denitrificans cytochrome c_{550}	1.6×10^4
Alcaligenes faecalis cytochrome c_{554}	$\sim3\times10^8$
[2Fe-2S] ferredoxin	slow
Spinach plastocyanin (pH 6)	slow ($<3\times10^3$)
Spinach plastocyanin (pH 6 with 8 mm $[Co(NH_3)_6]^{3+}$	7×10^4
Spinach plastocyanin (pH 6 with 20 mM $MgCl_2$)	2.7×10^4
Spinach plastocyanin (pH 6 with 0.1 M KCl)	4×10^3
Parsley plastocyanin (pH 7.5)	3.3×10^3
Anabaena variabilis plastocyanin (pH 7.5)	5.9×10^5
Rhus vernicifera stellacyanin	1.2×10^5
Pseudomonas aeruginosa azurin	9.6×10^5
Alcaligenes denitrificans azurin	4.0×10^5
Thiobacillus versutus amicyanin	1.3×10^5

[a] Data selected from *Adv. Inorg. Chem., 36* (1991) 377; *Adv. Chem. Ser., 226* (1990) 161; *Met. Ions Biol. Syst., 27* (1991) 291; *J. Chem. Soc., Dalton Trans.,* (1992) 2149. Data are presented in the same context as noted in relevant parts of footnote a of Table 1.

electron self-exchange reaction, the rate constant, k_{se} [5,26] can be written as

$$k_{se} = SK_a\nu_n K_{el} \exp\frac{\Delta G^*_r}{RT} \quad (25)$$

where S is the steric factor which in the case of proteins is assumed to reflect the extent to which electron transfer occurs at the exposed heme edge, K_a is the association constant for the formation of the transition state complex, ν_n is the nuclear frequency factor, K_{el} is the average probability of passing from the transition state to products, ΔG^*_r is the sum of the inner- and outer-sphere reorganisational free energies, R is the universal gas constant and T the absolute value of the temperature.

Table 7 summarises some of the results of calculations which have led to the various parameters in Eq. (25) being identified for cytochrome *c*, cytochrome c_{551} and cytochrome b_5. In calculating S, the steric factor, it is assumed that electron transfer occurs mainly through the exposed heme edge, so the fraction of the protein surface needs to be calculated and is included in Table 7 [26]. Since these calculations are based on a static model, as noted earlier the cytochromes are dynamic molecules with the heme opening and closing on the NMR time scale, some uncertainty may exist in the interpretation of the values obtained. The association constant K_a is calculated from the effective volume over which the reaction occurs multiplied by an electrostatic work term $\exp(-\omega_r/RT)$ [5,26] or

$$K_a = 4\pi Nr^2\delta(r)\exp\left(\frac{-\omega_r}{RT}\right) \quad (26)$$

where N is the Avogadro constant, r is the sum of the radii of the two electron transfer proteins, $\delta(r)$ is the range of intermolecular separation that contributes significantly to the rate (assumed to be 1.1 Å) and ω is the work required to bring the two proteins into the proper geometry for electron transfer. However, the K_a values calculated this way are only approximate because specific features of the protein surface are not taken into account. The terms required for calculation of K_a are also included in Table 7 as they are required for subsequent discussion. For calculation of $\nu_n K_{el}$ the expression $\nu_n K_{et} = 10^{13}\exp[-\beta(d-d_0)]$ was used, where d_0, taken as 3 Å, is the value of d (the distance between the two hemes in the electron transfer complex) at which K_{el} equals 1 and β is a system-dependent constant (see later) taken as 0.9 $Å^{-1}$ [26]. However, this value of β may not be completely appropriate on the basis of data now available as will be seen in a later discussion.

Since protein self-exchange electron transfer reactions commonly occur between species that are highly charged, rates are expected to be dependent on ionic strength. Theoretical models which assume that the electrostatic interactions are a result of the dipole moments and charges on the proteins (Table 1) enable the rate constant to be calculated as a function of ionic strength [26]. Values of k_{se} calculated from data obtained from the structural model extrapolated to zero ionic strength are also included in Table 7.

Table 7
Parameters obtained at 25 °C with an ionic strength of 0.1 M from cytochrome electron self-exchange data, and use of Eq. (25) and related equations presented in the text and in Ref. [26]

Parameter	Cytochrome *c*	Cytochrome c_{551}	Cytochrome b_5
Heme fraction surface area	0.007	0.012	0.038
Steric factor	0.0012	0.0036	0.0361
Radius (Å)	16.6	14.4	15.9
$4\pi r^2 N\delta(r)$ (m^{-1})	9.27	6.98	8.50
Work (kcal mol^{-1})	2.7	0.30	3.1
K_a (M^{-1})	0.097	4.2	0.045
Heme–heme distance (Å)	8.9	8.6	7.5
$K_{el}=\exp(-\beta(d-d_0)$	4.9×10^{-3}	6.5×10^{-3}	1.7×10^{-2}
$SK_a\nu_n\kappa_{el}$	5.9×10^{6}	9.8×10^{8}	2.9×10^{8}
k_{se} (exp.)	5.1×10^{3}	5.1×10^{6}	2.7×10^{3}
k_{se} (extrapolated to zero ionic strength)	5.1×10^{5}	2×10^{7}	6.9×10^{5}
ΔG_r^* (kcal mol^{-1})	4.2	3.1	6.85
λ (eV)	0.72	0.54	1.2
λ (kcal mol^{-1})	17	12	28

If the values of k_{se} are known from experiment and the values of the parameter S, K_a and $\nu_n K_{el}$ are estimated using the concepts described above, then ΔG^*_r may be calculated from Eq. (25). Furthermore, since for a self-exchange reaction [26]

$$\lambda = 4\Delta G^*_r \quad (27)$$

values of λ may be calculated where λ is the reorganisational energy of the reaction. Reorganisation energies based on the use of steric factor given in Table 7 are 0.72, 0.54 and 1.2 eV for cytochrome *c*, c_{551} and b_5, respectively, but they are strongly dependent on the value of the steric factor used [26]. For example, if the fraction of the surface area that is heme squared is used as the steric factor, as would be the case if electron transfer were to occur only through the exposed heme edge, instead of the values given in Table 7, the calculated λ values would be 0.4, 0.2 and 0.9 eV for cytochrome *c*, c_{551} and b_5, respectively [26].

Within the limitations for the model summarised by Eq. (25), the very fast rate of electron self-exchange for cytochrome c_{551} relative to cytochrome *c* and cytochrome b_5 is explained as resulting from the smaller reorganisational energy for cytochrome c_{551} [26]. The absolute magnitude of the electron self-exchange rate constant of around $10^7\ M^{-1}\ s^{-1}$ approaches the diffusion controlled value and is consistent with this concept. The diffusion controlled value if cytochrome c_{551} was considered to be equivalent to a simple inorganic complex is expected to be about $5\times10^9\ M^{-1}\ s^{-1}$ [26]. However, since only a small percentage of the surface area is reactive, then it may be considered that the cytochrome c_{551} electron self-exchange rate actually occurs at an essentially diffusion controlled rate as predicted when there is no significant energy barrier or reorganisational energy associated with an electron transfer process.

Data in Table 7 also enable the self-exchange rates for cytochrome c_{551} relative to cytochrome *c* to be qualitatively explained [26] according to the theoretical model described above. Cytochrome c_{551} is a smaller protein then cytochrome *c*, with a more exposed heme and a closer heme-edge to heme-edge distance in the complex (Table 7) as well as a small net charge and smaller dipole moment. All of these factors, which are incorporated into the pre-exponential term ($SK_a\nu_n K_{el}$) of Eq. (25) indicate that the electron transfer rate for cytochrome c_{551} should be about 170 times larger than for cytochrome *c*. Experimentally, the value obtained of $5.1\times10^6\ M^{-1}\ s^{-1}$ is three orders of magnitude faster than the value of $5.1\times10^3\ M^{-1}\ s^{-1}$ found for cytochrome *c*. According to the model the differences in the theoretically predicted (170) and experimentally determined (1000) factors therefore are attributable to the differences in the experimental free energy terms (reorganisational energy) which is lower for cytochrome c_{551} [26].

In comparing cytochrome *c* with cytochrome b_5 it can be noted that the two proteins are very similar in size, net charge and net dipole moment. However, the heme is more exposed in cytochrome b_5 which leads to a larger *S* factor for this protein. Additionally, the two hemes are able to get closer in the cytochrome b_5–cytochrome b_5 complex than in the cytochrome *c*–cytochrome *c* complex which leads to a larger value of $\nu_n K_{el}$ for cytochrome b_5, so that both the *S* and $\nu_n K_{el}$ factors lead to the prediction of a faster rate constant for cytochrome *c* than for cytochrome b_5 [26]. On this basis, the pre-exponential Eq. (25) in fact would lead to a prediction of a 50-fold increase in the rate for cytochrome b_5. The experimental values are in fact about equal which in terms of the model represented by Eq. (25) leads to the conclusion that the reorganisational energy for cytochrome b_5 is larger than for cytochrome *c*, although the reason why this should be

the case is not completely clear [26]. However, it can be noted that changes in the water solvent structure which occur when cytochrome *c* is involved in a redox process with another protein have been neglected in all of the above calculations and this feature is expected to be important as noted in an earlier discussion.

Sykes and co-workers [27] have also extensively discussed self-exchange protein–protein cross-reactions involving acidic and basic plastocyanins, cytochrome *f* and azurin. The high reactivity of cytochrome *f* and the importance of the properties of the basic *Anabena variabilis* plastocyanin relative to other plastocyanins were noted. Application of the Marcus theory enabled the self-exchange rate constants for acidic parsley (3.3×10^3 M^{-1} s^{-1}) and the basic *A. variabilis* (5.9×10^5 M^{-1} s^{-1}) plastocyanins to be calculated and the expected influence of the very different overall charge on the [Pc, Cu(II)]–[Pc, Cu(I)] self-exchange, estimated as -8, -7 in the case of parsley and $+1$, $+2$ for *A. variabilis*, is observed [27]. A mechanism for electron transfer involving contact of adjacent hydrophobic regions on the two plastocyanin surfaces giving a Cu···Cu separation of 12–14 Å was proposed [27]. Again emphasising the influence of charge, it was found that rate constants for the [Cyt.f, Fe(II)] reduction of four [Pc, Cu(II)] plastocyanins (acidic parsley, spinach, *Scenedesmus obliquus* and basic *A. variabilis*) are a factor of $\approx10^2$ less in the case of the basic form. The rate constant for *Pseudomonas aeruginosa* azurin with cytochrome *f* was also determined. Interestingly, the *A. variabilis* and azurin rate constants gave a [Cyt.f, Fe(II)[–[Cyt.f, Fe(III)] self-exchange of 5.0×10^5 M^{-1} s^{-1} whereas that obtained from the cross-reaction with the more highly charged parsley [Pc, Cu(II)] (2.3×10^8 M^{-1} s^{-1}) requires correction for the work terms, and is predictably out of line. Only one out of four cross-reactions of *A. variabilis* plastocyanin and azurin with $[Co(phen)_3]^{3+}$ (phen = 1,10-phenanthroline) and $[Fe(CN)_6]^{3-}$ provide a satisfactory fit to the Marcus theory [27]. This was attributed to the influence of a more localised protein charge on these reactions and further demonstrates the difficulty of applying the Marcus theory to the complex electron transfer data.

3.3. Electron transfer in protein–protein complexes

Redox active protein–protein complexes which participate in electron transfer reactions are formed in many situations, particularly when oppositely charged protein combinations are reacted together. Examples involving oppositely charged simple protein combinations include cytochrome *c*–cytochrome b_5, cytochrome *c*–cytochrome b_2, cytochrome *c*–cytochrome c_{551}, and cytochrome *c*–plastocyanin. Other examples involve physiological partners such as the cytochrome *c*–cytochrome *c* peroxidase combination. In most aspects, the transition state believed to exist in electron self-exchange reactions represents a special case of the transition state proposed for protein–protein complexes. However, unlike the self-exchange reactions where there is no free energy driving force ($\Delta G=0$), with protein–protein complexes, the free energy term now takes on an essential importance which necessarily introduces complexity into application of the Marcus or related theory (if one is brave enough to assume these reactions are amenable to this kind of description!!). Furthermore, in studying electron transfer reactions between proteins, complications may arise because the system may exhibit several conformational states and the important conformations with respect to the electron transfer step may not be known unambiguously. Other problems related to interpretation of the kinetics may also arise, but general features, as contained in Ref. [28], are summarised below.

Consider a protein P_1 which has a more negative reduction potential than protein P_2 but where either can be in the oxidised (ox) or reduced (red) state. In the simplest of interprotein reactions, described in Eq. (28), rapid association of (P_1^{red}) and (P_2^{ox}) is followed by slow electron transfer (k_{et}) and rapid dissociation

$$P_1^{red} + P_2^{ox} \rightleftharpoons P_1^{red}/P_2^{ox} \xrightarrow{k_{et}} P_1^{ox}/P_2^{red} \longrightarrow P_1^{ox} + P_2^{red} \quad (28)$$

of P_1^{ox} and P_2^{red}. If one of the reactants, say P_2^{ox}, is in pseudo-first-order excess, then $k_{obs}=k_{et}[P_2^{ox}]$.

A more general case is shown in Eq. (29) in which the intracomplex (internal) electron transfer reaction is induced by external oxidation (ox) or reduction (red) of the proteins by agents that are not shown explicitly.

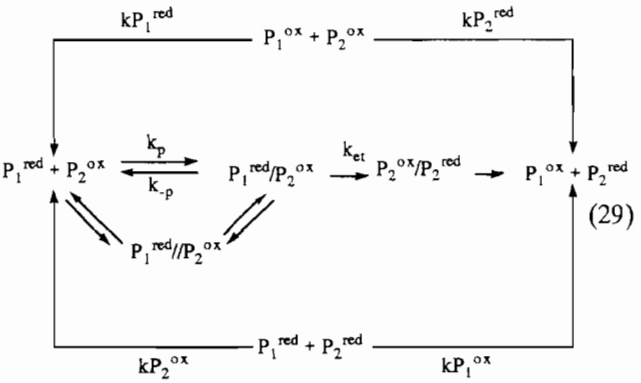

(29)

The proteins must be in excess over the exogenous oxidant or reductant, so that complete oxidation or complete reduction (of both P_1 and P_2) is avoided. The external reaction should be selective in the sense that $kP_1^{ox} > kP_2^{ox}$ or $kP_2^{red} > kP_1^{red}$, so that the yield of the unstable product, $P_1^{red}+P_2^{ox}$, will be higher than the yield of the stable one, $P_1^{ox}+P_2^{red}$. If the external oxidation or reduction is unselective ($kP_1^{ox} \approx kP_2^{ox}$ or

$kP_2^{red} \approx kP_1^{red}$) or, especially, if it is selective in the unfavourable sense ($kP_1^{ox} < kP_2^{ox}$ or $kP_1^{red} < kP_1^{red}$), the internal reaction may be difficult to follow, and measurement of k_{et} inaccurate. In principle, the proteins P_1 and P_2 may form multiple and interconverting complexes, which may undergo internal electron transfer reactions at different rates. In a limiting case represented by Eq. (29), the complex $P_1^{red}//P_2^{ox}$ is redox inactive, and the reaction occurs through the redox active one, P_1^{red}/P_2^{ox}. The stability of this precursor complex is defined by the association constant, $K_a = k_p/k_{-p}$. The equilibria (the interchange rate constants k_i and k_{-i}) involving the redox inactive $P_1^{red}//P_2^{ox}$ are seldom treated explicitly.

A more detailed mechanism, shown in Eq. (30), explicitly includes the successor complex, P_1^{ox}/P_2^{red}, and allows for the reversibility of each step. In principle, the precursor and the successor complex differ in thermodynamic stability, i.e., $k_p/k_{-p} \neq k_{-s}/k_s$, and in

$$P_1^{red} + P_2^{ox} \underset{k_{-p}}{\overset{k_p}{\rightleftharpoons}} P_1^{red}/P_2^{ox} \underset{k_{-et}}{\overset{k_{et}}{\rightleftharpoons}} P_1^{ox}/P_2^{red} \underset{k_{-s}}{\overset{k_s}{\rightleftharpoons}} P_1^{ox} + P_2^{red} \quad (30)$$

structure, but the successor complex generally is not observed. For this reason, and because the electron transfer step is usually irreversible ($k_{-et} = 0$) when the difference of the reduction potentials (i.e. the thermodynamic driving force) is appreciable, the scheme in Eq. (29) is adequate [28]. Under pseudo-first-order conditions, say with an excess of P_2^{ox}, the following three cases usually occur [28]. Firstly, if $k_{-p} + k_{et} \geq [P_2^{ox}]$ and $k_{et} \gg k_{-p}$, then $k_{obs} = k_p[P_2^{ox}]$ and second-order kinetics is found. Secondly, if $k_{-p} + k_{et} \gg k_p[P_2^{ox}]$ and $k_{et} \ll k_{-p}$, then $k_{obs} = K_a k_{et}[P_2^{ox}]$ and the second-order rate constant, $K_a k_{et}$, reflects both the rapid pre-equilibrium and the subsequent electron transfer step. Thirdly, if $k_{-p} + k_{et}$ is not $\geq k_p[P_2^{ox}]$ and $k_{-p} \approx k_{et}$, then $1/k_{obs} = 1/k_{et} + [(k_{et} + k_{-p})/(k_p k_{et}[P_2^{ox}])]$; then the limiting (also called saturation) kinetics is found and usually interpreted as formation of the precursor complex following by the rate-limiting electron transfer step.

The first and second cases are sometimes difficult to distinguish. The second case is the most common for the reactions between two proteins, and the third case is found occasionally [28]. When the driving force for the electron transfer reaction is small, the full mechanism represented by Eq. (30) must be considered.

The above situation refers to conditions that may be described as the bimolecular regime. When the diprotein complex is fully formed, which most commonly occurs when P_1 and P_2 bear large opposite charges (e.g. cytochrome *c* and plastocyanin) and the ionic strength of the solution is low, the kinetics may be analysed in terms of Eq. (31), which is analogous to Eq. (29). These conditions correspond effectively to the unimolecular regime and provide a similar situation to that encountered with chemically modified proteins. From an experimental point of view, if the unimolecular conditions prevail, then the value of k_{et} should not change as the concentration of P_1^{red}/P_2^{ox} is varied at least 10-fold. The external reactions kP_1^{red} and kP_2^{ox} may in fact involve the formation of ternary complexes with redox agents, or they may yield the redox inactive $P_1^{red}//P_2^{ox}$ as well as the redox active P_1^{red}/P_2^{ox}, although neither situation is shown in Eq. (31).

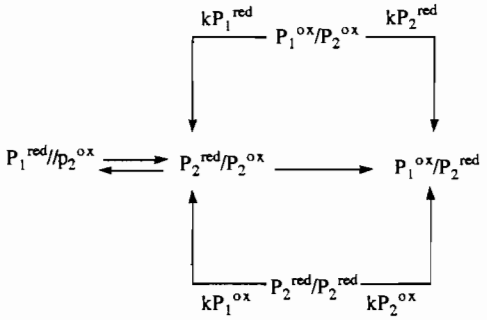

(31)

The main advantage of the unimolecular over the bimolecular regime is that the reaction k_{et} in the former case is unobscured by formation of the precursor complex and by dissociation of the successor complex. The diffusion processes leading to the bimolecular reactions are ideally suppressed by forming covalent linkages between the proteins. However, if the association is by electrostatic and hydrophobic forces and if the concentrations are relatively high, the possibility of bimolecular reactions must always be considered.

An unstable distribution of oxidation states in a diprotein complex can sometimes be achieved photochemically by exciting one of the redox centres into an electronic state that is a strong reductant, a strong oxidant, or both. This method is usually applied to protein complexes formed in the unimolecular regime. Eq. (32) shows the excited state, designated with an asterisk, as a reductant. The excited state may decay

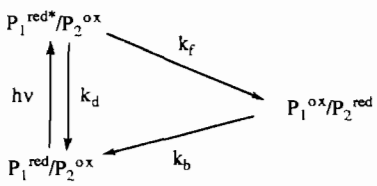

(32)

not only by the so-called forward electron transfer reaction, k_f, but also by various other processes (e.g. k_b and k_d). However, k_f may be calculated provided k_d and k_b are known to provide a measure of k_{et}.

The above summary which was adopted in the main from Ref. [28] is provided to show yet again how difficult it can often be to distinguish k_{et} from other steps. Experimentally, the reaction in Eq. (28) is normally studied by stopped-flow spectrophotometry and occa-

sionally by temperature jump methods. The external reactions in Eqs. (29) and (31) are usually reductions and need to be faster than the internal reaction of interest, k_{et}. Methods used for these studies are usually stopped-flow spectrophotometry, laser flash photolysis (usually with flavin semiquinones or flavin hydroquinones as reductants), and pulse radiolysis (with electrons or free radicals as reductants). The reactions in Eq. (32) arc studicd by laser flash photolysis and by transient absorption spectroscopy. Most kinetic measurements are made at pH 7.0, at or near room temperature. In some studies pH, temperature and ionic strength are varied. However, with all methods, it is always important, but often difficult, to establish whether the rate-limiting step in the overall reaction is actually electron transfer or some other process such as conformation change in one or both proteins, rearrangement of the precursor complex or change in solvation, etc. [26,28,29].

The second-order rate constant for a reaction between two differcnt proteins when the reaction occurs via formation of a protein–protein complex is expected to be related to the second-order electron self-exchange reactions obtained for the individual proteins. For example, given the data presented in Table 7 which have been derived or calculated for the individual proteins, rate constants for the redox cross-reaction between cytochrome *c*–cytochrome c_{551} and cytochrome *c*–cytochrome b_2 combinations can be predicted using procedures detailed in Refs. [26], [28] and [29] and summarised below.

Using thc samc formalism as for the electron self-exchange reactions gives

$$\Delta G_r^* = \frac{\Delta G_{11}^* + \Delta G_{22}^* + \Delta G_{12}^{0\prime}}{2} + \frac{(\Delta G_{12}^{0\prime})^2}{8(\Delta G_{11}^* + \Delta G_{22}^*)} \quad (33)$$

where ΔG_r^* is the reorganisational free energy of the electron transfer reaction between the two proteins, ΔG_{11}^* and ΔG_{22}^* are the reorganisational energies of the two reactions, and $\Delta G_{12}^{0\prime}$ is the free energy change for the electron transfer step, calculated from the differences in redox potential of the individual electron transfer reactions.

In the case of the reaction between cytochrome *c* and cytochrome c_{551}, the redox potentials of the two proteins are similar [26]. From Eq. (27) the reorganisational energy when $\Delta G_{12}^{0\prime} = 0$ is the arithmetic mean of the reorganisational energies of the two proteins, or approximately 3.8 kcal mol^{-1} in the case being considered. Using the net charges and dipole moments in Table 1 enables a work term of 2.0 kcal mol^{-1} to be calculated. This result, in combination with data in Table 7 and a heme–heme distance of 8.7 Å, allows the prediction [26] to be made of a rate constant of 3×10^4 M^{-1} s^{-1} (ionic strength = 0.1 M, 4°C). The experimentally determined second-order electron transfer rate constant between cytochrome *c* and cytochrome c_{551} at 0.1 M ionic strength and 4.5 °C is 1.6×10^4 M^{-1} s^{-1}. Thus, the predicted rate constant is in excellent agreement with that measured experimentally [26].

Substantial attention has been paid to the electron transfer reaction between cytochrome *c* and cytochrome b_5 [2,26]. At low ionic strength, the two cytochromes form a protein–protein complex that has been studied by modelling as well as optical and NMR spectroscopic techniques. From these studies it has been deduced that cytochrome *c* and cytochrome b_5 form a complex in which the two heme centres lie in parallel planes separated by a closest edge-to-edge distance of 8.5 Å, with a centre-to-centre separation of 16 Å. Using pulse radiolysis and flash photolysis, k_{et} values have been measured for various derivatives when the metal centres have been modified, but under conditions where >90% of the cytochrome b_5 was bound to cytochrome *c*. The driving forces and k_{et} values associated with these studies are given in Table 8. From the driving force versus k_{et} relationship, the reorganisation energy (λ value) was estimated to be 0.8 eV. Calculations based on self-exchange reorganisational energies of cytochromes *c* and b_5 give a value for λ of 0.95 eV [26]. The difference in the two estimates of λ presumably arises from errors in the approximations for bimolecular electron transfer calculations and from the assumption in the intracomplex electron transfer experiments that the substitution of one metal for another at the active site results in no change, other than altering the redox potential [26]. However, overall, these two estimates of the reorganisational energy, one derived from intracomplex electron transfer as a function of free energy and the other derived from bimolecular self-exchange data, are in satisfactory agreement [26].

Recent investigations into factors that control electron transfer in protein–protein complexes have been extensive [20,26–30] and different approaches to varying the driving force have been reported. Additionally, in order to probe the electron transfer pathway, site directed mutagenesis has been undertaken to modify

Table 8
Electron transfer rates and driving forces reported for cytochrome *c*–cytochrome b_5 protein–protein complexes

Donor–acceptor	$-\Delta G^\circ$ (eV)	k_{et} (s^{-1})
[Cyt.c, Fe(III)]/[Cyt.b_5, Fe(III)]	0.3	1.6×10^3
[^{3}porph-Cyt.c*]/[Cyt.b_5, Fe(III)]	0.35	5×10^4
[^{3}Zn-Cyt.c*]/[Cyt.b_5, Fe(III)]	0.75	5×10^5
[H_2porph-Cyt.c*]/[Cyt.b_5, Fe(III)]	1.1	8×10^3

[a] Data taken from *Prog. Inorg. Chem., 38* (1990) 259; *J. Am. Chem. Soc., 107* (1985) 739; *J. Am. Chem. Soc., 107* (1985) 7811.

a particular amino acid residue thought to be involved in electron transfer process. In summary [2], studies of long-range electron transfer between both physiological and non-physiological protein complexes suggest that, with the exception of the cytochrome *c*–cytochrome b_5 complex, rates generally increase with driving force according to Marcus-type predictions.

Refs. [2] and [26–29] may be consulted for further details of studies on electron reactions in protein–protein complexes. In this article, data obtained from a few representative examples are discussed, with the aim of demonstrating the relationship between electron transfer in protein–protein complexes and electron self-exchange reactions and in providing a background to enhance the understanding of the relationships of these solution phase reactions to electrochemical studies on the same systems where the reactions take place at the protein solution/electrode interface.

3.4. Electron transfer in modified proteins

As noted earlier, the preparation of chemically modified proteins should in principle provide a simpler method of measuring first-order intramolecular electron transfer rate constants than via studies of homogeneous redox reactions. Data derived from these studies therefore can be expected to enable the dependence on distance and driving force to be established in a reliable and unambiguous manner. However, even after extensive studies by several eminent research groups, the interpretation of the data reported remains cloudy and no universally self-consistent interpretation of the results has yet to emerge. For example, in reviewing the available data, examples where the opposite extremes of electron transfer rates being related to distance and driving force in a Marcus-like theoretical relationship or totally independent of redox centre distance have been found. Indeed anomalous data, or 'exceptions to the rule', are in abundance. Conclusions from this apparent conundrum are that many complexities associated with the electron transfer process have yet to be unravelled and that the experiments themselves and their interpretation remain intrinsically difficult.

To demonstrate the difficulty of interpreting data, reports of recent extensive studies may be compared under what appear to be rather contradictory headings.

3.4.1. Intramolecular electron transfer rates reported to be independent of redox centre distance

Scott et al. [30] conclude their extensive studies involving the preparation, characterisation and measurement of electron transfer rates of cytochrome *c* derivatives with glutamate or aspirate residues covalently modified with the cobalt-containing cage structure $[Co(diAMsar)]^{3+}$ (Scheme 4) by discussing the intriguing observation that the measured values of k_{et} (Fig. 5(a)) are independent of the heme–cobalt redox centre distance in contrast to theory based on the Marcus relationship which predicts a well-defined dependence on distance. The reversible half-wave potentials, $E^{r}_{1/2}$, values, which are equivalent to the standard redox potentials for the heme and the $Co^{2+/3+}$ reactions as well as their separation, which is a measure of the driving force for the electron transfer reaction, are almost derivative independent (Table 9). However, the $[Co(diAMsar)]^{3+}$ centre is attached to different locations on the protein surface so that the distance between the cobalt and heme centre varies in accordance with data also contained in Table 9. According to the Marcus theory, under conditions of constant driving force, as for this series of modified proteins, the linear dependence of log k_{et} versus distance given in Fig. 5(a) would be expected. This theoretically predicted result is very different to the result obtained experimentally which is that k_{et} is independent of distance. The conclusion of this study, that rate is independent of distance, seems improbable and further investigation of this intriguing result therefore seems to be warranted.

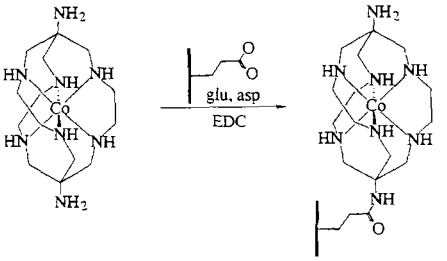

Scheme 4. Formation of a covalently modified cytochrome derivative by nucleophilic attack of an amino group of $[Co(diAMsar)]^{3+}$ at a carbodiimide-activated surface carboxylate (EDC). Reproduced by courtesy: *Met. Ions Biol. Syst., 27* (1991) 209.

3.4.2. Intramolecular electron transfer rates which have been proposed to depend on redox centre distance

The distance dependence of electron transfer in proteins has also been studied in ruthenated sperm whale myoglobin [2], where there are four surface histidines (His48, 81, 116, 12) at edge–edge distances from the metal porphyrin of 12.7, 19.3, 20.1 and 22.0 Å, respectively. While myoglobin does not function physiologically as an electron transfer protein, it does undergo Fe(III)/Fe(II) redox chemistry in a similar way to simple electron transfer metalloproteins and has been studied in this context both chemically and electrochemically (see later). The driving force for electron transfer from the Fe(II) heme to the a_5Ru(III)histidine is too small to allow observable electron transfer rates for the three long distance histidines (His81, His116, His12). Consequently, the driving force–distance relationship was determined using proteins in which the iron porphyrin was replaced by zinc and magnesium

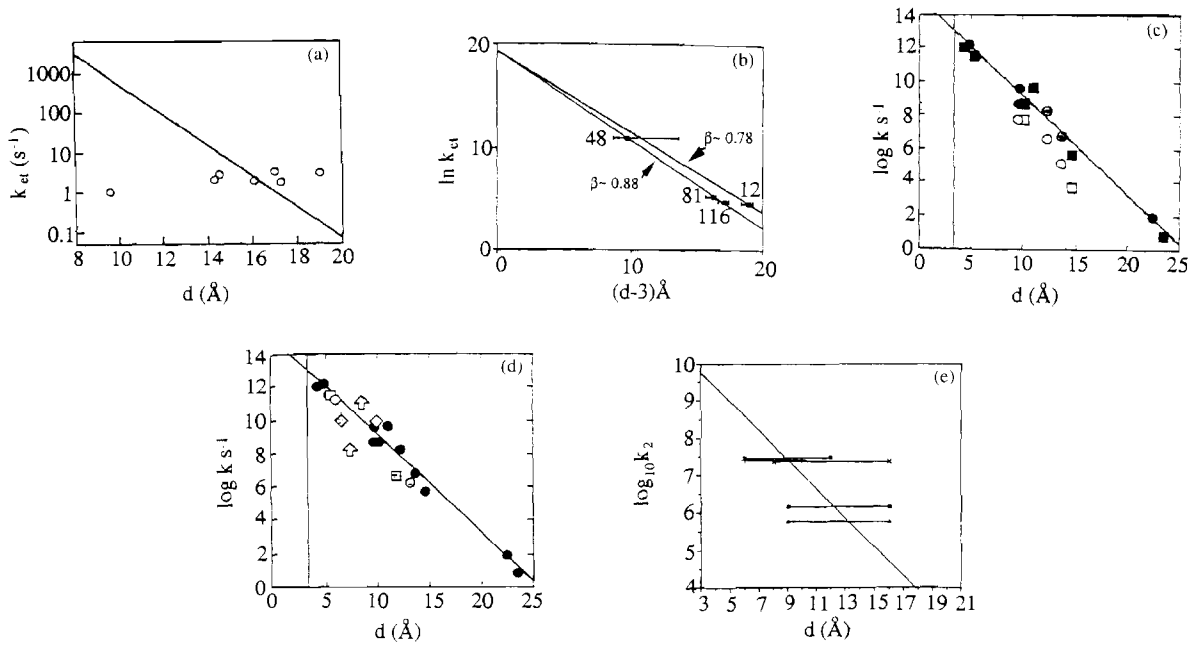

Fig. 5. Examples of different distance dependences reported for the rate of electron transfer in modified proteins. (a) Distance vs. rate dependence for the seven [Co(diAMsar)]–cytochrome *c* derivatives listed in Table 9 represented by open circles. Solid line represents the Marcus-type theoretical prediction with $\beta = 0.9$ Å^{-1}. (b) Distance vs. rate dependence for sperm whale myoglobin. Distance is reported as actual distance minus the van der Waals contact distance of 3 Å. Data taken from Ref. [2]. (c) Distance (edge carbon to edge carbon) vs. rate dependence reported for *Rb sphaeroides* (squares) and *Rp viridis* (circles). Filled and open symbols represent native rates, shaded symbols represent free energy optimized rates [32]. (d) Distance vs. rate dependence reported for a wide range of systems based on free energy optimised electron transfer rates as presented in Ref. [32]. Data reported in Fig. 5(c) (filled circles). Calculated minimum *Rp viridus* rates for Cyt.c_{551} to Cyt.c_{556} and Cyt.c_{551} to c_{559} (arrows) porphyrin–quinone (open square); iridium–organic (open circle); porphyrin–quinone (open diamond); ruthenium–Cyt.*c* (shaded square); ruthenium–myoglobin (shaded circle); biphenyl–organic (shaded diamond). (e) Distance vs. rate dependence reported for Ru(bipyridine)$_2$(dicarboxybipyridine)–cytochrome *c* modified proteins [35]. Data points are for derivatives modified at lysines 7 (▲), 13 (+), 25 (■), 27 (●) and 72 (×).

Table 9
Reduction potentials, redox centre distances and intramolecular electron transfer rate constants obtained for [Co(diAMsar)]–cytochrome *c* derivatives [a]

Derivative [b]	Distance [c] (Å)	k_{et}^{red} [d] (s^{-1})	k_{et}^{ox} [e] (s^{-1})	(k_{et})av. [f] (s^{-1})	$E^{r}_{1/2}$(heme) [g] (mV vs. NHE)	$E^{r}_{1/2}$(cobalt) [g] (mV vs. NHE)	$\Delta E^{r}_{1/2}$ [h] (mV)
E21	10±2	0.9±0.1	1.2±0.2	1.0±0.2	279	−369	648
E61	14±2	2.2±0.2	1.7±0.2	2.0±0.3	260	−361	621
E66	14±2	2.8±0.1	2.7±0.2	2.8±0.2	261	−379	640
E62	16±2	1.7±0.2	2.1±0.2	1.9±0.3	264	−357	621
E104	17±2	1.8±0.1	1.7±0.1	1.7±0.1	269	−375	644
E4	17±2	3.1±0.1	3.3±0.2	3.2±0.2	261	−374	635
D2	19±2	3.2±0.2	2.6±0.2	2.9±0.3	264	−378	642

[a] Data taken from Ref. [30].
[b] Details presented in Ref. [30].
[c] [Co(diAMsar)] cage to cytochrome heme edge distance estimated by molecular modelling.
[d] Rate measured using $([Ru(bpy)_3]^{2+})^*$ as a photo-reductant.
[e] Rate measured using $([Ru(bpy)_3]^{2+})^*$ as a photo-oxidant.
[f] Average rate obtained from oxidation and reduction.
[g] Reversible half wave potential obtained from voltammetric measurement at an edge plane pyrolytic graphite electrode.
[h] Separation in $E^{r}_{1/2}$ values which is, a measure of $\Delta G°$ or the driving force for the electron transfer reaction.

porphyrin. Fig. 5(b) summarises the data and a β value (slope of plot) of 0.88 is proposed from the log k_{et} versus distance plot on the basis of the His48, 81 and 116 data. In this study, the His12 data was considered to be unique and a separate β value of 0.78 was derived for this derivative. However, arguably, more data points are required to draw conclusions from a study of this kind as if the His48 data were to be regarded as unique

and only the His81, 116 and 12 considered as a triad, the result could be interpreted as being independent of distance as in the work of Scott et al. The triad of data discussed above also refers to rather long distance electron transfer reactions which are rather slow and therefore difficult to measure accurately and resolve from homogeneous processes, which occur on similar time scales. In a recent report [31], Winkler and Gray postulated that bimolecular electron transfer reactions may have contributed to the observed kinetics of this system. If so, then the rates for the His12, His81 and His116 systems may represent an upper limit to the true intramolecular electron transfer role. In summary, results of more extensive studies on this system would also be of considerable interest. More extensive data on ruthenium–His48 modified myoglobin derivatives do in fact appear to conform to a Marcus-type relationship [31].

An example of a linear driving force–distance plot containing many data points has been presented by Dutton and others [6,32–34] for photosynthetic reaction centre proteins (Fig. 5(c)). While again it may be argued that electron transfer reactions of a photosynthetic bacterium may be intrinsically different from that of the simple metalloproteins being considered in this review, data from other systems including metalloproteins to which a transition metal complex has been attached, also satisfactorily fit the same relationship.

Fig. 5(d) shows a comparison of rate data contained in Fig. 5(c) with the rates of electron transfer obtained for a number of organic–organic, organic–transition metal complex, bridged donor–acceptor systems and modified proteins (metalloproteins to which a transition metal complex has been peripherally attached) with all data being calculated in an analogous manner. The results from the chemical systems cluster about the linear rate–distance relation defined by the biological photosynthetic reactions. At van der Waals contact of donor and acceptor edge carbon atoms (approximately 3.6 Å), the intercept of the rate versus distance curve is 1.3×10^{13} s^{-1} which is much greater than in Fig. 5(b), but typical for a reaction that is adiabatic with nuclear motion along the reaction coordinate [32]. The slope of plot in Fig. 5(d) of 1.7 Å per decade (β value) while clearly different to that in Fig. 5(b) is in the middle of a range of other measurements made on more limited data sets. The results shown in Fig. 5(d) suggest that the photosynthetic reaction centre medium is biologically unremarkable in that many media, independent of their specific, chemical features, share a common rate–distance relationship between the redox centres.

In another study, where a linear distance–driving force dependence is reported, Durham et al. [35] labelled cytochrome *c* at specific lysine groups with Ru(bipyridine)$_2$(dicarboxybipyridine). Laser flash photolysis experiments with some of the cytochrome derivatives showed that the excited state of the ruthenium complex undergoes an electron transfer reaction with the heme. Results of k_{et} values calculated from these experiments together with the redox centre distances were used as the basis for comparing experimental data with Marcus theory calculations shown in Fig. 5(e). The estimated redox centre distances obviously contain a good deal of uncertainty. The reorganisational energy barrier for electron transfer required in the Marcus calculation was estimated to be 78 kJ based on self-exchange data for Cyt.*c* and $[Ru(bpy)_3]^{2+}$ and the driving force was estimated to be 1.05 V based on an $Ru^{3+/2+}$ $E°$ value of 1.31 V versus NHE for Ru(bpy)-(dcphy) and 0.26 versus NHE for $Fe^{3+/2+}$ for cytochrome *c*. The best line fit to the data in Fig. 5(e) gives $\beta=0.9$ $Å^{-1}$ and $\lambda=43$ kJ using the free energy relationship

$$k_{et}=\frac{10^{13}\exp[-\beta(d-3)]\exp[-(\lambda+\Delta G°)^2]}{4\lambda RT} \quad (34)$$

where the pre-exponential term was set at 10^{13}. The value of β calculated from the slope of the plot in Fig. 5(e) must be regarded as having considerable uncertainty. If a statistical analysis of the data had been provided, it would probably be concluded that the fact that the reported slope is similar to that in Fig. 5(b) is not especially significant. Furthermore, the contrast with the data obtained for the Co(diAMsar) derivatives where no dependence on distance has been reported is most striking and at this stage the reasons for the difference between what should be closely related situations has yet to be satisfactorily explained.

3.4.3. Further example where k_{et} does not appear to be a function of driving force or distance or predicted by the Marcus relationship

In other studies on the electron transfer reactions of modified proteins, the dependence of rate on free energy or driving force generally has been examined by replacing an ammine or other ligand on a ruthenium centre and varying the redox potential at the ruthenium site or in the case of hemoglobin, by varying the metal in the porphyrin [31]. In these studies, the distance between the redox centres has been assumed to be fixed. Some of the data reported in these studies are summarised in Table 10 and while some kind of dependence of k_{et} on driving force is observed, the degree to which data conform to a Marcus-type theory is far from clear. Some ot the anomalies in the rate-free energy relationship that have been noted in studies on modified proteins are considered below.

Another example of an apparent anomaly is contained in the work of Isied [36] who noted that the dependence of electron transfer rates on distance for some ruthenium modified cytochrome *c* complexes appears to be directional. After inspection of their data (Table 11) it may be concluded that on varying the $E°$ value, the

Table 10
Electron transfer rates in ruthenated metalloproteins [a]

Modification site	Protein	Direction of electron transfer	r_c [b] (Å)	$-\Delta G°$ [c] (eV)	k_{et} (s^{-1})
His 33	cytochrome *c* (horse heart)	$Ru^{II} \rightarrow Fe^{III}$	11.7	0.18	30
His 83	azurin (*P.a.*)	$Ru^{II} \rightarrow Cu^{II}$	11.8	0.24	2.2 [a]
His 59	myoglobin (sperm whale)	$Ru^{II} \rightarrow Fe^{III}$	12.7	−0.02	0.02
His 59	plastocyanin (*A.v.*)	$Ru^{II} \rightarrow Cu^{II}$	11.9	0.26	<0.08
His 32	plastocyanin (*S.o.*)	$Ru^{II} \rightarrow Cu^{II}$	10–12	0.29	<0.26
His 100	stellacyanin (*Rh.v.*)	$Ru^{II} \rightarrow Cu^{II}$	~16.1		0.05
His 42	HiPiP (*Rh.v.*)	$Ru^{II} \rightarrow Cu^{II}$	7.9	0.27	18
His 47	cytochrome c_{551}	$Ru^{II} \rightarrow Fe^{III}$	7.9	0.18	13

[a] Data taken from Refs. [2,15] with the average value of k_{et} given for azurin. Symbols are those used in Ref. [2].
[b] Redox centre distance.
[c] Free energy driving force.

Table 11
Reported rates of intramolecular electron transfer (k_{et}) and reduction potentials (E_f^0) of ruthenium modified cytochrome *c* proteins [a]

Ruthenium modified Cyt.*c* [b]	E_f^0 [c] (V)	[process][d]	k_{et} (s^{-1})	Direction of electron transfer
Native horse heart cytochrome *c*	0.26	[Fe(III)/Fe(II)]		
cis[$(NH_3)_4Ru(OH)$]	−0.01	[Ru(III)/Ru(II)]	5×10^2	Ru → heme
[$(NH_3)_5Ru$-]	0.13	[Ru(III)/Ru(II)]	55	Ru → heme
[Ru(bpy)(bpy$^-$)(py)]	−1.2	[Ru(III)/Ru(II)]	2.8×10^5	Ru → heme
[Ru(bpy)(bpy$^-$)(im)]	−1.2	[Ru(II)*/Ru(II)]	2.0×10^5	Ru → heme
[$Ru(bpy)_2$(py)]	0.92	[Ru(II)*/Ru(II)]	40	heme → Ru
[$Ru(bpy)_2$(im)]	0.79	[Ru(III)/Ru(II)]	55[e]	heme → Ru
Ru(bpy)(terpy)	0.74	[Ru(III)/Ru(II)]	44	heme → Ru
$Ru(bpy)_2OH_2$	0.65	[Ru(III)/Ru(II)]	~50	heme → Ru

[a] Unless otherwise stated data taken from Ref. [36].
[b] bpy = 2,2′-bipyridine, bpy$^-$ = the bipyridine radical anion, terpy = 2,2′,2″-terpyridine, im = imidazole, py = pyridine.
[c] E_f^0 is the formal redox potential of the Cyt.*c* or substituted Cyt.*c* vs. the normal hydrogen electrode.
[d] [Fe(III)/Fe(II)] and [Ru(III)/Ru(II)] are metal based processes whereas [Ru(II)*/Ru(II)] is a ligand based process.
[e] It is important to note that Winkler and co-workers (*J. Am. Chem. Soc., 113* (1991) 7056) report a value of 2.6×10^6 s^{-1} for this process which casts doubt on the validity of the slow rates reported for the heme–Ru electron transfer process (see text).

rate for the Ru → heme electron transfer process increases significantly with driving force. However, for the reverse heme → Ru process, the rate constants are rather slow and almost independent of $E°$ or driving force. The mechanism proposed to interpret these results is summarised in Eq. (35)

$$Ru^{II}Cyt.c^{III} \underset{k_{-1}}{\overset{k_1}{\rightleftharpoons}} Ru^{III}Cyt.c^{*II} \overset{K_{eq}}{\rightleftharpoons} Ru^{III}Cyt.c^{II} \qquad (35)$$

where for the forward reaction, $k_{obs} = k_1$ and for the reverse reaction, $k_{obs} = k_{-1}/K_{eq}$. In this mechanism, it is proposed that [Cyt.c, Fe(III)] is reduced to an activated intermediate, [Cyt.c*, Fe(II)], which undergoes a conformational change to the stable form of [Cyt.c, Fe(II)]. According to this mechanism, the rate of formation of the activated intermediate, k_1 is measured when the reduction of cytochrome *c* is studied. In contrast, for the oxidation of cytochrome *c*, an initial pre-equilibrium reaction is required prior to forming the same activated intermediate. The presence of this initial reaction depresses the observed rate of intramolecular oxidation to k_{-1}/K_{eq} and thereby explains why a significantly decreased intramolecular rate apparently is observed for oxidation for the cytochrome *c*. This mechanism is one of many that could be proposed to interpret the directional nature of the result, and if correct, reinforces the concept developed in the early part of this review that structural changes accompanying electron transfer in reactions of cytochrome *c* cannot necessarily be neglected. However, it needs to be recognised that the attractiveness of the mechanism in Eq. (35) is probably only its simplicity. Furthermore, as noted elsewhere great care has to be made to exclude artifacts, particularly when very slow rate constants are being reported. These apparently anomalous data have also been considered by Winkler and Gray in a recent review [31]. These authors refer to a study from their own laboratory (see footnote in Table 11) which gives a rate constant for the oxidation of the ferroheme by $[Ru(bpy)_2(im)(His33)]^{3+}$ of 2.6×10^6 s^{-1}. Furthermore,

no evidence was found in their study for a ferroheme oxidation process proceeding at a slower rate (55 s^{-1}). Consequently, additional studies are required to confirm the validity of reaction scheme (35) before further speculation is warranted.

Additional examples of 'anomalous rates', relating to a lack of an obvious dependence on driving force or distance have arisen in the work by Sykes et al., which is summarised in Refs. [2] and [15] and Table 10. For example, cytochrome c_{551} has been ruthenated at His47 and the Ru(II) to Fe(III) rate is 13 s^{-1} for a redox centre separation of 7.9 Å [2,15]. However, while the driving force for electron transfer in this example is the same as for horse heart cytochrome *c* modified at His33, the rate of electron transfer is actually slower (13 versus 30 s^{-1}) even though the 3.8 Å shorter separation distance would lead to the prediction of a much faster rate. Similarly, in comparing data obtained from modified azurins, modified plastocyanins and the high-potential iron–sulfur protein [4Fe–4S] ferredoxins, it has been noted by Sykes et al. [15] that although the distance between the ruthenium label and the protein metal centre does not vary greatly from that in modified cytochrome *c*, significantly different rates of electron transfer were obtained, relative to the value of 30 s^{-1} obtained for cytochrome *c*. For example, for the copper proteins which have an estimated distance redox centre of 8–12 Å, the reactions were slower than expected for both azurin (k_{et} 1.9 s^{-1}) and for the plastocyanins (k_{et} <0.26 and <0.1 s^{-1} for *S. obliquus* and *A. variabilis*, respectively) on the basis of cytochrome *c* data. In contrast, as noted above for Cyt. c_{551} (k_{et} 13 s^{-1}) the electron transfer rates are of the same order of magnitude as for cytochrome *c*. Similar difficulties exist in comparing the high-potential iron–sulfur protein [4Fe–4S] ferredoxin rates with other proteins and no clear correlation between electron transfer rates with distance and driving force could be drawn from these studies. It may, therefore be concluded that the question as to whether the electron transfer step, conformational change or some other step is the rate-limiting step in modified protein electron transfer reactions has not yet been always unambiguously answered. Additionally, as noted on several occasions, the solvent and proton rearrangements accompanying electron transfer have rarely been considered and whether a rigid model is valid in both oxidation states is questionable.

Gray and co-workers [31,37,38] in a series of extensive studies on ruthenium modified cytochrome *c* have reported that electron transfer rates do not correlate well with distance, but rather with the effective tunnelling pathway ($\sigma\ell$) (see Fig. 6) which may be calculated on the basis of a theory developed by Onuchic et al. [39,40].

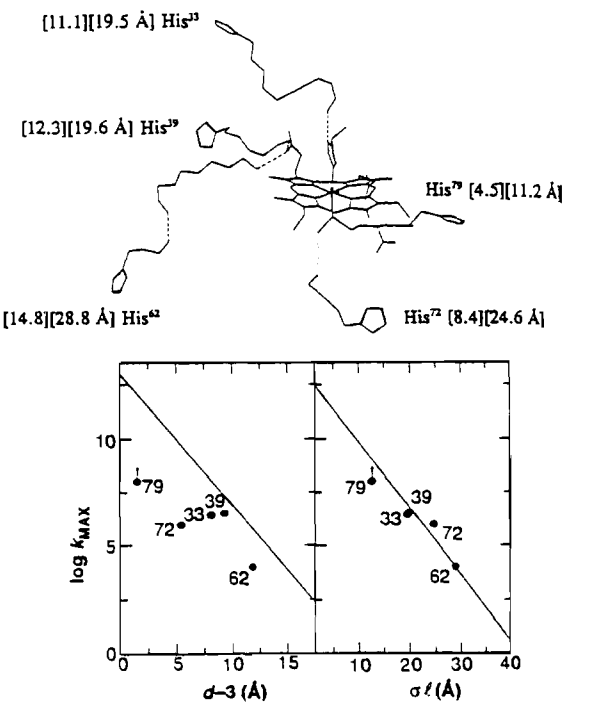

Fig. 6. Upper: electron-tunnelling pathways in ruthenium histidine modified cytochrome *c* proteins. Edge–edge distances, and tunnelling paths lengths ($\sigma\ell$) are indicated in brackets ([*d*], [$\sigma\ell$]). Lower: correlation of activationless electron transfer rates in ruthenium modified cytochromes with *d* and $\sigma\ell$. Reproduced by courtesy: *Science, 258* (1992) 174.

The work of Dutton referred to above led to the conclusion that $\ln(k_{et})$ is linearly related to the donor–acceptor distance. However, in the pathway dependent model, rates are predicted to vary with factors relevant to each step in the pathway and the factors associated with each step are quantified by calculating the effective tunnelling pathway length ($\sigma\ell$). Data in Fig. 6 obtained as ruthenium modified cytochrome *c* [37,38,41] in fact suggest that the electron transfer rate decreases exponentially with $\sigma\ell$ but not with direct donor–acceptor distance. As noted above, Dutton and co-workers [34] recently suggested that the uniform medium model may be used to describe a broad range of natural and synthetic electron transfer systems. Thus, whereas Dutton was able to fit to a single exponential, data encompassing rates over twelve orders of magnitude (20 Å), Gray et al. have reported that this uniform medium model is unsatisfactory when examining individual subclasses of electron transfer reactions, such as those found with chemically modified cytochrome *c*. This dilemma is highlighted by comparing the experimental data reported by Gray to Dutton's line of best fit (Fig. 6) and noting that discrepancies of several orders of magnitude exist for some data points. The pathway analysis therefore suggests that the structure of the intervening protein medium is critical in determining the role of individual protein electron transfer

reactions. The difficulty at the moment is that both the Dutton and Gray concepts appear convincing when considered in isolation. However, the experiments, the theories, the preparation of compounds, the interpretation of structural data (bond distances) and allowance for structural (conformational volume) changes that occur with cytochrome *c* are all either difficult or fraught with dilemmas.

Given the existence of a range of apparent anomalies with respect to the dependence of k_{et} on distance and driving force, it has been proposed that there are intrinsically 'good' and 'bad' pathways for electron transfer between the protein and inorganic redox centres in the modified protein, as in the Gray type approach. In a similar vein, Sykes et al. [15] had speculated previously that factors other than distance driving force, and conformational gating, as proposed by Isied [36], may be involved in governing the rates of electron transfer.

To pursue the concept of 'good' and 'bad' pathways in more detail, some of the data are now presented with emphasis on the electron transfer pathway rather than distances and driving force. For example, the rates of electron transfer (k_{et} is $<0.08\ s^{-1}$ for *A.v.* plastocyanin and $<0.26\ s^{-1}$ for *S.o.* plastocyanin ruthenated at His59 as noted above) are anomalously low both relative to modified cytochrome *c* and other proteins for which data are listed in Table 10. The rates also are slow with respect to expectations based on structural considerations. As noted in Section 1, the inner-sphere reorganisation energy for blue copper proteins should be small, because the geometry at the copper site is essentially unaltered as a result of the electron transfer process. Furthermore, the outer-sphere reorganisation energy also is expected to be small, since the Cu metal site is buried within the protein lattice and no solvent molecules are proximal to the metal. Finally, the ruthenium-labelled histidines in the plastocyanins are also thought to be similar in structure to modified histidines in other proteins, so no structural impediment to fast electron transfer has been identified in His59 ruthenated plastocyanins.

The concept of the importance of the reaction pathway was introduced in Section 3 to explain data obtained from proteins with chemical redox reagents when redox inactive reagent was added. The modified rates (Fig. 4) for ferrodoxin led to the suggestion of specific binding sites. In homogeneous redox reaction studies, where plastocyanin reacts with the $[Co(phen)_3]^{3+}$, the route for electron transfer is thought to be from the Tyr83/Asp42 to the metal centre. According to the 'good' and 'bad' pathway concept, this electron transfer process could be regarded as occurring via a favourable route because the electron transfer rate in the $[Co(phen)_3]^{3+}$–plastocyanin precursor complex is $26\ s^{-1}$ even though the driving force is only 20 mV [2,15]. Additionally, reaction of $[a_5RuIm]^{2+}$ with the *A.v.* and *S.o.* plastocyanins results in $k_{et} > 5 \times 10^3\ s^{-1}$ [15] so that obviously fast rates of electron transfer can be achieved with modified plastocyanins and favourable electron transfer routes [15]. On the basis of the 'good' and 'bad' electron transfer pathway model, it may therefore be concluded that a_5Ru^{3+}–plastocyanin modification at His59 [2,15] may not provide an optimal site for electron transfer because the electron transfer pathway from this site to the metal centre is 'bad'. That is, the nature of the intervening medium is the factor which is dominant in determining the observed rate. Fig. 7(a) shows the relative positions of the copper and ruthenium redox centre in the His59 modified plastocyanin. The

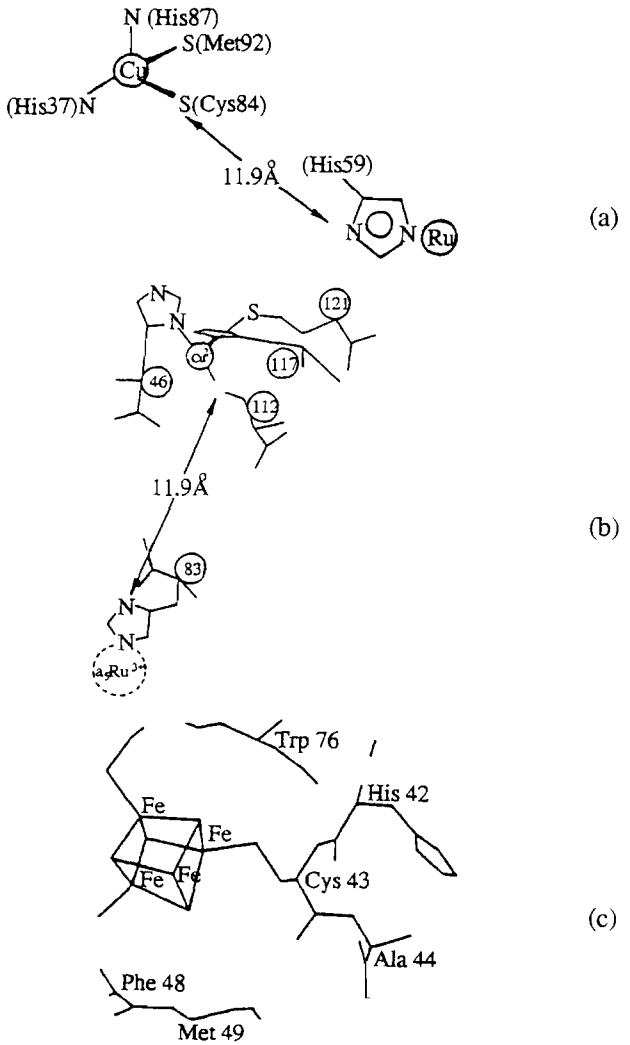

Fig. 7. Representation of the relative locations of the protein metal redox centre and ruthenium redox centre in a range of modified proteins. (a) Ruthenium modified *Anabena variabilis* plastocyanin. Reproduced by courtesy: *J. Am. Chem. Soc., 110* (1988) 5880. (b) Ruthenium modified (His83) azurin. Reproduced by courtesy: *J. Am. Chem. Soc., 105* (1983) 7765; (c) Ruthenium modified (His42) $[Fe_4S_4]$ ferredoxin. Reproduced by courtesy: *J. Chem. Soc., Dalton Trans.,* (1988) 2843.

redox centres are separated by a distance of about 11.9 Å. Unfortunately, from the point of view of the 'good' and 'bad' pathway model, a convincing answer to the question as to why this particular modified protein complex gives rise to a particularly unfavourable route has yet to be provided.

The relationship of the donor and acceptor sites in *Pseudomonas aeruginosa* azurin ruthenated at His83 is shown in Fig. 7(b). In this case, the redox centre separation distance is also about 11.9 Å. However, as noted above, the intramolecular Ru(II)-to-Cu(II) electron transfer rate of 2.2 s^{-1} in the $a_5Ru(His83)^{2+}$–$Az(Cu^{2+})$ complex again is low in comparison with modified heme protein electron transfer rates over similar distances and with similar driving forces (Table 10). On the basis of this reaction pathway model, the slow rate could be interprcted to result from poor electronic coupling between the ruthenium and copper centres and the electron transfer process would be regarded as occurring over an unfavourable pathway. Similarly, when the blue copper protein *Rhus vernicigera* stellacyanin was labelled with a a_5Ru^{3+} at both exposed histidines, His32 and 100, the Ru(II) to Cu(II) electron transfer rate constant of 0.05 s^{-1} appears to be small. As is the case with the slow reactions observed for azurin and plastocyanin, again this could be the consequence of having an unfavourable electron transfer pathway.

An even more remarkable rate anomaly, if distance were to be the only important parameter, is provided by data obtained for the [4Fe–4S] ferredoxin protein modified by a_5Ru^{3+} at His42 (Fig. 7(c)). In this modified protein, the estimated through-space distance from the [4Fe–4S] cluster to the a_5Ru^{3+} His42 is only 7.9 Å. Despite this very short through-space electron transfer distance and a respectable driving force of ~0.27 eV, k_{et} (Ru to the [4Fe–4S] cluster) is only 18 s^{-1}, a value which is about two orders of magnitude lower than expected by comparison with cytochromc *c* rates and assuming an exponential dependence of k_{et} on r_e and use of the Marcus relationship with a β value of 0.9 $Å^{-1}$. The rate is also remarkably slow in view of the short through-bond pathway available since His42 is adjacent to Cys43 which is bonded directly to the iron sulfur cluster (Fig. 7(c)). This would be regarded as a very unfavourable pathway on the 'good' and 'bad' reaction pathway model.

3.5. Summary of data derived from chemical redox investigations

The data cited and discussed above represents only a small fraction of the extensive total body of literature now available. However, despite the intense activity in studies of both intermolecular electron transfer reactions involving metalloproteins and inorganic complexes, and intramolecular electron transfer reactions within protein–protein complexes and modified proteins, additional experiments conducted over wider ranges of distances and driving forces in situations where systematic structural changes can be made, still appear to be required before a clearer and less ambiguous picture of the electron transfer process can emerge. Despite the fact that there are examples where electron transfer rates increase with driving force and decrease with distance as expected theoretically, exceptions or at least apparent exceptions to this result are prevalent. The exceptions imply that the medium through which the electron transfer reaction has to take place is often more important than the distance or driving force of the reaction and that theoretical models which take into account the nature of the electron transfer route are required [37–44]. However, gating steps or conformational or other structural changes which accompany the electron transfer process and which effectively provide a barrier to the electron transfer, the dynamic nature of the redox centres in at least one oxidation state and other ambiguities inherently present in this complex subject may be more important than has commonly been believed in many reactions. Indeed, given the significant complexity of the studies, it is likely that reinterpretations of much of the data will occur in the next few years as some of these or other nuances are recognised and incorporated into the interpretation.

4. Electron transfer at the metalloproteins/electrode interface

Armed with the knowledge available from the chemically based redox studies in Section 3, it would be expected that the electrochemical data on metalloproteins could be readily explained in equivalent terms. In principle, all that has to happen in an electrochemical experiment is that electron transfer should takc place at the electrode/solution interface and provided the electron transfer distance is not too great and structural changes accompanying electron transfer are small, the rate should be fast, i.e. the value of k_s should be large. Conversely, if the distance of closest approach to the electrode is too great or gross structural changes have to take place, then it would be predicted that slow rates of electron transfer (small k_s values) would be found. However, there are some important nuances in the electrochemistry that need consideration, and some concepts derived from chemically based redox reactions do not always translate in an intuitively obvious manner from the chemical to the electrochemical domains. For example, concepts based on rate versus distance relationships described in Section 3 for chemical redox reactions need not apply in an exactly analogous manner under electrochemical conditions because the solution in the electrode/solution interface region has special (double layer) properties that are significantly different to the bulk solution. Nevertheless, understanding of

the differences and similarities of electrochemical and chemical studies of the redox reactions may provide important fundamental new insights into protein electron transfer reactions.

4.1. Theory of electrode kinetics in voltammetry

If only the electron transfer component of Eq. 7(a) and (b) is considered, then an electron transfer process at an electrode can be written as:

$$P_o + e^- \overset{E^\circ, k_s, \alpha}{\rightleftharpoons} P_r \tag{36}$$

where P_o is the oxidised form of the protein and P_r the reduced form and E°, k_s and α are as described previously.

Many approaches to the theoretical description of Eq. (36) are available. The initial observation that the rate of electron transfer is potential dependent formed the basis of the empirical Tafel plot [8]. This concept was extended by Butler and also by Erdey-Gruz and Volmer to give what is now known as the Butler–Volmer equation [8]. This equation is

$$i = i_o\{\exp[(-\alpha nF/RT)(E-E^\circ)] - \exp[\{(1-\alpha)nF/RT\}(E-E^0)]\} \tag{37}$$

where $i_o = nAFk_s[P_o]^{(1-\alpha)}[P_r]^{\alpha}$. The basis of Eq. (37) is that the net current, i, is the sum of the current from the forward (i_f) and the backward reactions (i_b) of Eq. (36), which in turn are dependent upon the rate of each reaction with $i_f = nAF[P_o]k_f$ and $i_b = nAF[P_r]k_b$. The potential dependence of each reaction rate constant is as follows

$$k_f = k_s \exp[(-\alpha nF/RT)(E-E^\circ)] \tag{38}$$

$$k_b = k_s \exp[\{1-\alpha)nF/RT\}(E-E^\circ)] \tag{39}$$

where k_f is the rate of the forward process in Eq. (36) and k_b is the rate of the backward reaction, n is the number of electrons transferred in the rate determining step, R is the universal gas constant, T is the absolute temperature, F is the Faraday constant and k_s, E° and α are as defined previously. It is generally considered that Butler–Volmer kinetics are obeyed if k_f and k_b are exponentially dependent upon potential and α is independent of potential. The role played by α can be considered from Eqs. (38) and (39). If the driving force (i.e. $-nF(E-E^\circ)$) is increased, only a fraction, equivalent to α, of the additional energy is used to increase the apparent rate constant. Usually α is found to be close to 0.5.

Developments of electron transfer theory, which enabled data from chemical and electrochemical redox studies to be compared, were introduced by Hush who extended the statistical mechanical treatments of Marcus to the case of electrode kinetics [12,45]. In this approach, the homogeneous and heterogeneous charge transfer reactions are considered to be conceptually equivalent and the electrode is regarded as a molecule with adjustable reactivity.

With the extended theory, the equations relating current, potential and reaction rate are still expressed in the traditional form equivalent to the Butler–Volmer formulation to give

$$i = nAFk(E)\{[P_o] - [P_r]\exp[nF(E-E^\circ)/RT]\} \tag{40}$$

but with

$$k(E) = k_s^t \exp[(\alpha n - Z_i)F\phi_s/RT]\exp[-\alpha nF(E-E^\circ)/RT] \tag{41}$$

and

$$\alpha = \tfrac{1}{2} + \frac{F(E-E^\circ-\phi_s)}{4\lambda} \tag{42}$$

where $k(E)$ is the potential dependent rate, Z_i is the ionic charge of the relevant species, ϕ_s is the electrical potential of the electron transfer site which is usually considered to be close to the site of the outer Helmholtz plane. The reorganisation energy of the molecule in an electron transfer reaction as noted previously is associated with changes in bond length, bond angle and solvent reorganisation and is symbolised by the term λ. The term k_s^t is the true standard heterogeneous rate constant and is related to the reorganisation energy and the collision frequency, Z, as in Eq. (43)

$$k_s^t = Z \exp(-\lambda/4RT) \tag{43}$$

where $Z = \sqrt{RT/2\pi M}$, with M being the molar mass of P_o and P_r. The intrinsic or measured heterogeneous rate constant, k_s, is related to the true standard rate constant as in Eq. (44)

$$k_s = k_s^t \exp[(-\alpha n - Z_i)F\phi_s/RT] \tag{44}$$

In Eq. (44), the exponential term is a double layer correction and if ϕ_s is independent of potential then both k_s and k_s^t will be constant. The above discussion is limited to molecules undergoing electron transfer reactions where bonds are not formed or broken via interaction with the electrode or within the molecule during the course of the heterogeneous electron transfer process. These reactions for which the theory is relevant were referred to as outer-sphere electron transfer reactions in the discussion of chemically derived redox data.

A quantum mechanical approach to the problem of electron transfer at electrodes, developed by Levich and Dogonadze [46], leads to a theory that has many similarities with the statistical mechanical approach. A discussion of the physical significance and interpretation of α in each of the theoretical models is contained in Ref. [47].

In the case where a surface-confined process is observed, Butler–Volmer type equations are still applicable, but of course it is the surface concentrations that are important and the electron transfer rate constant has the units of s^{-1} which are different from the units of the heterogeneous charge transfer rate constant (cm s^{-1}). Apart from this difference, the formulation of the equations for surface base processes are analogous to the solution soluble case and are available in Ref. [48]. However, in spite of the availability of sophisticated theoretical models, most experiments are analysed in terms of the apparent rate constant k_s rather than k_s^t and the apparent charge transfer coefficient. The potential-dependence of α has been investigated with frequently conflicting results. Molecules which are neutral and have small reorganisation energies appear to exhibit a potential dependent α value. Neutrality ensures that the molecule is unaffected by the electrostatic forces in the double layer and this decreases the uncertainties brought about by applying the so-called double layer corrections. It follows from Eq. (42) that the smaller the reorganisation energy, the larger the potential dependence of α. The organisation energy is the sum of the inner-shell and outer-shell contributions; the inner-shell reorganisation energy is dependent on bond length and bond angle variations whereas the outer-shell energy is dependent upon the solvent. Unfortunately, from an experimental point of view, the rate constant is also dependent on λ and α as can be seen from Eqs. (43) and (44). Consequently, this means that large potential dependencies of α are predicted to occur with fast rates of electron transfer. However, accurate measurement of fast rate processes is difficult to achieve. The dependence of α on potential is therefore usually neglected because of the relative insensitivity of the rate constant with respect to λ under conditions where reliable rate constant data can be obtained. Many aspects of the problem of electron transfer at the electrode surface have been reviewed in Refs. [8], [46] and [47].

4.2. Voltammetry of surface attached metalloproteins

In a stimulating paper, Chidsey [49] showed that when a ferrocene group is attached at a range of fixed distances from a gold electrode surface by the self-assembly of a mixed thiol monolayer of $(\eta^5\text{-}C_5H_5)(\eta_5\text{-}C_5H_4)CO_2(CH_2)_{16}SH$ and $CH_3(CH_2)_{15}SH$ that rate constants from 1 s^{-1} to 2×10^4 s^{-1} are obtained and that a Marcus type relationship between rate constant and distance of the ferrocene centre to the electrode is observed with a reorganisation energy of 0.85 eV and a pre-exponential factor of 7×10^4 s^{-1} eV^{-1}. This study highlights how electrochemical methods may be used to systematically probe the dependence of electron transfer rates on distance and medium. Unfortunately, although this is just the knowledge that ideally could be obtained from electrochemical studies of metalloprotein electron transfer reactions, data of this kind has yet to be achieved from electrochemical measurements.

Fundamental features of electrochemical techniques that must be appreciated and which introduce differences relative to chemical redox studies are that electrodes have a potential dependent charge and that the electrode/solution interface has a double layer region of molecular dimensions where the electrode/solution interface is structured in a potential dependent manner [8]. Proteins, as noted in Section 1, are themselves also highly charged, but unlike the electrode they often have an asymmetrical rather than symmetrical charge distribution. Consequently, specific electrostatic interactions at the electrode/solution interface may be expected at all potentials irrespective of the apparent overall charge on the protein. That is, the asymmetric charge distribution on a protein provides the possibility of having negatively or positively charged surface sites, irrespective of the overall charge, and therefore it is likely that proteins will adsorb at an electrode surface at all potentials irrespective of the sign or magnitude of the charge on the electrode. This implies that proteins are electroactive in a non-redox as well as redox sense and diffusion of protein to an electrode may occur at all potentials to achieve adsorption and not just at potentials where electron transfer takes place. In understanding the voltammetry of proteins, it is therefore likely that features associated with adsorption will have to be considered and in the extreme case proteins may be reduced or oxidised solely in the electrode attached or adsorbed state. An example of the ability of proteins to adsorb at a solid interface, despite an apparently unfavourable charge situation, is provided in the work of van Dulm et al. [50] who showed that adsorption of negatively charged proteins may occur even at a negatively charged polystyrene surface.

If the adsorption of the protein onto the electrode surface does not result in denaturation of the protein and if the surface-attached rate of electron transfer is fast, then it is likely that the voltammetry of adsorbed protein will occur at or near to the reversible potential for the native form of the protein. However, note that units of the rate constant for the electron transfer rate constant are s^{-1} for the case when electron transfer takes place in the surface attached state and not cm s^{-1} as is the case when electron transfer occurs across a solution/electrode interface. In this surface attached case, it may be predicted that the electrochemically derived data for the electron transfer process should be very closely related to that found in protein–protein or modified protein complexes, the electrode now being considered to be attached to a specific site. Assuming a distance of less than 10 Å can be achieved between

the point of attachment of the protein to the electrode and the metal centre, where k_{et} in the chemical redox sense would be predicted to be in the range of 10^8 to 10^{10} s^{-1} according to the data presented in Fig. 5(d) then it would seem likely that a very fast surface based electron transfer pathway should be available to accommodate the electron transfer process, if distance is the only consideration. However, as noted in the chemical redox studies, the pathway may be crucial. A fast rate of electron transfer in the electrochemical context will lead to the observation of current flowing at potentials near $(E_f^0)_{attached}$, whereas if the electron transfer rate is slow, then the current for the electrochemical redox process will occur at potentials well removed from $(E_f^0)_{attached}$. Consequently, electrochemical measurements made in the potential region of $(E_f^0)_{attached}$ and which detect current flow in this potential region are in a sense selectively filtering the fast pathways from the slow ones.

Fig. 8(a) shows a cyclic voltammogram for reduction of cytochrome *c* immobilised into a lecithin lipid monolayer and deposited onto an SnO_2 electrode by the Langmuir–Blodgett technique [51]. Fig. 8(b) shows the analogous experiment at a 4,4′-bipyridyl modified gold electrode where to a first-order approximation adsorption and/or surface attachment is absent and the redox process involves transport of cytochrome *c* by diffusion from the bulk solution, followed by electron transfer at the electrode/solution interface and finally diffusion of reduced cytochrome *c* back to the bulk solution. In both cases, a measurable current is observed at or near the reversible redox potential. In the case where cytochrome *c* is physically attached to the electrode surface (Fig. 8(a)) a symmetrical peak-shaped curve is observed and the peak current shows a linear dependence on scan rate v, as theoretically expected for an electroactive species confined to an electrode surface. In contrast, in the solution phase experiment, an asymmetrical peak shaped curve is observed and a linear dependence of peak current on $v^{1/2}$ is found experimentally and expected theoretically (Fig. 8(b)). In Fig. 8(b), the peak-to-peak potential separation for the reduction and oxidation component of the experiment is close to the Nernstian value of 57 mV expected for a reversible process at 25 °C which implies that it is the rate of diffusion rather than the rate of the electron transfer step that is rate determining on the time scale of this experiment. Furthermore, for this diffusion controlled process, the average of the oxidation and reduction peak potential is +0.020 V versus SCE which is identical, within experimental error, to the potentiometrically determined E_f^0 value, again as theoretically predicted if diffusion control is observed at all potentials including E_f^0. All data imply that the rate of electron transfer is very fast between cytochrome *c* and an electrode surface, irrespective of whether the protein is surface attached or undergoes electron transfer at the solution/electrode interface without direct attachment to the electrode surface.

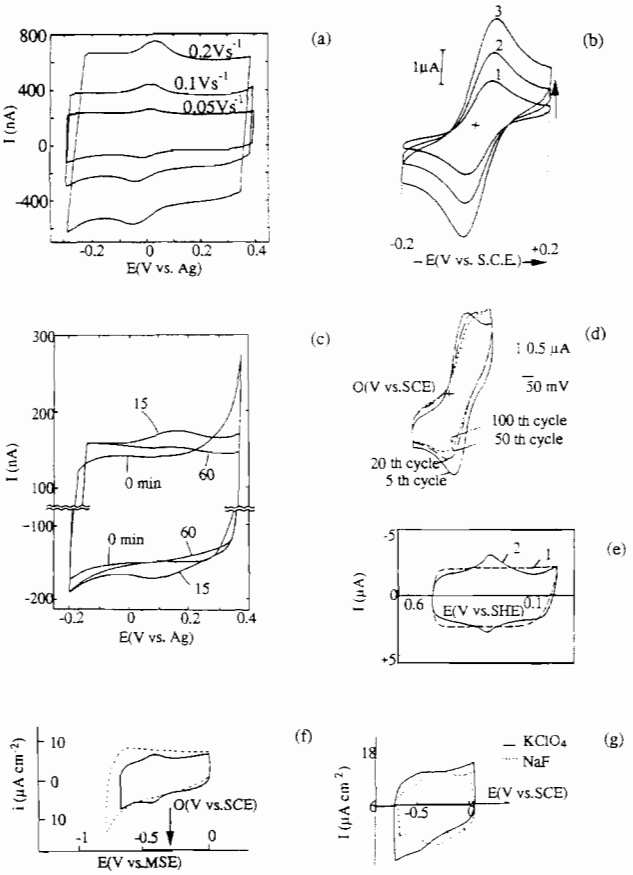

Fig. 8. Cyclic voltammograms of cytochrome *c*: (a) immobilised on an SnO_2 electrode by the Langmuir–Blodgett technique (reproduced by courtesy: *J. Electroanal. Chem., 216* (1987) 289); (b) at a gold electrode in the presence of 10 mM bipyridyl using scan rates of (a) 20, (b) 50 and 100 mV s^{-1} (reproduced by courtesy: *Adv. Inorg. Chem., 36* (1991) 341); (c) obtained under conditions of (a) but as a function of time using a scan rate of 100 mV s^{-1}; (d) at an edge plane graphite electrode using a scan rate of 20 mV s^{-1}; (e) adsorbed onto a pyrolytic graphite carbon electrode using a scan rate of 10 mV s^{-1} (reproduced by courtesy: *J. Electroanal. Chem., 253* (1988) 581); (f) adsorbed onto a bis(4-pyridyl) disulfide modified gold electrode using a scan rate of 5 mV s^{-1} (reproduced by courtesy: *J. Electroanal. Chem., 264* (1989) 157); (g) adsorbed onto a large gold electrode using a scan rate of 300 mV s^{-1} (reproduced by courtesy: *J. Electroanal. Chem., 147* (1983) 324). Other details of experimental conditions are available in the original literature.

The embedding of cytochrome *c* into a lipid monolayer [51] leads to the observation of stable voltammograms for periods in excess of 1 h. In contrast, if cytochrome *c* is physically attached by adsorption onto the surface of the SnO_2 electrode (Fig. 8(c)), rather than embedded, then the peak currents gradually increase for 15 min and then decrease. From visible light experiments [51] it was ascertained that despite the time dependence of the peak current, that cytochrome *c* still remains on the surface ($\geq 0.8 \times 10^{-11}$ mol cm^{-2}) even after the

electrode was transferred from the buffered media present in the electrochemical cell to water for 2 h. This time dependence of the voltammetry at an SnO_2 electrode therefore was attributed to either denaturation or structural modification to a non-native form of cytochrome *c*. A time-dependent response has also been made with repetitive cycling experiments at carbon electrodes (Fig. 8(d)) where a change in wave shape occurs from peak shaped to sigmoidal shaped as the electrode becomes self-blocked by what appears to be the formation of a voltammetrically insulating layer of adsorbed protein. However, in solution studies, time-dependent voltammetry or even the complete absence of voltammetry does not necessarily represent slow electron transfer [52–56]. Rather, a partial blocking of the surface by a modified or denatured form of the protein which is electroinactive at the reversible potential may leave a residual array of electroactive sites. If the residual sites are sufficiently small and well spaced, voltammetry occurs by radial rather than linear diffusion [52–56]. That is, when mass transport occurs via diffusion, a change from a peak shaped to a sigmoidal shaped curve may take place as more of the surface becomes blocked. In the extreme, if the entire surface is blocked, then of course no response will be observed at potentials around E_f^0, but this does not necessarily mean that the rate of electron transfer is slow.

Spectroscopic studies by Collinson and Bowden [57] on the conformational state of cytochrome *c* electrostatically adsorbed on tin oxide electrodes reveal that no major structural changes occur in either the reduced or oxidised forms and that cytochrome *c* is predominantly absorbed in its electroactive form. The E_f^0 values of adsorbed cytochrome *c* and the fast rate of electron transfer are consistent with spectroscopic data in the sense that both indicate that it is the native form that is electroactive. A small shift in the E_f^0 value of about 20 mV relative to the solution value [58], may reflect a small conformational change induced by adsorption and electrostatic electrode–cytochrome *c* interactions [58]. Consequently, some aspects of the time dependence of surface-attached material have not been unambiguously explained.

The voltammetry of cytochrome *c* immobilised on a pyrolytic graphite electrode also produces a well-defined response (Fig. 8(e)) in the reversible redox potential region as is the case when this protein is attached to an SnO_2 electrode (Fig. 8(a)) or bis(4-pyridyl)disulfide modified gold (Fig. 8(f)) electrode. However, at a bare gold electrode, adsorbed and presumably structurally modified (non-native) protein is reduced at considerably more negative potentials than native cytochrome *c* (Fig. 8(g)).

A carefully defined electrode treatment method was required to form sufficient suitable sites to immobilise cytochrome *c* on the pyrolytic graphite electrode to obtain the result shown in Fig. 8(e). The equilibrium potential calculated from the voltammetry of the adsorbed cytochrome *c* was equal to the reversible redox potential. The electrode kinetics of the immobilised cytochrome *c* were also analysed as a function of scan rate. Thc fact that the potentials are equal to the reversible value and independent of scan rate up to 0.01 V s^{-1} was taken to indicate that the electron transfer step was fast and not rate determining on this time scale [59,60]. The dependence on scan rate at higher scan rate and the temperature and electrolyte dependence was attributed to conformational changes and the data have been analysed in terms of inner- and outer-sphere reorganisational energies. Similar conclusions have been reached in studies of Cyt.*c* immobilised on a gold electrode surface modified with bis(4-pyridyl)disulfide [61]. In summary, for much of the data obtained under a variety of conditions it is plausible to propose that the slow step may be associated with small conformational or other structural changes and not electron transfer. Even though the SnO_2 electrode data were treated as a case of slow electron transfer without considering the influence of structural change, the reported rate constant of 2 s^{-1} is still consistent with a fast rate of electron transfer. In a series of detailed studies, Bowden et al. [62,63] have studied the voltammetry of cytochrome *c* adsorbed onto carboxylic acid-terminated self-assembled monolayer electrodes of the alkane thiol–gold type. Fig. 9 shows some experimental and theoretical square wave voltammograms for this system. The average rate constant determined was $1.1 \pm 0.3\ s^{-1}$, although some non-ideality is noted [61]. Albery et al. report an even faster value of 50 s^{-1} [10] for the surface-attached electron transfer rate when the diffusion and cytochrome *c* surface process were separated by detailed analysis of the voltammetric data.

There are numerous other studies on the voltammetry of electrode attached metalloproteins (see Refs. [64–73] for example) and some dissolution of material with time or other form of time dependence or evidence for a conformational change of the structure of the attached metalloprotein etc. make it clear that the assumptions required to use the simple theory [57] are not always met. The use of the simple theory outlined earlier requires, in addition to the requirements noted in chemical redox studies, that (i) lateral interactions among adsorbed species are negligible, (ii) all surface sites are equivalent and (iii) that processes involving solution-soluble species in both oxidation states are negligible. To meet all these assumptions places high demands on the experimental design and is unlikely to be readily achieved with complex molecules such as metalloproteins. Thus, unfortunately, while the highly informative experiments of the Chidsey-type described above where electrochemical establishment of k_{et} versus

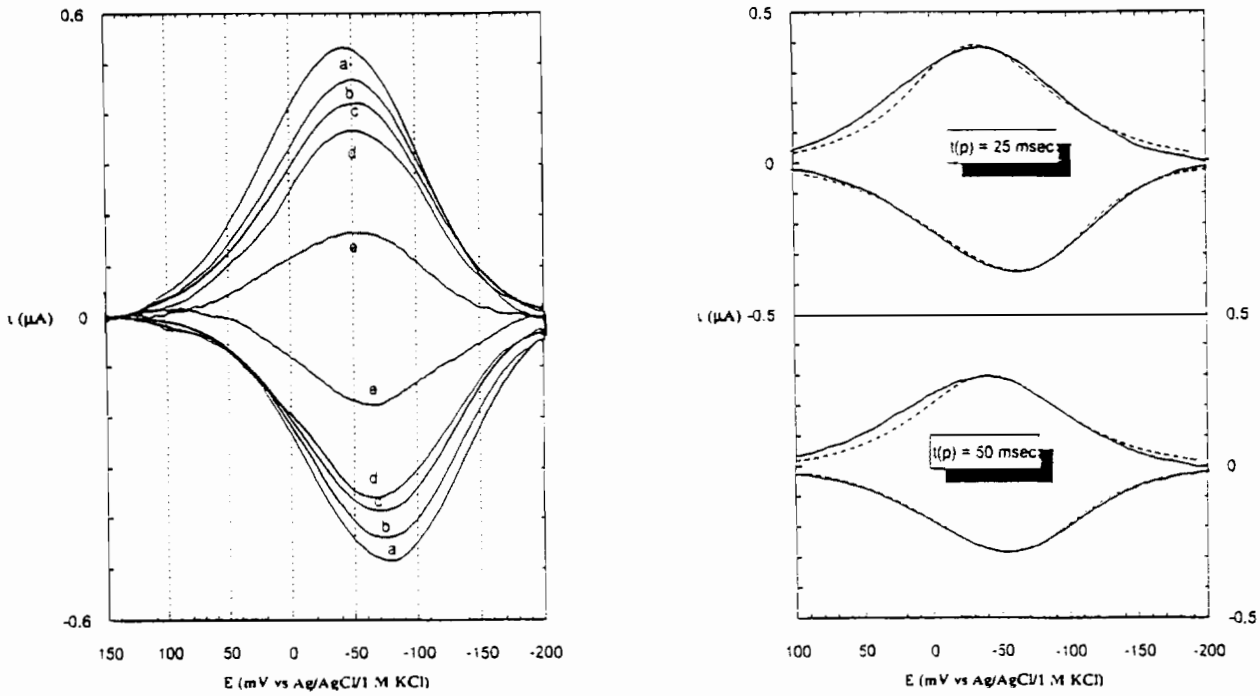

Fig. 9. Square wave voltammograms of cytochrome *c* adsorbed onto a 16-mercapto hexadecanoic acid modified gold electrode. (Left hand side) Experimental square voltammograms obtained with pulse widths, [$t(p)$], of (a) 10 , (b) 17.5, (c) 25, (d) 37.5, (e) 250 ms. (Right hand side) Comparison of experimental (——) and calculated ($E_f^0 = -0.048$V, $k_{et} = 0.8$ s^{-1}, $\alpha = 0.45$) (– – –) square wave voltammograms. Reproduced by courtesy: *Anal. Chem., 65* (1993) 683.

distance relationships was achieved with ferrocene materials [49], these relationships are unlikely to be achieved in the immediate future via electrochemical studies of metalloproteins.

4.3. Voltammetry of metalloproteins in the solution phase where mass transport to and from the electrode surface occurs by diffusion

Fig. 10 shows an example of a voltammogram obtained for cytochrome *c* at a carbon microelectrode where radial diffusion must occur irrespective of whether or not blocking of the electrode surface occurs by adsorbed and denatured cytochrome *c*. In data obtained at microelectrodes, the wave shape is consistent with a reversible process and the half wave potential $E_{1/2}$ is equal to the reversible formal potential E_f^o. Analysis of the voltammogram therefore implies that diffusion rather than the rate of electron transfer is rate determining. Simulations of these experiments which are also included in Fig. 10 demonstrate that k_s must be greater than 0.1 cm s^{-1} [52]. Other data based on a microscopic model of electron transfer are consistent with k_s values ≥ 1 cm s^{-1} [52–56].

A picture of very fast rates of heterogeneous electron transfer ($k_s \geq 0.1$ cm s^{-1}) is emerging from electrochemical studies for many of the simple electron transfer proteins that have been studied in detail [52–56] (e.g. plastocyanin, cytochrome *c*, azurin, ferredoxin). In a

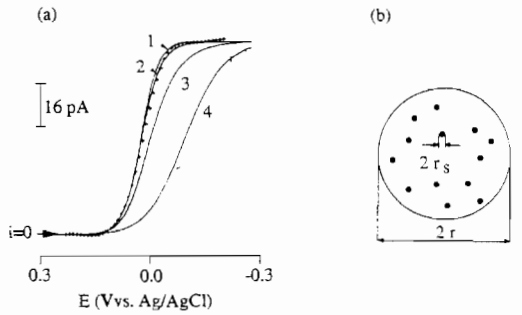

Fig. 10. (a) Voltammograms at microdisc electrodes; experimental (+) and simulated (– – –) data; for reduction of 660 μm cytochrome *c* in 100 mM $NaClO_4$, 5 mM phosphate buffer (pH 7) at a carbon microdisc electrode with $r = 6.3$ μm, using a scan rate of 0.5 V s^{-1}. Simulation parameters are $r_s = 0.14$ μm; number of active sites = 25; $D = 8.0 \times 10^{-7}$ cm^2 s^{-1}; $\alpha = 0.5$; $\nu = 0.5$ V s^{-1} for rate constants (1) $k_s = \infty$; (2) $k_s = 1.0$ cm s^{-1}; (3) $k_s = 0.1$ cm s^{-1}; (4) $k_s = 0.01$ cm s^{-1}. (b) The model used for calculations which consist of a finite number of non-interacting electroactive microdisc sites of radius r_s within a microdisc electrode of radius r, with the remainder of the microelectrode being electroinactive. Reproduced by courtesy: *J. Electroanal. Chem., 314* (1991) 191.

sense, this is a logical conclusion from the fact that current flow normally is detected at or near the reversible potential and this is the voltammetric region of potential that has been focussed on. A misunderstanding that no current or only a small current at the reversible potential corresponds to slow electron transfer seem

to have been made via conclusions reached on the basis of a macroscopic model. Fig. 11(a) and (b) contains a collection of examples of the voltammetry of metalloproteins where the current magnitude and wave shape is critically dependent on the nature of the electrode and solution conditions. In several of these cases, it is tempting to describe the changes as resulting from an increase or decrease in rate of electron transfer when either the solution or the electrode surface conditions are modified. In fact, in each case, detailed analysis reveals that if significant change in wave shape is observed at the reversible potential it is most likely that it is the nature of the electrode surface and therefore the mass transport process that is being altered and not the rate of electron transfer [52–56]. For example, in Fig. 11(a), the change from a peak to sigmoidal shaped voltammetric response may be attributed to a decrease in the number of available electroactive sites at the edge plane relative to basal plane graphite electrode and therefore an increase of radial relative to linear diffusion, rather than to a change in heterogeneous charge transfer rate constant. Fig. 11(c) and (d) show what would happen if a change in k_s actually had occurred in the extreme cases where mass transport is solely by linear or radial diffusion, respectively.

Recollecting the influence of the addition of positively charged complexes to homogeneous rate data, where for example, it has been found that k_{obs} for the oxidation of the reduced form of ferredoxin by $[Co(NH_3)_5(C_2O_4)]^+$ decreases on addition of $[Cr(NH_3)_6]^{3+}$ (Fig. 4) because of competitive binding of $[Cr(NH_3)_6]^{3+}$ and $[Co(NH_3)_5(C_2O_4)]^+$ and electrostatic considerations, then it is tempting to explain the changes in the voltammetry of ferredoxin in the presence and absence of $[Cr(NH_3)_6]^{3+}$ in analogous terms. However, in the voltammetric response, the change observed for negatively charged ferredoxin from no response to sigmoidal to peak shaped with increasing concentration of $[Cr(NH_3)_6]^{3+}$ (Fig. 12) (and vice versa for positively charged cytochrome *c* as in Fig. 11(b) (3) and (4)) predominantly reflects the increasing or decreasing contribution of radial and linear diffusion and not a change in k_s. With the microscopic model of electron transfer [52–56] the interpretation of the data is that no measurable current response at potentials near E_f^0 for the native form corresponds to a fully blocked surface. A sigmoidal response corresponds to a partially blocked surface and a peak-shaped response to a highly electroactive surface with relatively few blocked sites. Applications of the microscopic model have also been developed for membrane-modified electrodes [74,75] and all the data illustrate the care which must be taken before true k_{et} and/or k_s values can be calculated.

As intimated in Section 1, simple metalloproteins are ideally designed to achieve fast rates of electron transfer. The current flowing at potentials near to the

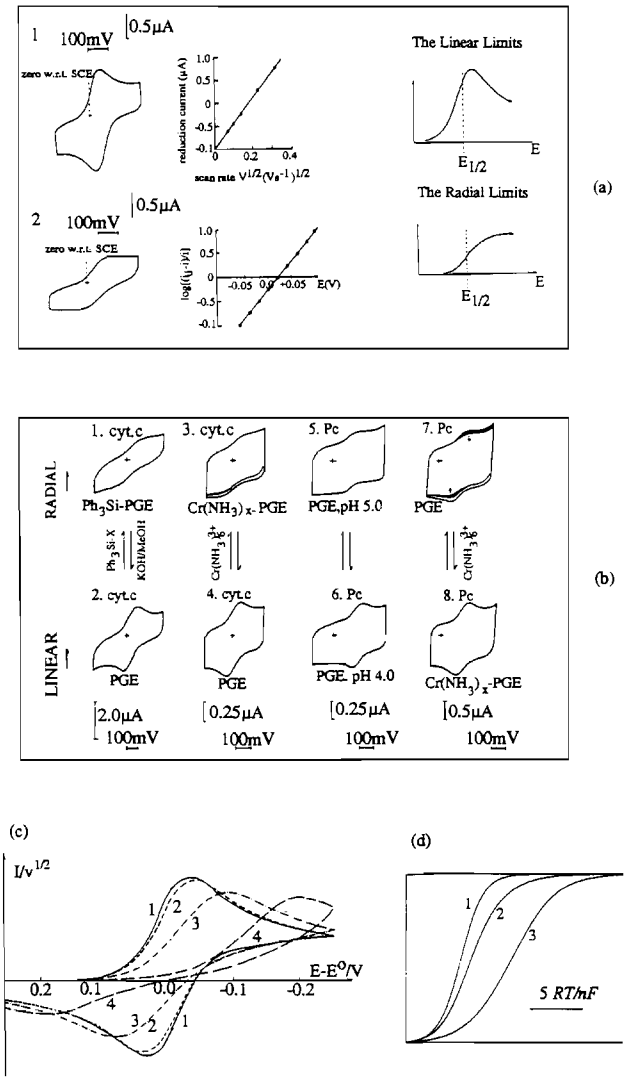

Fig. 11. Range of shapes actually observed (a,b) and those predicted (c,d) in the voltammetry of metalloproteins dissolved in aqueous media at a pyrolytic graphite electrode (PGE) according to the microscopic model described in detail in Refs. [53] and [56]. (a) Cytochrome *c* at (1) a polished edge plane electrode and (2) a freshly cleaved basal plane PGE. Also shown are a plot of peak current for the reduction process at the edge plane electrode vs. the square root of the scan rate, $v^{1/2}$, verifying the predominance of linear diffusion at the polished edge plane surface and a plot of log $[(i_d - i)/i]$ vs. the potential E verifying the predominance of radial diffusion at the basal plane electrode. Reproduced by courtesy: *J. Am. Chem. Soc., 111* (1989) 9185. (b) (1) Cytochrome *c* at a Ph_3Si-modified PGE; (2) as in (1) but at a bare PGE; (3) cytochrome *c* at a $[Cr(NH_3)_6]^{3+}$-modified PGE; (4) as in (3) but at a bare PGE; (5) plastocyanin at a bare PGE at pH 5.0; (6) as in (5) but at pH 4.0; (7) plastocyanin at a bare PGE; (8) as in (7) but at a $[Cr(NH_3)_6]^{3+}$-modified PGE. Reproduced by courtesy: *J. Am. Chem. Soc., 111* (1989) 9185. (c) Effect of decreasing the rate of k_s on transient cyclic voltammograms with mass transport by linear diffusion: (1) reversible response or fast k_s, (2–4) progressively decreasing values of k_s. See Ref. [8] for further details. (d) Effect of decreasing the rate of k_s on steady state voltammograms obtained at a single microdisc electrode with mass transport by radial diffusion: (1) reversible, (2) quasi-reversible, (3) irreversible cases. Reproduced by courtesy: *Anal. Chim. Acta, 216* (1989) 177.

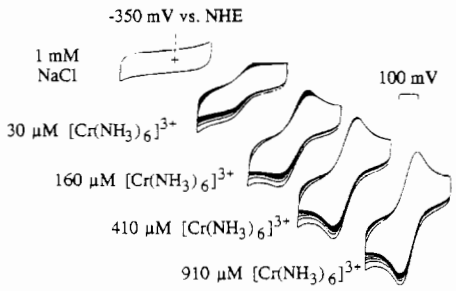

Fig. 12. Cyclic voltammograms for reduction of *Clostridium pasteurianum* 2[4Fe–4S] ferredoxin at an edge plane pyrolytic graphite electrode in the presence of increasing concentrations of $Cr(NH_3)_6^{3+}$. Scan rate = 20 mV s^{-1}; temperature = 25 °C. Reproduced by courtesy: *J. Electroanal. Chem., 217* (1987) 331.

reversible potential of the native form could in fact be regarded as the summation of the current flowing from all the fast reaction pathways for the native form of the metalloprotein. In this sense, metalloproteins appear to act like switches under voltammetric conditions with pathways for electron transfer being either extremely fast or extremely slow. However, with data presented so far, it must be emphasised that the deliberate choice of only providing results of measurements at or near reversible potentials of the native form of the metalloprotein has actually led to a de facto filtering of the fast electron transfer reaction pathways for the native form being achieved. In line with this argument it logically follows that voltammetric studies should also include examination of potentials well removed from the reversible potential. If this is done, additional valuable insights may be gained. For example, Fig. 8(g) shows that at a gold electrode in NaF electrolyte, reduction of adsorbed cytochrome *c* occurs at potentials that are several hundred mV more negative than the reversible potential of native cytochrome *c*. Similarly, at alkaline pH values, a well-defined response is observed for reduction of cytochrome *c* at more negative potentials (Fig. 13(a)) than the native form suggesting that the additional process at more negative potentials results from reduction of a structurally different form of cytochrome *c* [76–78].

In a detailed study of voltammetry and pH-linked conformational changes, Barker and Mauk [78] have demonstrated how the voltammetry of functionally distinct native and alkaline forms of cytochrome *c* are inter-related. In the alkaline form, it is believed that the thio ether of methionine 80 is replaced by a nitrogenous ligand from perhaps a deprotonated amino group of a surface lysine residue. Scheme 5 summarises the proton and conformational equilibria believed to be involved in the alkaline conversion of both ferric and ferrocytochrome *c*. The voltammetry of yeast iso-1-cytochrome *c* at an edge-oriented pyrolytic graphite electrode at neutral and alkaline pH and at two scan rates of 20 mV s^{-1} and 2V s^{-1} is shown in Fig. 13(b).

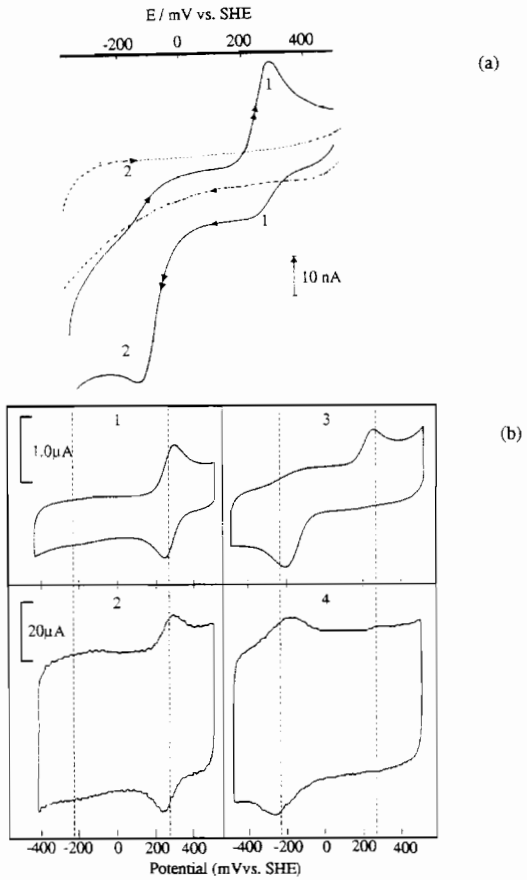

Fig. 13. (a) Cyclic voltammograms (solid line) for reduction of horse heart cytochrome *c* at pH 9.30 at a 4,4-bipyridyl modified gold electrode clearly showing the presence of two processes (designated as 1 for the native form and 2 for the base form). Scan rate = 5 mV s^{-1}, T = 25 °C, dotted line is for the electrolyte without cytochrome *c*. Reproduced by courtesy: *J. Electroanal. Chem., 141* (1982) 91. (b) Cyclic voltammograms (first scans) of yeast iso-1-cytochrome *c* at a pyrolytic graphite electrode and pH 7.1 (1 and 2) and pH 10.3 (3 and 4). Sweep rates were 20 mV s^{-1} (1 and 3) and 2 V s^{-1} (2 and 4). Vertical dashed lines indicate the reversible potential at pH 7.1 of the native form and of the reversible potential at pH 10.3 of the alkaline form. Reproduced by courtesy: *J. Am. Chem. Soc., 114* (1992) 3619.

As for horse heart cytochrome *c* two processes are observed with their relative importance being a function of both scan rate and pH.

The major response observed at neutral pH has a reversible potential of 275 mV versus SHE and is attributed to the native conformation of cytochrome *c*. This process is essentially reversible at both scan rates shown in Fig. 13(b). The voltammetry at pH 10.3 where yeast iso-1-ferricytochrome *c* is predominantly in the alkaline form is similar to that for the horse heart protein. At high pH and slow scan rates, two electron transfer processes are observed neither of which are chemically reversible. On the first negative potential direction scan, no response corresponding to the reduction of the native form is observed. Rather, a reduction process is observed at a much more negative

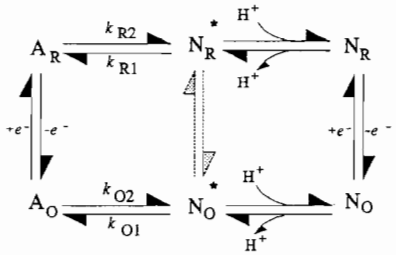

Scheme 5. A minimal scheme describing the conformational equilibria involved in the alkaline transition of cytochrome *c*. N and A refer to the native (Met/His ligation) and alkaline (putative Lys/His ligation) conformations of the protein respectively. Subscripts O and R refer to oxidised and reduced iron. Superscript * denotes a single deprotonated state with respect to the native structure and the rates k_{O1}, k_{O2}, k_{R1}, k_{R2}, describe conformational changes. This scheme omits the changes in protonation accompanying the change of redox state in each individual conformational state. Reproduced by courtesy: *J. Am. Chem. Soc., 114* (1992) 3619.

potential. On the reverse or positive potential direction scan, no oxidation peak is seen at potential values when the alkaline form is reduced, but an oxidation current is observed close to that expected for the oxidation of the native form of the protein. However, the voltammetry in alkaline media is dramatically dependent on sweep rate (Fig. 13(b)). At a scan rate of 2 V s^{-1}, the response at pH 10.3 consists essentially of a single reversible wave with a reversible potential of −230 mV versus SHE. At this scan rate, no electrochemistry is observed around the reversible potential of the native form of the protein. The response at pH 10.3 at the scan below 200 mV s^{-1} is also dependent on the scan number (data not shown). On the second and subsequent cycles a chemically reversible process is observed which is centred on the reversible potential of the native protein (~230 mV). The reduction current observed for both of the reduction processes (second cycle) at a scan rate of 2 V s^{-1} is also a function of pH. Over the pH range 6.5–10.5, the appearance of the reversible wave at around −200 mV versus SHE, attributable to the base form, directly mirrors the disappearance of the wave around +270 mV, attributed to the native form of cytochrome *c*. Using what appears to be only different nomenclature, Bixler et al. [79] have suggested that the process that occurs at negative potentials in the presence of guanidine may be defined as the voltammetry of the folded form of cytochrome *c* whereas the voltammetry of the native form refers to the unfolded form. These authors described their data in terms of the square reaction scheme.

$$\begin{array}{ccc} \text{Fe(III) Cyt.c (folded)} & \rightleftharpoons & \text{Fe(III) Cyt.c (unfolded)} \\ -e^- \downarrow\uparrow +e^- & & -e^- \downarrow\uparrow +e^- \\ \text{Fe(II) Cyt.c (folded)} & \rightleftharpoons & \text{Fe(II) Cyt.c (unfolded)} \end{array} \quad (45)$$

The voltammetry of iso-1-cytochrome *c* can be qualitatively explained by reference to Scheme 5 in which the process at the more positive potentials due to the one-electron reduction, and reoxidation, of native cytochrome *c* is symbolised as ($N_O N_R$) while the process at the more negative potential and which is dominant at high pH and high sweep rates is assigned to the one-electron reduction and reoxidation of the alkaline form is represented by the ($A_O A_R$) notation. According to Scheme 5, both electrochemical reactions for iso-1-cytochrome *c* are coupled to pH dependent conformation reactions which can occur either before or after the electron transfer reactions. However, importantly, once the existence of these steps is recognised and they are deconvoluted from the electron transfer steps, it is clear that the heterogeneous charge transfer steps for both electron transfer processes are very fast. That is, apparent complications in the voltammetry around the E_f^0-value for the native form are a direct result of structural changes accompanying the electron transfer step and not of the electron transfer process itself. The acid–base (folded and unfolded) forms of cytochrome *c* represent major structural change. However, of course many minor conformational changes may also accompany a change in redox state as noted earlier and in Refs. [18,19] and [80–82]. These nuances of the redox processes should also be incorporated into the interpretation of chemically derived redox data. However, such features are not as readily detected in chemically based studies and may be more readily overlooked, or as easily understood as is the case in voltammetric studies. The dependence of cyclic voltammograms on pressure [20] as summarised in Fig. 14, is a direct reflection of the subtleties that may be introduced by structural (volume) change and shows how this feature is readily detected electrochemically.

The relationship between structural change and its influence on redox reactions is an important, but often unsatisfactorily resolved subject. Simplistically, it is often argued that structural change is synonymous with slow rates of electron transfer. However, of course, this need not be the case. The following argument demonstrates that structural change and electron transfer are often separable. In inorganic and organic chemistry, many compounds exist in different conformational or isomeric forms. In principle, conformer C_1, may be reduced to iso-structural conformer $[C_1]^-$ and conformer C_n to $[C_n]^-$ according to Eq. (46), with the processes having reversible potentials of $(E_f^0)_1$ and $(E_f^0)_n$, respectively.

$$\begin{aligned} C_1 + e^- &\overset{(E_f^0)_1}{\rightleftharpoons} [C_1]^- \\ C_n + e^- &\overset{(E_f^0)_n}{\rightleftharpoons} [C_n]^- \end{aligned} \quad (46)$$

Additionally, the conformational interconversion reactions

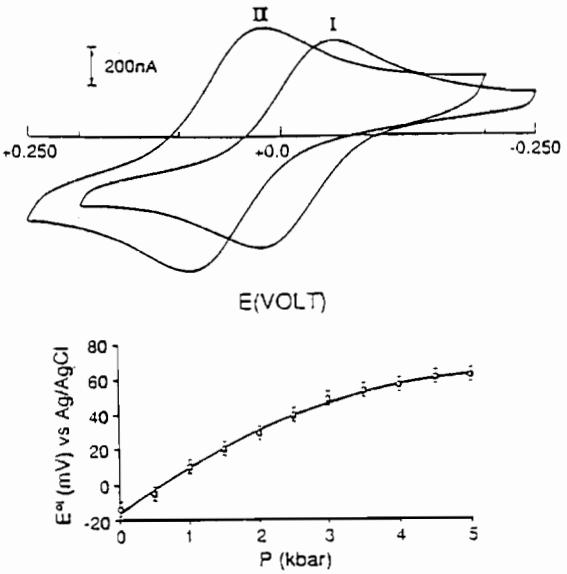

Fig. 14. (a) Cyclic voltammograms of cytochrome *c* at pH 7.0 vs. Ag/AgCl (0.1 M NaCl) at a cysteine modified gold electrode at ambient pressure (I) and at 4 k bar (II). (b) Pressure dependence of the formal potential of cytochrome *c*. Reproduced by courtesy: *J. Am. Chem. Soc., 114* (1992) 9660.

$$C_1 \underset{k_{-1}}{\overset{k_1}{\rightleftharpoons}} C_n \quad \text{and} \quad [C_1]^- \underset{k_{-2}}{\overset{k_2}{\rightleftharpoons}} [C_n]^- \tag{47}$$

may occur prior to or after the electron transfer process to give a square reaction scheme

$$\begin{array}{ccc} C_1 + e^- & \overset{(E_f^0)_1}{\rightleftharpoons} & [C_1]^- \\ \downarrow\uparrow & \times & \downarrow\uparrow \\ C_n + e^- & \overset{(E_f^0)_n}{\rightleftharpoons} & [C_n]^- \end{array} \tag{48}$$

where the cross symbol, ×, represents the homogeneous cross redox reaction

$$[C_n]^- + C_1 \underset{k_{-3}}{\overset{k_3}{\rightleftharpoons}} C_n + [C_1]^- \tag{49}$$

Depending on the separation of the $(E_f^0)_n$ values and the rates of the conformational interconversion (k_1, k_{-1}, k_2, k_{-2}) and cross redox reactions (k_3, k_{-3}), an apparently simple one-electron process, a complex series of processes or a voltammetric time scale dependent response can be observed [17,83]. These square type reaction schemes which involve structurally related compounds having different E_f^0 values are now widely recognised in inorganic and organic voltammetry [17] and they are also emerging as being important in the interpretation of metalloprotein electrochemistry [84]. Such square schemes may equally well apply to chemically based redox reactions, although they are often more difficult to detect.

In accordance with the above concept, the influence of many factors on the reversible potential may be probed by voltammetry. A brief overview of some of these factors is presented below. Numerous papers are available which relate voltammetrically determined E_f^0 values and substituent effects obtained for a series of inorganic or organic compounds. In organic chemistry, the variation of E_f^0 with variation of the 'R group' in an homologous series is often analysed [85] in terms of electronic or inductive effects or Hammett or Taft substituent parameters. In inorganic or organometallic chemistry, ligand substituent or ligand additivity effects have also occupied a great deal of attention [86]. Studies on modified forms of cytochrome *c* and on different forms of plastocyanin also provide well-defined examples of what may be termed substituent effects.

In a particularly interesting study, McLendon and co-workers [87] have voltammetrically measured the E_f^0 values of a series of yeast iso-1-cytochrome *c* proteins obtained by site replacement using oligonucleotide directed mutagenesis. Data are summarised in Table 12. Site replacements, at heme residues 38, 52 and 82 combine to cause large shifts in the E_f^0 values of cytochrome *c*. The data also show that multiple replacements lead to synergistic shifts in potential. Eukaryotic cytochrome *c* proteins have an essentially invariant redox potential (±20 mV). Many investigators have tried to modulate the E_f^0 value [87–90]. However, apart from some of the studies where the axial ligation has been varied and the site replacement studies referred to above, the changes in the cytochrome *c* redox potential observed after structural modification have usually been small (less than 50 mV).

As a further example of what may be called a substituent effect, the reversible potentials obtained [91] as a function of pH with positively charged (+1) *A. variabilis* plastocyanin may be compared to the values (k_{obs}) for the negatively charged (−9) spinach, poplar, cucumber and parsley plastocyanin [16b] (Fig. 15). The considerable shift of E_f^0 is also observed with data obtained via rate measurements [28]. The dependence

Table 12
Reversible potentials of iso-1-cytochrome *c* mutants [87]

Protein	E_f^0 (mV vs. SHE)
Normal (R38 N52 F82)	285
F82S	247
R38A	239
N52I	231
R38A N52I	212
R38A F82S	203
N52I F82S	189
R38A N52I F82S	162

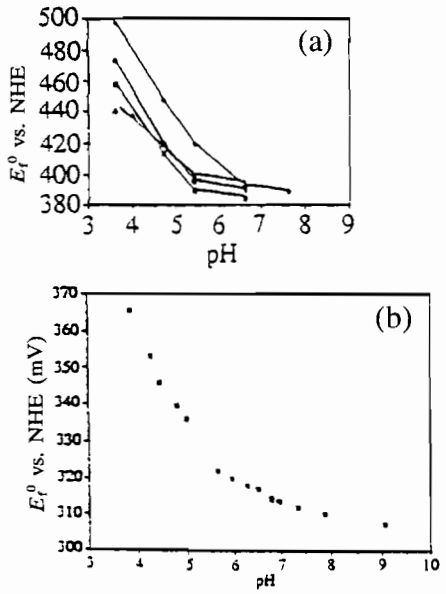

Fig. 15. pH dependence of voltammetrically determined reversible potentials for (a) poplar (▲), cucumber (■), spinach (●) and parsley (◆) plastocyanines and (b) positively charged *A. variabilis* plastocyanin. Reproduced by courtesy: (a) *Inorg. Chem., 31* (1992) 5007; (b) Ref. [91].

on pH for *A. variabilis* is also different to that found for the negatively charged plastocyanins. Apparently the substituent effect which modifies the structure and which leads to a change from an overall negative to a positive charge is thermodynamically important.

The fact that metalloproteins are highly charged entities implies that electrolyte and medium effects could be significant. The variation of formal potential for cytochrome *c* with phosphate buffer concentration has been measured by Hagen [92]. At pH 7, a small shift to more negative potentials is observed with increasing phosphate concentration. This has been attributed to an ionic strength effect [92]. However, small variations in values of E_f^0 with changes in buffer and electrolyte composition also are evident in other literature data [92] and it is difficult to distinguish between specific anion binding and non-specific ionic strength effects.

The E_f^0 value for cytochrome *c* has been studied as a function of pH in 20 mM potassium phosphate buffer [93] at a glassy carbon electrode. The slight decrease in E_f^0 with increase in pH is consistent with the proposed ionic strength dependence. Data as a function of pH have also been obtained in 20 mM potassium phosphate buffer containing 0.1 M $NaClO_4$ to maintain the ionic strength constant and are almost independent of pH. Table 13 provides the reversible potential data [94] for cytochrome *c* at a gold microelectrode (i) in the absence of added electrolyte, (ii) with addition of $NaClO_4$, (iii) with addition of potassium phosphate buffer to a solution containing sodium perchlorate electrolyte. Data for reduction of the inorganic compound, $[Ru(NH_3)_6]^{3+}$, are also included in Table 13. Importantly, the reversible half-wave potential data for both the cytochrome *c* and $[Ru(NH_3)_6]^{3+/2+}$ processes are almost independent of the ionic strength and whether or not buffer is present which suggests that despite the high overall charge on cytochrome *c*, medium effects on E_f^0 are small and similar to medium effects observed for less highly charged inorganic and organic compounds. In a recent paper, McDevitt and Addison [95] have pointed out that the metal centre in native cytochrome *c* is situated inside a folded protein and that this non-polar low dielectric medium is a significant factor determining the magnitude of the E_f^0 value. In this sense, it is therefore perhaps not surprising that modifications to the solution and electrolyte compositions which take place at distances well removed and insulated from the metal centre are not highly significant in determining the E_f^0 value, despite the high overall charge on cytochrome *c*.

While the medium effects on E_f^0 values are small, some very significant electrolyte composition effects have been observed on the shapes of cyclic voltammograms as noted previously. For example, Fig. 12 shows voltammograms obtained at a graphite electrode for a negatively charged ferredoxin as a function of positively charged $[Cr(NH_3)_6]^{3+}$ concentration. In the absence of $[Cr(NH_3)_6]^{3+}$, no response is observed in the reversible potential region. With increasing $[Cr(NH_3)_6]^{3+}$ concentration, the current magnitude increases as the wave shape changes from no response to a sigmoidal shaped wave and then to a peak shaped response. According to the microscopic model [52–56], the presence of positively charged $[Cr(NH_3)_6]^{3+}$ sites on the graphite electrode surface increases the number of electroactive sites available for reduction of negatively charged proteins such as ferredoxin and changes the mass transport mechanism from predominantly radial diffusion at a blocked electrode (low $[Cr(NH_3)_6]^{3+}$ concentration) to predominantly linear diffusion (high $[Cr(NH_3)_6]^{3+}$ concentration). Exactly the inverse effect takes place with positively charged cytochrome *c* [96] or *A. variabilis* plastocyanin [91] where the well-defined peak shaped response at graphite electrodes is suppressed by addition of positively charged cations such as Mg^{2+} or $[Cr(NH_3)_6]^{3+}$. The sign of the overall charge therefore appears to be significant in determining the shape of the voltammetric responses.

In the fifteen years or so since the initial recognition that voltammetric studies of metalloproteins can be undertaken routinely, it is now emerging that not only are the voltammetrically determined E_f^0 values in excellent agreement with earlier potentiometric determinations, but that structural and medium influences on E_f^0 are similar to those observed for decades with simple organic and inorganic compounds. In many

Table 13
The dependence of $E^{r}_{1/2}$ (E_f^0) on electrolyte composition and concentration for the cytochrome *c* and $[Ru(NH_3)_6]^{3+/2+}$ redox processes [94 [a]]

	Ultra-pure water		37 mM $NaClO_4$		Buffer/$NaClO_4$	
	$[Ru(NH_3)_6]^{3+}$	Cyt.*c*	$[Ru(NH_3)_6]^{3+}$	Cyt.*c*	$[Ru(NH_3)_6]^{3+}$	Cyt.*c*
$E^{r}_{1/2}$ (mV vs. SCE)	−230	+30	−225	+20	−225	+20
Nernst slope (mV)	54.8	56.1	57.9	60	58	58.2

[a] Data obtained at a modified gold microelectrode under steady state conditions.

senses, it can therefore be concluded that there is nothing special in metalloprotein voltammetry nor indeed in metalloprotein redox chemistry. The voltammetry of electron transfer metalloproteins seems to be charactcrised by rapid heterogeneous electron transfer at the electrode/solution interface and the only effects specifically related to the proteins seem to arise from their ready denaturation and the sensitivity of the voltammetry of native protein to electrodes blocked by adsorbed and/or denatured protein or impurities present in the protein. The critical factors required to observe well-defined voltammetry appear to be a suitable electrode surface which inhibits electrode blocking and/or highly pure protein. In essence, provided the oxidised or reduced forms of metalloproteins can diffuse to and from a suitable electrode surface, then almost ideal voltammetric responses are observed for the native form of a metalloprotein in the potential region corresponding to the reversible potential.

4.4. Voltammetry of protein–protein complexes

The voltammetry of both surface attached and solution soluble proteins suggests that heterogeneous electron transfer is fast and probably not the rate-determining step in the majority of voltammetric experiments reported to date. To extend the data base available on which to compare chemically and electrochemically derived data, a brief survey of voltammetric data obtained with protein–protein complexes [97] is presented. These data further illustrate that metalloprotein electrochemistry is dominated by fast electron transfer processes.

4.4.1. Cytochrome c–plastocyanin complex

Fig. 16(a) shows cyclic voltammograms obtained at an edge plane graphite electrode for individual solutions of cytochrome *c* (1) and plastocyanin (2) which may be compared to that obtained with 1:1 mixture of each protein (3) which corresponds to conditions where the protein–protein complex is formed. In each case, a response near the reversible potential is obtained suggesting that fast electron transfer occurs for the cytochrome *c*–plastocyanin complex as well as for the individual proteins.

The voltammetry of the cytochrome *c*–plastocyanin complex has also been further investigated [97] by

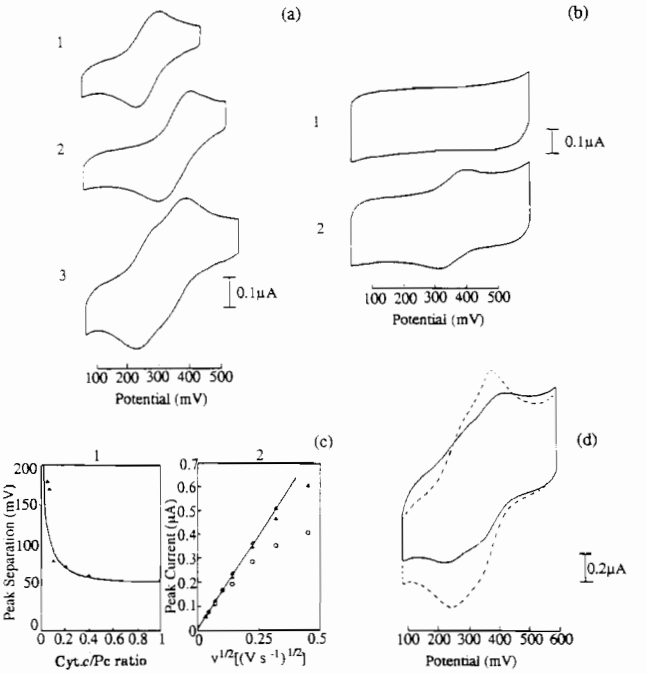

Fig. 16. (a) Cyclic voltammograms of (1) cytochrome *c* (50 μM), (2) plastocyanin (50 μM) and $Cr(NH_3)_6^{3+}$ (2 μM), and (3) cytochrome *c* and plastocyanin (50 μM each) at an edge-plane graphite pyrolytic electrode; pH 7.0. Scan rate: 5 mV s^{-1}. (b) Cyclic voltammogram of (1) Zn(II) cytochrome *c* alone (75 μM), (2) Zn(II) cytochrome *c* and plastocyanin (34 μM each) at an edge-plane graphite pyrolytic electrode. Scan rate: 10 mV s^{-1}. (c) (1) Variation of peak separation with Zn(II) cytochrome c/plastocyanin ratio. Scan rate: 20 mV s^{-1}, (2) variation of peak current with the square root of scan rate, $\nu^{1/2}$, at different Zn(II) cytochrome c/plastocyanin ratios. Ratios: open triangle = 1:1; filled triangle = 1.6; open circle = 1:12. Other conditions as for Fig. 16(b). (d) Cyclic voltammogram of cross-linked (1:1) cytochrome c/plastocyanin (– ~ –) and a 1:1 mixture of 'free' proteins (---) (50 μM). Other conditions as for Fig. 16(b). Reproduced by courtesy: *Biochemistry, 29* (1990) 3213.

substituting Zn(II) cytochrome *c* for Fe(III) cytochrome *c*. Zn(II) cytochrome *c* is redox inactive between potentials of −550 and +850 mV but is structurally identical to the native protein. Fig. 16(b) shows the cyclic voltammograms resulting from a 1:1 mixture of Zn(II) cytochrome *c* and plastocyanin at an edge plane graphite electrode. In this case, only one wave is observed, at a potential of +345 mV, which is attributable to reduction of the plastocyanin component of the complex. As expected the peak currents are proportional

to the plastocyanin concentration rather than the Zn(II) cytochrome *c* concentration. While the shape of the voltammograms changes from sigmoidal to peak shaped (represented by the decrease in 'peak' separation shown in Fig. 16(c)) as the Zn(II) cytochrome *c* to plastocyanin ratio increases, again this change in shape is consistent with a change from radial to linear diffusion as the number of surface active sites increases, presumably supplied by the Zn(II) cytochrome *c* molecules. No change in the response is observed at ratios of Zn(II) cytochrome *c* to plastocyanin of greater than 1:1. There is no difference in the response for the 1:1 mixture at KCl electrolyte concentrations of 1, 5, 10, 20 or 50 mM (constant 20 mM cacodylate buffer), suggesting that the results obtained are independent of the extent of complexation between these two highly charged proteins. All data arc consistent with a very fast rate of electron transfer for the cytochrome *c*–plastocyanin complex.

As noted in Section 1 it has been proposed that protein–protein interactions are highly dynamic and that complexes of different orientations may exist between two interacting proteins. To see if cross-linking the two proteins inhibits the electrochemical response, covalently linked cytochrome *c*–plastocyanin complexes were prepared and studied voltammetrically [97]. The voltammetric responses of the covalent complex at a graphite electrode arc shown in Fig. 16(d). Also shown in Fig. 16(d) is the response of the 'free' 1:1 mixture of cytochrome *c* and plastocyanin. While it is difficult to quantify the details of the response, it is obvious that the linked proteins also give rise to two well-defined responses, which are characterised by fast rates of electron transfer.

4.4.2. *Cytochrome c–cytochrome b_5 complex*

Fig. 17(a), (b) and (c) shows cyclic voltammograms obtained at a graphite electrode for a 1:1 mixture of cytochrome *c* and cytochrome b_5 as well as each protein alone. The two separate redox processes are better resolved than for the cytochrome *c*–plastocyanin complex because of the larger redox potential differences between these two proteins.

The measured reversible potentials for cytochrome *c* and cytochrome b_5 calculated from averaging the reduction and oxidation peak are +270 and −5 mV, respectively. Titration experiments suggest that the peak separations at a given scan rate decrease as the cytochrome *c* to cytochrome b_5 ratio increases until the ratio is 1:1, in thc same manner observed for the cytochrome *c*–plastocyanin complex. However, again this probably reflects a change from predominantly radial to predominantly linear diffusion.

Fig. 17(d) and (e) depicts analogous experiments carried out when Zn(II) cytochrome *c* is substituted for Fe(III) cytochrome *c* which confirms that cytochrome

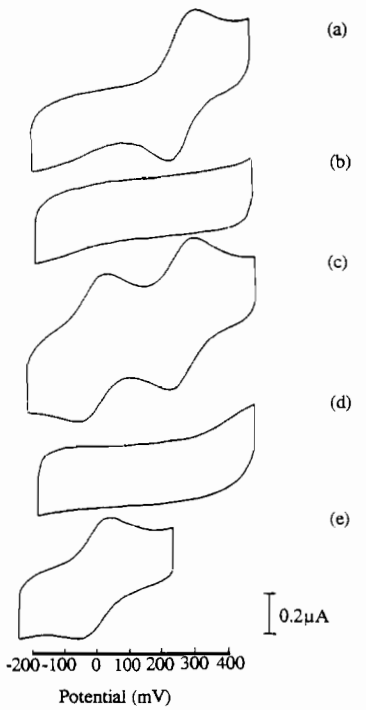

Fig. 17. Cyclic voltammograms of (a) cytochrome *c* alone (95 μM), (b) cytochrome b_5 alone (95 μM), (c) cytochrome *c* with cytochrome b_5 (95 μM each), (d) Zn(II) cytochrome *c* alone (75 μM), and (e) cytochrome b_5 with Zn(II) cytochrome *c* (75 μM each) at an edge-plane pyrolytic graphite electrode; pH 7.0. Scan rate: 10 mV s^{-1}. Reproduced by courtesy: *Biochemistry, 29* (1990) 3213.

c modifies the electrochemistry of cytochrome b_5. However, again, it should not be concluded that the absence of current at the reversible potential is attributable to slow electron transfer. Rather, the presence of a blocked electrode or the absence of a suitable electron transfer site probably causes the change in voltammetry. In summary, the same picture of fast heterogeneous rates of electron transfer emerges for the protein–protein complex, as is the case with the voltammetry of the cytochrome *c*–cytochrome b_5, individual proteins.

4.5. *Voltammetry of modified proteins*

When discussing the chemically derived electron transfer rates of ruthenated and other modified proteins, most of the reversible potentials reported (see Table 9 for examples) were actually obtained from voltammetric studies. In general, a voltammetric response for both the metal and protein redox centres is observed for the modified proteins at potentials close to the values expected on the basis of data obtained from the protein or metal complex, respectively. In particular, reversible voltammetry is observed for the modified protein at the potential expected for the native protein, so that again fast heterogeneous electron transfer is assumed to occur at the electrode modified protein interface. Fig. 18 shows the comparison of the voltam-

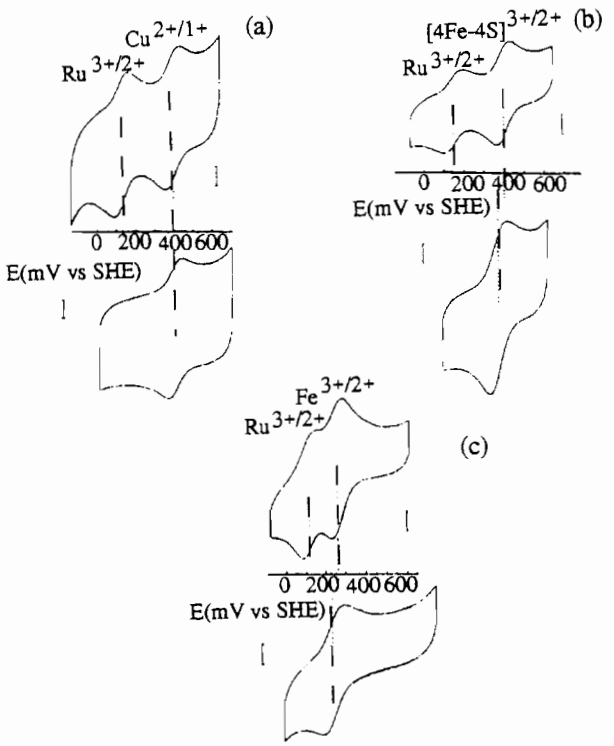

Fig. 18. Cyclic voltammograms of *S. obliquus* plastocyanin, *C. vinosum* $[Fe_4S_4]$ ferredoxin, *P. stutzeri* cytochrome c_{551} and their Ru derivatives: (a) (bottom) 100 μM native Pc (current scale 1.0 μA), (top) 100 μM Pc (His59) $Ru(NH_3)_5$, (pH 7.0, temperature 2 °C, scan rate 20 mV s^{-1}, current scale 0.2 μA); (b) (bottom) native 100 μM $[Fe_4S_4]$ (pH 7.0, temperature 4 °C, scan rate 10 mV s^{-1}, current scale 0.1 μA), (top) 130 μM $[Fe_4S_4]$ (His42) $Ru(NH_3)_5$, (pH 7.0, temperature 1 °C, scan rate 10 mV s^{-1}, current scale 0.2 μA); (c) (bottom) 150 μM native cytochrome c_{551} (pH 7.0, temperature 25 °C, scan rate 10 mV s^{-1}, current scale 0.2 μA), (top) 100 μM cytochrome c_{551} (His47) $Ru(NH_3)_5$ (pH 7.0, temperature 25 °C, scan rate 20 mV s^{-1}, current scale 0.4 μA). Broken vertical lines indicate positions of E_f^0. Reproduced by courtesy: *Inorg. Chem., 29* (1990) 4858.

metry [98] of ruthenium modified plastocyanin, cytochrome *c* and [4Fe–4S] ferredoxin and the native proteins to verify this feature.

4.6. Conclusions from the voltammetric data

The voltammetric data surveyed above imply that after allowance is made for blocked electrodes giving rise to small electroactive areas and mixtures of radial and linear diffusion, the existence of conformationally different forms of the protein, conformational changes accompanying electron transfer and adsorption of proteins, there is at least one pathway for which the rate of electron transfer between the native form of simple metalloproteins and an electrode is intrinsically fast. Given that metalloproteins are dynamic molecules, it is conceivable that concurrently with diffusion towards or away from the electrode, that rotational diffusion (giving rise to conformational changes) can occur in a time-resolved sense from the electron transfer process. If this occurs, then a suitable configuration can be achieved for electron transfer at the solution/electrode interface with solution soluble forms of the protein with virtually no structural change being required during the actual electron transfer step. Furthermore, for the simple electron transfer metalloproteins discussed in this article, there does not appear to be any reason why the metal centre cannot approach within 10 Å of the electrode, and if this is the case, then there would appear to be no barrier to prevent rapid electron transfer.

An alternative, but phenomenologically equivalent explanation of the observation of fast heterogeneous electron transfer rates for a wide range of proteins has been proposed by Hawkridge and co-workers [99]. After noting that fast rates of electron transfer have been reported for cytochrome *c* and cytochrome c_{553} under a wide range of conditions both at bare metal electrodes, carbon electrodes and modified electrodes, and recognising that these two heme proteins differ from each other considerably with respect to their size, redox potential, surface charge at neutral pH, dipole moment, conformation and biological function, Hawkridge and co-workers proposed [99] that early attempts to model the cytochrome *c* reactions at electrodes based on the need for suitable hydrophobicity of the electrode surface/solution interface, suitable electrostatic and dipole–dipole interactions and weak adsorption need to be reconsidered. Recent work [52] has actually demonstrated that these factors are important in determining the effective available electrode areas for electron transfer but that they do not necessarily catalyse or inhibit the heterogeneous charge transfer rate constant itself. In accordance with a fundamental electrochemical concept, if a diffusion controlled current is observed at the reversible potential, then this means that the diffusion process rather than the heterogeneous electron transfer step is rate determining, which is the case for simple electron transfer metalloproteins, and which by definition therefore means that k_s is fast.

Voltammetric data suggest that for simple proteins the distance between the metal redox centre and the electrode is not critical and that dynamic rotational diffusion may mean no special factors need be introduced to explain the facile nature of electron transfer reactions of metalloproteins at electrodes. Fast rates of electron transfer are assumed to be common because distances of electron transfer never need to exceed more than about 10 Å in the simple metalloproteins considered in this review. Alternatively, it may be argued that the electron transfer reactions may involve electron tunnelling reactions between the metal centre and the electrode. Using an electrochemical quantum model,

it has been calculated that the threshold tunnelling distance leading to substantial decreases in electron transfer rates is around 18 Å [100]. The distance of closest approach between the protein metal redox centre and electrode for the metalloproteins considered in the electrochemical component of this review certainly would be less than 18 Å regardless of molecular orientation at an electrodc/solution intcrface even after including relevant solvent terms.

The application of shorter time domain voltammetric methods than have been applied so far, may enable the electron transfer rate to be resolved from the diffusion process in a manner which may enable a k_s versus distance relationship to be observed. However, k_s values are probably so fast that reliable k_s versus electron transfer distance correlations are going to be difficult to elucidate unambiguously at the electrode solution interface and therefore theory relating homogeneous electrochemical and homogeneous chemical redox reactions presented in this review is difficult to utilise. Furthermore, double layer corrections required to determine k_s^t are also difficult to include in the theory.

One metalloprotein that may have a protein–electrode electron transfer distance in excess of 18 Å and which therefore could exhibit small values of k_s is myoglobin [100]. As noted in the section on chemical redox data, while myoglobin does not function physiologically as an electron transfer carrier, it will undergo oxidation and reduction at the heme centre. Many examples of homogeneous redox rate data are available for this protein and rates are slow (Fig. 5(b)). Myoglobin is a small heme protein found in muscle cells [99]. A single polypeptide chain of 153 amino acid residues surrounds the porphyrin ring containing the iron and the structure is similar to one of the four units of hemoglobin. X-ray diffraction and other data show that the sequences of the amino acids are similar for many species. Further details known are that (a) 70% of the polypeptide chain is α-helical, (b) the polar residues in the chain are distributed over the outer surface of the molecule and are hydrogen-bonded to water, (c) the non-polar residues occur either on the inner surfaces of the α-helices and stabilise the heme, and (d) only the edge of the heme with the two propionic acid groups is exposed to polar solvent so that the iron centre may be well removed from the electrode surface.

The electron transfer process which occurs when myoglobin is either rcduced or oxidised at an electrode can be represented by Eq. (50).

$$[\text{myoglobin, Fe(III)}] + e^- \overset{Ef^0, k_s, \alpha}{\rightleftharpoons} [\text{myoglobin, Fe(II)}] \quad (50)$$

Quasi-reversible electron transfer kinetics have been reported for sperm whale myoglobin at tin-doped indium oxide electrodes [101] with a value of $k_s = (2.6 \pm 0.5) \times 10^{-5}$ cm s^{-1} and $\alpha = (0.48 \pm 0.05)$ being obtained from cyclic voltammetry, single step chronoabsorptometry and derivative voltabsorptometry (the latter two methods couple optical spectroscopic methods with the electrochemistry). Fig. 19(a) and (b) shows large peak-to-peak separations in cyclic type experiments which are consistent with slow rates of electron transfer. Other studies of the electrochemistry of myoglobin provide a range of rates of electron transfer [101–109] and apparently adsorption, protein purity and the nature of the electrode are all important in determining the reported value of k_s and α. Thus, unfortunately, the true k_s value for myoglobin is not yet clear, but there is a possibility that it may be slower than other metalloproteins because of the long distance required for the charge transfer process.

Some information is known on the structural changes which accompany the myoglobin electron transfer step [111]. The iron atom of [myoglobin, Fe(II)] lies 55 pm out of the mean porphyrin plane, with the bond between the His93 nitrogen and the Fe(II) centre making an 11° angle from the normal to the heme. The porphyrin, itself, bends toward the iron giving a domed effect. In [myoglobin, Fe(III)], the iron is pulled a distance of 15 pm into the heme plane, and the angle with the normal becomes 4°, with the domed effect remaining. This change within the heme is known to be accompanied by a conformational change in the helical structure.

The iron in the heme is coordinated at the fifth position to a nitrogen atom in the imidazole ring of His93. When the iron is in its natural reduced form, the sixth position is free to bind to species such as dioxygen, carbon monoxide or nitric oxide. A water molecule is usually the sixth ligand in the oxidised

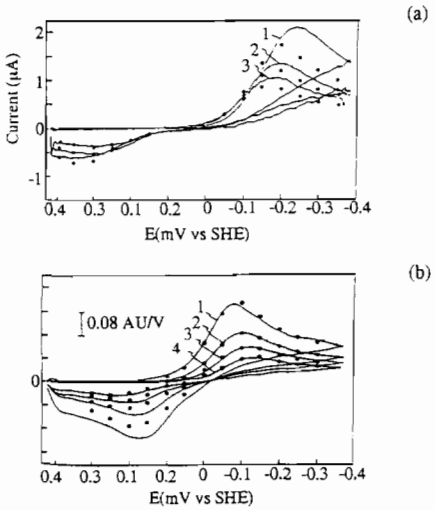

Fig. 19. (a) Cyclic voltammograms for 54 μM myoglobin. Scan rates: 1, 200; 2, 100; 3, 50 mV s^{-1}. (b) Derivative cyclic voltabsorptammograms of 63 μM myoglobin. Scan rates: 1, 2.48; 2, 6.30; 3, 12.4; 4, 24.6 mV s^{-1}. Dots show calculated values. Reproduced by courtesy: *J. Electroanal. Chem., 237* (1987) 81.

form. In both the oxidised and reduced forms, the nitrogen of His64, is thought to make contact with the bound dioxygen or water. While the interpretation of a slow k_s value for myoglobin is open to question and values are probably only apparent k_s values and certainly not k_s^t, a correlation with homogeneous redox data may exist for myoglobin in the sense that k_s and k_{et} values are both very slow. Further electrochemical studies on this protein may therefore be valuable in understanding rate–distance relationships.

In reality, most electrochemical data for myoglobin as well as other proteins are probably complicated by the presence of a mixture of adsorption and diffusion (linear and radial), as well as the fact that both bulk solution and surface-based processes occur simultaneously. This, of course, leads to almost mind-boggling difficulty in interpretation of data since structural changes and dynamics of the protein and electrode/solution interface also need to be understood and included in the theoretical description. To solve these problems will almost certainly require a combination of electrochemical and spectroscopic methods. Spectral techniques such as NMR have been successfully applied to study the dynamics of the redox proteins [112] and IR methods and other spectroscopic methods applied in conjunction with electrochemistry should also be useful in this context [113] as may in situ surface methods such as ellipsometry and tunnelling microscopy [114] to probe the interfacial region. In this sense, it is probably too premature to apply Marcus–Hush type theories to electrode processes as too many ambiguities still exist in the interpretation of the majority of the data.

Finally, it is obvious that numerous electrochemical studies involve addition of reagents to solutions to promote well-defined voltammetry. Most attention in these studies has been devoted to the modification that occurs at the electrode surface, but these reagents could also modify the protein. Of course, modifications of proteins may also occur with chemical-based redox studies. In many studies it has been implied that the modifications to the electrode surface and/or protein are innocent in the thermodynamic sense. That is, it has been assumed that the E_f^0 values are unaltered by the modification of proteins at sites well removed from the metal centre. However, recent detailed studies suggest that this approximation is not necessarily a good one. For example, the studies by Rivera et al. [115] related to cytochrome b_5 have been summarised as follows.

(i) Reversible cyclic voltammetry of recombinant rat outer membrane cytochrome b_5 is observed at a gold electrode modified with β-mercaptopropionic acid.

(ii) The voltammetric response associated with electron transfer between the negative electrode surface and the negatively charged cytochrome b_5 is promoted by the addition of divalent metal ions such as Mg^{2+} or Ca^{2+} and by the positively charged species poly-L-lysine.

(iii) The titration of cytochrome b_5 (0.1 mM) with poly-L-lysine results in a gradual positive shift of the $E_{1/2}$ value which levels off at +8 mV versus NHE when the poly-L-lysine:cytochrome b_5 ratio reaches a value of 2:1. Since the further addition of poly-L-lysine has no effect on the $E_{1/2}$ value of the protein, it may be concluded that a complex is formed in which two molecules of poly-L-lysine bind to each molecule of cytochrome b_5.

(iv) When the cytochrome b_5–poly-L-lysine complex (0.1 mM) is titrated with Mg^{2+} or Ca^{2+} ions, the $E_{1/2}$ value shifted gradually in the negative direction and levels off at −40 mV versus NHE when the concentration of divalent ions reaches 85 mM.

(v) There is a large dependence of the reduction potential of cytochrome b_5 on the type (Mg^{2+}, Ca^{2+}, $[Cr(NH_3)_6]^{2+}$ etc.) and concentration of multivalent ions present in solution. A reduction potential of −102 mV versus NHE is obtained from cytochrome b_5 (0.60 mM) by spectroelectrochemical titration in the presence of 0.4 mM $[Ru(NH_3)_6]^{3+}$ and 1 mM methyl viologen, pH 7.0, ionic strength = 0.1 M. This value is approximately 100 mV more negative than the reduction potentials reported for microsomal cytochromes b_5 obtained from other sources.

(vi) The differences in reduction potential observed for cytochrome b_5 in the presence of $MgCl_2$ or poly-L-lysine are believed to be due to modification of surface charge near the heme brought about by the binding of $MgCl_2$ or poly-L-lysine. The results indicate that the large density of positive charge introduced by the binding of two molecules of poly-L-lysine results in a positive shift of reduction potential, while the binding of Mg^{2+} to the surface of the protein does not reverse the negative charge on the surface of the cytochrome b_5.

(vii) The reduction potential of cytochrome b_5 may be modulated by physiological concentrations of Ca^{2+} or Mg^{2+} ions and by complex formation with complementarily charged physiological partner proteins.

When the cytochrome b_5 data [115] is combined with equivalent data reported for plastocyanin [91] as well as other data presented in this article, and it is recognised that Mg^{2+} and Ca^{2+} are biologically relevant, then it may be concluded that the importance of redox inactive cations in modulating the in vitro electron transfer of redox active metalloproteins may need to be carefully considered or even re-evaluated in future investigations. At the very least, the role of charged reagents employed in chemical or electrochemical investigations cannot be assumed to be innocent without detailed investigation.

5. Conclusions based on comparison of chemical and electrochemical metalloprotein redox data

The general conclusion reached after critical evaluation of metalloprotein electron transfer data is that there are still many complexities and apparent contradictions that remain to be unravelled. A major difficulty with both solution phase chemical and electrochemical studies of simple metalloproteins is the separation of diffusion and conformational changes that occurs at sites well removed from the metal protein centre from the homogeneous or heterogeneous electron transfer step. Furthermore, the molecules are dynamic and even in the case of electron transfer reactions associated with chemically modified proteins and electrochemical electron transfer reactions of proteins attached to electrode surfaces, the problem of separating the conformational and electron transfer steps still remains. As noted in Section 1, cytochrome *c* for which by far the most metalloprotein redox data are available, represents a particularly complex redox reaction, given that rather substantial conformational changes are known to take place during the course of the overall Fe(III)/Fe(II) redox process. Additionally, significant changes in reversible potentials occur when mutant forms of this metalloprotein are synthesised [87] suggesting that considerable mechanistic and kinetic variations are likely to occur with the mutant forms. Furthermore, the presence of biologically relevant redox inactive cations such as Mg^{2+} and Ca^{2+} may significantly modulate both thermodynamic and kinetic aspects of the electron transfer process. In many electron transfer studies it is therefore still not clear whether or not structural changes have been adequately deconvoluted in studies when electron transfer rates are reported. However, intrinsically, if steps involving structural change can be resolved from the electron transfer step there seems no reason why the true electron transfer rate should not be very fast for most simple electron transfer metalloproteins. Finally, on the basis of this overview, it may be proposed that applying both chemical and electrochemical methodologies to the complex problem of electron transfer reactions should be attempted in a broader context than is presently the case. The problem being addressed is inherently far more difficult than is the case with small organic or inorganic molecules so that the probable synergistic value of tackling the problem from more than one approach should not be overlooked.

In voltammetric work, detailed studies have shown that after careful treatment of the mass transport problem and careful attention to treatment of the electrodes and purity of the protein, k_s values for biologically important simple electron transfer metalloproteins generally are fast, although with myoglobin the rates may be slower than for cytochrome *c*, plastocyanin and other moieties considered in this review. For proteins bound to an electrode surface, where less data are available, results again suggest that after allowance is made for conformational changes that the rate of the electron transfer step is very fast.

In the field of chemical redox chemistry, there are reports of slow rates of electron transfer in the literature where the electron transfer distance should be small and little structural change accompanies the redox process. Interestingly, these slow rates do not commonly translate to slow rates of heterogeneous electron transfer at the electrode/protein interface. In the case of cytochrome *c*, rotational diffusion and/or conformational changes may still have to be deconvoluted from the rate data, and gating mechanisms may be operative so that reported rates do not necessarily measure or reflect the true rate of electron transfer. Even with studies on modified proteins, and particularly for overall slow reactions it is always likely to be difficult to separate the diffusion controlled homogeneous pathway from the electron transfer step, as is required, and from conformational changes which may be relatively fast in what are probably dynamic molecules. However, based on chemical intuition as much as science, it seems more likely in time that many of the slow rates reported to date will be demonstrated to be a result of incomplete deconvolution of reactions coupled to electron transfer and that the general picture will emerge that there is at least one pathway for electron transfer in simple proteins that is an intrinsically fast process no matter how the electron transfer process is initiated, or whether the electrochemical step is examined via a homogenous or heterogeneous technique. There may, in fact, be a range of pathways available which is detected by different time domain methods of measurement. For example, voltammetry at or near E_f^0 will selectively detect k_s values close to the diffusion controlled limit. With chemical methods, slower pathways may in fact be easier to detect than the close to diffusion controlled pathways. At present, it has not been possible to successfully demonstrate that homogeneous k_{et} and electrochemical k_s^1 values are compatible using existing theory. This could be because a Marcus-type theory is not applicable to these complex processes or else the required data has not been obtained free of artifacts related to structural or other changes accompanying the electron transfer step. However, unambiguously, it can be concluded that a great many more studies will be required to achieve a further understanding of this complex and fascinating field of metalloprotein electron transfer reactions.

Acknowledgements

The topic for this overview of metalloprotein redox chemistry from both chemical and electrochemical per-

spectives was conceived during the author's period of leave from La Trobe University at the Inorganic Chemistry Laboratory, Oxford University, in 1991 as the Robert Boyle Fellow in Analytical Chemistry. A.M.B. therefore has much pleasure in expressing his gratitude to the Trustees of the Royal Society of Chemistry Analytical Chemistry Trust for making the award on the occasion of the 150th Anniversary of the Society and, coincidentally the 300th Anniversary of the death of Robert Boyle. Much of the motivation for writing this review came from encouragement and advice from Allen Hill who acted as the host for the period of the Fellowship. The author would also like to acknowledge other colleagues at the Inorganic Chemistry Laboratory, for invaluable scientific discussion which led to some of the concepts contained in this review and for hospitality during the period of the Fellowship. Finally, the author expresses his appreciation to La Trobe University for granting leave to take up the Fellowship.

References

[1] C.J. Murphy, M.R. Arkin, Y. Jenkins, N.D. Ghatlia, S.H. Bossmann, N.J. Turro and J.K. Barton, *Science, 262* (1993) 1025; R. Baum, *Chem. Eng. News,* (Nov. 29) (1993) 52.

[2] B.E. Bowler, A.L. Raphael and H.B. Gray, *Prog. Inorg. Chem., 38* (1990) 259, and refs. therein.

[3] L. Poulos and B.C. Finzel, in M.T.W. Hearn (ed.), *Peptide and Protein Reviews,* Vol. 4, Marcel Dekker, New York, 1984, pp. 115–171.

[4] H. Pelletier and J. Kraut, *Science, 258* (1992) 1748.

[5] H. Taube, *Electron Transfer Reactions of Complex Ions in Solution,* Academic Press, New York 1970; *Pure Appl. Chem., 44* (1975) 25; (b) A. Haim, *Acc. Chem. Res., 8* (1975) 264; *Prog. Inorg. Chem., 30* (1983) 273; (c) R.A. Marcus and N. Sutin, *Biochim. Biophys. Acta, 811* (1985) 265.

[6] R.M. Baum, *Chem. Eng. News,* (Feb. 22) (1993) 20.

[7] L.-H. Guo and H.A.O. Hill, *Adv. Inorg. Chem., 36* (1991) 341, and refs. therein.

[8] (a) A.J. Bard and L.R. Faulkner, *Electrochemical Methods,* Wiley, New York, 1980; (b) R. Greef, R. Peat, L.M. Peter, D. Pletcher and J. Robinson, *Instrumental Methods in Electrochemistry,* Ellis Horwood, Chichester, UK, 1985, and refs. therein.

[9] (a) F.A. Armstrong, *Struct. Bonding (Berlin), 72* (1990) 137; (b) *Perspect. Bioinorg. Chem., 1* (1991) 141; (c) *Adv. Inorg. Chem., 38* (1992) 117.

[10] W.J. Albery, M.J. Eddowes, H.A.O. Hill and A.R. Hillman, *J. Am. Chem. Soc., 103* (1981) 3904.

[11] R.J.P. Williams, *Biochim. Biophys. Acta, 1058* (1991) 71, and refs. therein.

[12] (a) R.A. Marcus, *J. Chem. Phys., 24* (1956) 966; (b) *Ann. Rev. Phys. Chem., 15* (1964) 155; (c) P.N. Barlett, P. Tebbutt and R.G. Whitaker, *Prog. React. Kinet., 16* (1992) 55.

[13] B.L. Vallee and R.J.P. Williams, *Proc. Natl. Acad. Sci. U.S.A., 59* (1968) 498.

[14] (a) P.M. Colman, H.C. Freeman, J.M. Guss, M. Murata, V.A. Norris, J.A.M. Ramshaw and M.P. Venkatappa, *Nature (London), 272* (1978) 319; (b) J.M. Guss and H.C. Freeman, *J. Mol. Biol., 169* (1983) 521; (c) J.M. Guss, P.R. Harrowell, M. Murata, V.A. Norris and H.C. Freeman, *192* (1986) 361.

[15] (a) M.G. Segal and A.G. Sykes, *J. Am. Chem. Soc., 100* (1978) 4585; (b) J.D. Sinclair-Day and A.G. Sykes, *J. Chem. Soc., Dalton Trans.,* (1986) 2069; (c) M.P. Jackman, J.D. Sinclair-Day, M.J. Sisley, A.G. Sykes, L.A. Denys and P.E. Wright, *J. Am. Chem. Soc., 109* (1986) 6443; (d) J.M. McGinnis, J.D. Sinclair-Day, A.G. Sykes, R. Powls, J. Moore and P.E. Wright, *Inorg. Chem., 27* (1988) 2306; (e) A.G. Sykes, *Adv. Inorg. Chem., 36* (1991) 377; (f) P. Osvath, G.A. Salmon and A.G. Sykes, *J. Am. Chem. Soc., 110* (1988) 7114; (g) M.P. Jackman, J.M. McGinnis, R. Powls, G.A. Salmon and A.G. Sykes, *J. Am. Chem. Soc., 109* (1988) 5880, and refs. therein.

[16] (a) F.A. Armstrong, H.A.O. Hill, B.N. Oliver and D. Whitford, *J. Am. Chem. Soc., 107* (1985) 1473; (b) F.N. Büchi, A.M. Bond, R. Codd, L.N. Huq and H.C. Freeman, *Inorg. Chem., 31* (1992) 5007, and refs. therein.

[17] D.H. Evans and K.M. O'Connell, *Electroanal. Chem., 14* (1986) 113.

[18] G.V. Louie and G.D. Brayer, *J. Mol. Biol., 210* (1989) 313.

[19] A.M. Berghuis and G.D. Brayer, *J. Mol. Biol., 223* (1992) 959, and refs. therein.

[20] M.T. Cruañes, K.K. Rodgers and S.G. Sligar, *J. Am. Chem. Soc., 114* (1992) 9660.

[21] R.J.P. Williams, *Adv. Chem. Ser., 226* (1990) 3.

[22] P.L. Drake, R.T. Hartshorn, J. McGinnis and A.G. Sykes, *Inorg. Chem., 28* (1989) 1361.

[23] J.D. Rush, W.H. Koppenol, E.A.E. Garber and E. Margoliash, *J. Biol. Chem., 263* (1988) 7514.

[24] A.G. Sykes, *Met. Ions Biol. Syst., 27* (1991) 291, and refs. therein.

[25] M.J. Therien, M. Selman, H.B. Gray, I.-J. Chang and J.R. Winkler, *J. Am. Chem. Soc., 112* (1990) 2420.

[26] D.W. Dixon and X. Hong, *Adv. Chem. Ser., 226* (1990) 161.

[27] D.G.A. Harshani de Silva, D. Beoku-Betts, P. Kyritsis, K. Govindaraju, R. Powls, N.P. Tomkinson and A.G. Sykes, *J. Chem. Soc., Dalton Trans.,* (1992) 2145, and refs. therein.

[28] N.M. Kostic, *Met. Ions Biol. Syst., 27* (1991) 129.

[29] G. McLendon, *Met. Ions Biol. Syst., 27* (1991) 183, and refs. therein.

[30] R.A. Scott, D.W. Conrad, M.K. Eidsness, A.C.F. Gorsen and S.A. Wallin, *Met. Ions Biol. Syst., 27* (1991) 199.

[31] J.R. Winkler and H.B. Gray, *Chem. Rev., 92* (1992) 369, and refs. therein.

[32] (a) C.C. Moser, K. Warncke, J.M. Keske and P.L. Dutton, *Inorg. Biochem., 43* (1991) 91; (b) C.C. Moser, J.M. Keske, K. Warncke and P.L. Dutton, in A. Muller (ed.), *Electron and Proton Transfer in Chemistry and Biology, Proc. Bielefeld Workshop, Bielefeld, Germany, Sept. 1990.*

[33] M.R. Gunner and P.L. Dutton, *J. Am. Chem. Soc., 111* (1989) 3400, and refs. therein.

[34] C.C. Moser, J.M. Keske, K. Warncke, R.S. Farid and P.L. Dutton, *Nature (London), 355* (1992) 796, and refs. therein.

[35] B. Durham, L.P. Pan, S. Hahm, J. Long and F. Milett, *Biochemistry, 28* (1989) 8659; *Adv. Chem. Ser., 226* (1990) 181.

[36] S.S. Isied, *Adv. Chem. Ser., 226* (1990) 91; *Met. Ions Biol. Syst., 27* (1991) 1.

[37] H.B.Gray and J.R. Winkler, *Pure Appl. Chem., 64* (1992) 1257.

[38] D.N. Beratan, J.N. Onuchic, J.R. Winkler and H.B. Gray, *Science, 258* (1992) 1740, and refs. therein.

[39] J.N. Onuchic, D.N. Beratan, J.R. Winkler and H.B. Gray, *Annu. Rev. Biophys. Biomol. Struct., 21* (1992) 349, and refs. therein.

[40] D.N. Beratan, J.N. Betts and J.N. Onuchic, *Science, 252* (1992) 1285, and refs. therein.

[41] D.S. Wuttke, M.J. Bjerrum, J.R. Winkler and H.B. Gray, *Science, 256* (1992) 1007.

[42] D.S. Wuttke, M.J. Bjerrum, I.-J. Chang, J.R. Winkler and H.B. Gray, *Biochim. Biophys. Acta, 1101* (1992) 168.

[43] J.N. Onuchic and D.N. Beratan, *J. Chem. Phys., 92* (1990) 722.

[44] D.N. Beratan, J.N.Betts and J.N. Onuchic, *J. Phys. Chem., 96* (1992) 2852.
[45] (a) R.A. Marcus, *J. Chem. Phys., 43* (1965) 679; *Electrochim. Acta, 13* (1968) 955; (b) N.S. Hush, *J. Chem. Phys., 28* (1958) 962; *Trans. Faraday Soc., 57* (1961) 557; *Electrochim. Acta, 13* (1968) 1005.
[46] (a) V.G. Levich, in P. Delahay and C.W. Tobias (eds.), *Advances in Electrochemistry and Electrochemical Engineering,* Interscience, New York, 1966, pp. 249–371; (b) R.R. Dogonadze, in N.S. Hush (ed.), *Reactions of Molecules at Electrodes,* Wiley-Interscience, New York, 1971, Ch. 3.
[47] (a) J.P. Brenet and K. Traore, *Transfer Coefficients in Electrochemical Kinetics,* Academic Press, London, 1971; (b) M.J. Weaver, in A.F. Silva (ed.), *Trends in Interfacial Electrochemistry,* Reidel, Dordrecht, Netherlands, 1986, pp. 281–299.
[48] (a) H. Angerstein-Kozlowska and B.E. Conway, *J. Electroanal. Chem., 95* (1979) 1; (b) E. Laviron and L. Roullier, *J. Electroanal. Chem., 115* (1980) 65; (c) H. Daifuku, K. Aoki, K. Tokuda and H. Matsuda, *J. Electroanal. Chem., 183* (1985) 1.
[49] C.E.D. Chidsey, *Science, 251* (1991) 919.
[50] P. van Dulm, W. Norda and J. Lyklema, *J. Colloid Interface Sci., 82* (1981) 77, and refs. therein.
[51] T. Yukota, K. Itoh and A. Fujishima, *J. Electroanal. Chem., 216* (1987) 289.
[52] A.M. Bond and F. Büchi, *J. Electroanal. Chem., 314* (1991) 191.
[53] A.M. Bond and H.A.O. Hill, *Met. Ions Biol. Syst., 27* (1991) 431.
[54] F.A. Armstrong, A.M. Bond, H.A.O. Hill, I.S.M. Psalti and C.G. Zoski, *J. Phys. Chem., 93* (1989) 6485.
[55] F.A. Armstrong, A.M. Bond, H.A.O. Hill, B.N. Oliver and I.S.M. Psalti, *J. Am. Chem. Soc., 111* (1989) 9185.
[56] A.M. Bond, *Anal. Proc., 29* (1992) 132; *30* (1993) 218.
[57] M. Collinson and E.F. Bowden, *Anal. Chem., 64* (1992) 1470.
[58] J.L. Willit and E.F. Bowden, *J. Phys. ,Chem., 94* (1990) 8241.
[59] V.A. Bogdanovskaya, M.R. Tarasevich, R. Hintsche and F. Scheller, *J. Electroanal. Chem., 253* (1988) 581.
[60] V.A. Bogdanovich, M.R. Tarasevich, E.D. German and E.F. Gavrilova, *Elektrokhimiya, 25* (1989) 964.
[61] I. Taniguchi, M. Iseki, T. Eto, K. Toyosawa, H. Yamaguchi and K. Yasukouchi, *Bioelectrochem. Bioenerg., 13* (1984) 373.
[62] M.J. Tarlov and E.F. Bowden, *J. Am. Chem. Soc., 113* (1991) 1847.
[63] J.H. Reeves, S. Song and E.F. Bowden, *Anal. Chem., 65* (1993) 683.
[64] K. Niki, *Denki Kagaku Oyobi Kogyo Butsuri Kagaku, 61* (1993) 382.
[65] N. Nakashima, K. Abe, T. Horohashi, K. Hamada, M. Kunitake and O. Manabe, *Chem. Lett.,* (1993) 1021.
[66] D. Datta, H.A.O. Hill and H. Nakayama, *J. Electroanal. Chem., 324* (1992) 307.
[67] M. Caselli, M. Della Monica and M. Portacci, *J. Electroanal. Chem., 319* (1991) 361.
[68] M. Collinson, E.F. Bowden and M.J. Tarlov, *Langmuir, 8* (1992) 1247.
[69] Z. Salamon and G. Tollin, *Bioelectrochem. Bioenerg., 25 (1991) 447.*
[70] J.N. Butt, F.A. Armstrong, J. Breton, S.J. George, A.J. Thomson and E.C. Hatchikian, *J. Am. Chem. Soc., 113* (1993) 6663.
[71] J.N. Butt, A. Sucheta, L.L. Martin, B. Shen, B.K. Burgess and F.A. Armstrong, *J. Am. Chem. Soc., 115* (1993) 12587.
[72] A. Szucs, G.D. Hitchens and J.O'M. Bockris, *Electrochim. Acta, 37* (1992) 403.
[73] T. Sagara, K. Niwa, A. Sone, C. Hinnen and K. Niki, *Langmuir, 6* (1990) 254.
[74] Z. Salamon and G. Tollin, *Bioelectrochem. Bioenerg., 27* (1992) 381.
[75] Z. Salamon and G. Tollin, *Bioelectrochem. Bioenerg., 26* (1991) 321.
[76] J. Haladjian, R. Pilard, P. Bianco and P.-A. Serre, *J. Electroanal. Chem., 9* (1982) 91.
[77] C.D. Rodrigues, F. Farchione, A.G. Wedd and A.M. Bond, *J. Electroanal. Chem., 218* (1987) 251.
[78] P.D. Barker and A.G. Mauk, *J. Am. Chem. Soc., 114* (1992) 3619.
[79] J. Bixler, G. Bakker and G. McLendon, *J. Am. Chem. Soc., 114* (1992) 6938.
[80] Q. Chi and S. Dong, *J. Electroanal. Chem., 348* (1993) 377.
[81] D.D. Schlereth and W. Maentele, *Biochemistry, 32* (1993) 1118.
[82] D. Moss, E. Nabedryk, J. Breton and W. Maentele, *Eur. J. Biochem., 187* (1990) 565.
[83] A.M. Bond and K.B. Oldham, *J. Phys. Chem., 87* (1983) 2492; *89* (1985) 3739.
[84] A.M. Bond, in F.A. Schultz and I. Taniguchi (eds.), *Proc. Fifth Int. Symp. Redox Mechanisms and Interfacial Properties of Biological Importance,* The Electrochemical Society, Pennington, NJ 1993, pp. 21–33.
[85] P. Zuman, *Substituent Effects in Organic Polarography,* Plenum, London, 1967.
[86] A.B.P. Lever, *Inorg.Chem., 29* (1990) 1271.
[87] S. Komar-Panicucci, J. Bixler, G. Bakker, F. Sherman and G. McLendon, *J. Am. Chem. Soc., 114* (1992) 5443.
[88] A.L. Raphael and H.B. Gray, *Proteins: Struct. Function, Genet., 6* (1989) 338.
[89] A.L. Raphael and H.B. Gray, *J. Am. Chem. Soc., 113* (1991) 1038.
[90] T.N. Sorrell and P.K. Martin, *J. Am. Chem. Soc., 111* (1989) 766.
[91] (a) D.D. Niles, *B.Sc.(Hons.) Thesis*, Department of Chemistry, University of Sydney, 1992; (b) D.D. Niles, H.C. Freeman, I. Harvey, P.A. Lay and A.M. Bond, *Inorg. Chem.,* submitted for publication.
[92] W.R. Hagen, *Eur. J. Biochem., 182* (1989) 523.
[93] K.B. Koller and F.M. Hawkridge, *J. Electroanal. Chem., 239* (1988) 291.
[94] I.S.M. Psalti, *D. Phil. Thesis,* Oxford University, UK, 1991.
[95] M.R. McDevitt and A.W. Addison, *Inorg. Chim. Acta, 204* (1993) 141.
[96] F.A. Armstrong, P.A. Cox, H.A.O. Hill, V.J. Lowe and B.N. Oliver, *J. Electroanal. Chem., 217* (1987) 331.
[97] S. Bagby, P.D. Barker, L.-H. Guo and H.A.O. Hill, *Biochemistry, 29* (1990) 3213.
[98] F.A. Armstrong, J.N. Butt, K. Govindaraju, J. McGinnis, R. Powls and A.G. Sykes, *Inorg. Chem., 29* (1990) 4858.
[99] S.-C. Sun, D.E. Reed, J.K. Cullison, L.H. Rickard and F.M. Hawkridge, *Mikrochim. Acta (Wien), III* (1988) 97.
[100] M.R. Tarasevich, in S. Srinivasan, Yu.A. Chizmadzhev, J.O'M. Bockris, B.E. Conway and E. Yeager (eds.), *Comprehensive Treatise of Electrochemistry,* Vol. 10, Plenum, New York, 1985, pp. 285–288.
[101] B.C. King and F.M. Hawkridge, *J. Electroanal. Chem., 237* (1987) 81, and refs. therein.
[102] B.C. King, F.M. Hawkridge and I. Taniguchi, in F.A. Schultz and I. Taniguchi (eds.), *Proc. Fifth Int. Symp. Redox Mechanisms and Interfacial Properties of Molecules of Biological Importance,* The Electrochemical Society, Pennington, NJ, 1993, pp. 87–96.
[103] J.F. Rusling and A.E.F. Nassar, *J. Am. Chem. Soc., 115* (1993) 11891.
[104] K.M. Faulkner and A.L. Crumbliss, *Chemtracts: Inorg. Chem., 4* (1992) 389.
[105] K. Nishiyama, *Kagaku (Kyoto), 48* (1993) 72.
[106] B.C. King, F.M. Hawkridge and B.M. Hoffman, *J. Am. Chem. Soc., 114* (1992) 10603.

[107] I. Taniguchi, K. Watanabe, M. Tominaga and F.M. Hawkridge, *J. Electroanal. Chem., 333* (1992) 331.
[108] D.D. Schlereth and W. Maentele, *Biochemistry, 31* (1992) 7494.
[109] J.F. Castner and F.M. Hawkridge, *J. Electroanal. Chem., 143* (1983) 217.
[110] J.F. Stargardt, F.M. Hawkridge and H.L. Landrum, *Anal. Chem., 50* (1978) 93.
[111] R.E. Dickerson and I. Geis, *Hemoglobin: Structure, Functions, Evolution and Pathology,* Benjamin/Cummings, Menlo Park, CA, 1983, pp. 20–60, and refs. therein.
[112] (a) F.A. Armstrong, P.C. Driscoll, H.A.O. Hill and C. Redfield, *J. Inorg. Biochem., 28* (1986) 171; (b) *Biochem. Soc. Trans., 15* (1987) 767; (c) P.C. Driscoll, H.A.O. Hill and C. Redfield, *Eur. J. Biochem., 170* (1987) 279.
[113] D. Moss, E. Nabedryk, J. Breton and W. Mäntele, *Eur. J. Biochem., 187* (1990) 565.
[114] T.R.I. Cataldi, I.G. Blackham, G.A.D. Briggs, J.B. Pethica and H.A.O. Hill, *J. Electroanal. Chem., 290* (1990) 1.
[115] M. Rivera, M.A. Wells and F.A. Walker, *Biochemistry, 33* (1994) 2161.